AFSC PROCESSED REPORT 2025-04

NOAA FISHERIES

Alaska Fisheries Science Center
Resource Assessment and Conservation Engineering Division
Midwater Assessment and Conservation Engineering Program

Results of the Acoustic-Trawl Survey of Walleye Pollock (*Gadus chalcogrammus*) in the Gulf of Alaska, February and March 2023 (DY2023-03 and DY2023-04)

APRIL 2025

AFSC Processed Report

This document should be cited as follows:
McKelvey, D., McCarthy, A., and Jones, D. 2025. Results of the acoustic-trawl survey of walleye pollock (*Gadus chalcogrammus*) in the Gulf of Alaska, February and March 2023 (DY2023-03 and DY2023-04). 2025. AFSC Processed Rep. 2025-04, 92 p. Alaska Fish. Sci. Cent., NOAA, Natl. Mar. Fish. Serv., 7600 Sand Point Way NE, Seattle WA 98115.

This document is available online at: https://repository.library.noaa.gov/

Results of the Acoustic-Trawl Survey of Walleye Pollock (*Gadus chalcogrammus*) in the Gulf of Alaska February and March 2023 (DY2023-03 and DY2023-04)

by

Denise McKelvey, Abigail McCarthy, and Darin Jones

Resource Assessment and Conservation Engineering Division

Alaska Fisheries Science Center

National Marine Fisheries Service

National Oceanic and Atmospheric Administration

7600 Sand Point Way, NE

Seattle, WA 98115

April 2025

Abstract

Scientists from the Alaska Fisheries Science Center conducted acoustic-trawl surveys in the Gulf of Alaska during late winter 2023 to estimate the distribution and abundance of walleye pollock (*Gadus chalcogrammus*; hereafter pollock) at several of their main spawning grounds. These pre-spawning walleye pollock surveys covered the Shumagin Islands, Pavlof Bay, and Morzhovoi Bay (Shumagin cruise DY2023-03; February 15-21) and Shelikof Strait, Chirikof shelfbreak, and Marmot Bay area (Shelikof cruise DY2023-04; March 04-17).

The abundance of pollock was estimated for each subarea surveyed during the Shumagin Islands cruise. Pollock in the Shumagin Islands were estimated to be 550 million fish weighing 48,868 metric tons (t). The overall length range was between 10 and 55 cm fork length (FL) with modal lengths at 12 cm and 35 cm FL, corresponding with the historical length of age-1 fish, and age-3 fish, respectively. Pollock in Pavlof Bay were estimated to be 18 million fish weighing 5,537 t and pollock in Morzhovoi Bay were estimated to be 6 million fish weighing 4,021 t.

The abundance of pollock was estimated for each subarea surveyed during the Shelikof Strait cruise. Pollock in Shelikof Strait were estimated to be 287 million fish weighing 258,110 t. Although the overall length composition ranged between 11 and 67 cm FL, there was a notable absence of fish < 30 cm FL. Modal lengths were 44-46 cm FL. Thirty percent of the biomass in Shelikof Strait comprised 5 year old fish from the 2018 year class, and another 23% of the biomass were 11 year-old fish from the 2012 year class. Pollock in the Chirikof shelfbreak area were estimated to be 70 million fish weighing 39,875 t and pollock in Marmot Bay were estimated to be 63 million fish weighing 9,284 t.

These estimates were based on an analysis where length-frequency distributions of all species were assigned to observed backscatter using biological data and species compositions of the hauls nearest that backscatter. Estimates included a correction for escapement of fishes and other catch from the survey trawl (i.e. net selectivity). Results from Shelikof Strait were compared with an analysis that did not include net selectivity. The Shelikof Strait no-selectivity analysis estimated slightly more biomass (2%) than the primary analysis.

CONTENTS

INTRODUCTION

The Midwater Assessment and Conservation Engineering (MACE) Program of the Alaska Fisheries Science Center (AFSC) conducts annual acoustic-trawl (AT) surveys in the Gulf of Alaska (GOA) during late winter. The goal of these surveys is to estimate the distribution and abundance of pre-spawning walleye pollock (*Gadus chalcogrammus*; hereafter pollock) at several of their main spawning grounds (i.e., pre-spawning surveys). In the Shumagin Islands area, these surveys covered the Shumagin Islands and intermittently, Sanak Trough, Pavlof Bay, and Morzhovoi Bay. In the Shelikof Strait area, these surveys covered Shelikof Strait and, intermittently, Chirikof shelfbreak and Marmot Bay. Historically, the Shumagin Islands area has been surveyed annually in the winter since 1994, (except in 1997-2000, 2004, 2011, 2019, and 2021-2022). The Shelikof Strait area has been surveyed annually in winter since 1981 (except in 1982, 1987, 1999, and 2011). This report presents the AT survey results from the Shumagin Islands, Pavlof Bay, and Morzhovoi Bay from February 15 to 21, 2023 (cruise DY23-03), and the Shelikof Strait, Chirikof shelfbreak, and Marmot Bay from March 4 to 17, 2023 (cruise DY23-04).

METHODS

All activities were conducted aboard the NOAA ship *Oscar Dyson*, a 64-m stern trawler equipped for fisheries and oceanographic research. The survey followed established AT methods as specified in NOAA protocols for fisheries acoustics surveys and related sampling[1]. The acoustic units used here are defined in MacLennan et al. (2002).

Survey itineraries are listed in Appendix I and scientific personnel in Appendix II. All survey dates and data were recorded and reported using UTC time zone, where Alaska Standard Time = UTC – 9 hours. Survey dates for the Shumagin Islands area were modified from the original schedule due to the ship's transit delay to Kodiak, Alaska, and due to medical emergencies during the cruise (Appendix I).

[1] National Marine Fisheries Service (NMFS) 2014. NOAA protocols for fisheries acoustics surveys and related sampling (Alaska Fisheries Science Center), 26 p. Prepared by Midwater Assessment and Conservation Engineering Program, Alaska Fish. Sci. Center, Natl. Mar. Fish. Serv., NOAA.

Acoustic Equipment, Calibration, and Data Collection

Acoustic measurements were collected with a Simrad EK80 scientific echosounder (Bodholt and Solli 1992, Simrad 2018). Data were collected with five split-beam transducers (18, 38, 70, 120, and 200 kHz) mounted on the bottom of the vessel's retractable centerboard, which was extended 9.15 m below the water surface.

Two standard sphere acoustic system calibrations were conducted to measure acoustic system performance (Table 1). The vessel's dynamic positioning system was used to maintain the vessel location during calibration. Local water temperature and salinity were measured and used to estimate absorption and sound speed. A tungsten carbide sphere (38.1 mm diameter) suspended below the centerboard-mounted transducers was used to calibrate the 38, 70, 120, and 200 kHz systems. The tungsten carbide sphere was then replaced with a 64 mm diameter copper sphere to calibrate the 18 kHz system. A two-stage calibration approach was followed for each frequency. On-axis sensitivity (i.e., transducer gain and s_A correction) was estimated from measurements with the sphere placed in the center of the beam following the procedure described in Foote et al. (1987). Transducer beam characteristics (i.e., beam angles and angle offsets) were estimated by moving the sphere in a horizontal plane using the EK80's calibration utility (Jech et al. 2005, Simrad 2018). For the February 12th calibration in Uyak Bay, the 18 kHz transducer beam characteristics were not estimated using the copper sphere due to too many fish in the water column. Instead, the 18 kHz transducer beam characteristics were estimated using the tungsten carbide sphere. The equivalent beam angle (for characterizing the volume sampled by the beam) and angle sensitivities (for conversion of electrical to mechanical angles) cannot be estimated from the calibration approach used because that requires knowledge of the absolute position of the sphere (see Demer et al. 2015). Therefore, the factory default values for equivalent beam angle and angle sensitivities for each transducer were used during calibration.

Raw acoustic data were recorded using EK80 software (version 21.15.2) at a nominal ping interval of 1.1 seconds, and analyzed from 16 m below the sea surface to within 0.5 m of the sounder-detected bottom to a maximum depth of 1,000 m. Data shallower than 16 m were excluded to account for the acoustic near-field range of all transducers (Simmonds and MacLennan 2005). Data within 0.5 m of the seafloor were also excluded to account for the bottom-associated acoustic dead zone (Ona and Mitson 1996). The raw acoustic data were

analyzed using Echoview post-processing software (version 13.0.396, Echoview Software Pty Ltd).

Trawl Gear and Oceanographic Equipment

Midwater and near-bottom acoustic backscatter were sampled using an LFS1421 trawl[2]. The headrope and footrope of the LFS1421 trawl each measure 76.8 m (252 ft), with meshes tapering from 650 cm (256 in.) in the forward sections to 3.8 cm (1.5 in.) in the section immediately preceding the codend (mesh sizes are stretched measurements unless otherwise noted). To increase retention of small organisms, the LFS1421 codend was fitted with a knotless nylon 7.9 mm (5/16 in.) mesh, 3.2 mm (1/8 in.) square-opening codend liner.

The LFS1421 trawl was fished with four 45.7 m (150 ft) bridles (1.9 cm (0.75 in.) dia.), 5 m^2 Series-2000-V trawl doors without shoes during the Shumagin cruise and with 4" shoes (918 kg (2,024 lb) each) during the Shelikof cruise. For both cruises, the trawl was fished with 227 kg (500 lb) tom weights attached to each wingtip. Average trawling speed was 1.7 m s^{-1} (3.3 knots). LFS1421 trawl vertical net openings and headrope depths were monitored with a Simrad FS70 third-wire netsonde attached to the headrope. The vertical net opening of the LFS1421 trawl ranged from 12.5 to 23.0 m (41.0 to 75.5 ft) and averaged 16.2 m (53.1 ft) while fishing.

A stereo camera system (Camtrawl; Williams et al. 2010) was attached to the starboard panel forward of the codend on the LFS1421 trawl. The Camtrawl was used to capture stereo images for species identification and length measurement of individual fish and other taxa as they pass through the net toward the codend. The Camtrawl images also included depth and time stamps, which were used to identify taxa associated with distinct backscatter layers separated by depth but could not be differentiated in the codend catch. Images were viewed and annotated using procedures described in Williams et al. (2010).

Physical oceanographic data were collected during the cruise at trawl locations, at calibration locations, and continuously along transects. Water temperature profiles were obtained at trawl locations with a temperature-depth probe (SBE 39, Sea-Bird Scientific) attached to the trawl headrope. Additional temperature-depth profile measurements were taken from

[2] LFS1421 trawl (LFS Marine, NOAA, 1421 Research Trawl, designed and built in 2018/2019 to MACE specifications; hereafter LFS1421)

conductivity-temperature-depth (CTD) casts with a Sea-Bird CTD (SBE 911plus) system at the calibration site. Sea surface temperature data were measured along transects using the ship's sea surface temperature flow through system (SBE 38, Sea-Bird Scientific, accuracy ± 0.002°C) located near the ship's bow, approximately 1.4 m below the surface. At times when the SBE 38 was not operating, sea surface temperatures were taken from the Furuno T-2000 temperature probe (accuracy ± 0.2°C) located amidships 1.4 m below the surface. The SBE 38 was used 95% of the time in the Shumagin Islands survey and 99% of the time in the Shelikof Strait survey. Sea surface temperature and other environmental data were recorded using the ship's Scientific Computing Systems (SCS).

Survey Design

Generally, the pre-spawning pollock surveys in the Shumagin Islands area occur in February while surveys in the Shelikof Strait areas occur in March. To gauge whether survey timing was appropriate, we evaluated the maturity condition of pollock during catch processing (described below). We consider the survey timing appropriate if < 10% of the female pollock are in the spawning or spent maturity stages.

The survey consisted of a series of parallel transects except in areas where it was necessary to reorient transects to maintain a perpendicular alignment to the isobaths or navigate around landmasses. Spatial coverage and predetermined transect location and spacing were chosen to be consistent with previous surveys. However, in the Shumagin Islands, transect spacing was increased from 1-1.5 nmi spacing to 2 nmi in Unga Strait, and from 1 nmi spacing to 2 nmi spacing off Renshaw Pt. to save time. In Shelikof Strait, the planned transect start and end locations matched those from 2022. The surveys were conducted 24 hours per day for both cruises but fishing operations were limited to 12 hours per day during the Shumagin cruise because of vessel staffing shortages.

Trawl hauls were conducted to identify the species and size composition of acoustically-observed fish aggregations and to determine biological characteristics of pollock and other specimens. Catches were sorted to species and weighed. When large numbers of small and large pollock were encountered, the predominant size groups in the catch were sampled separately (e.g., age-1 vs. larger sizes). Fork length (FL), body weight, sex (FL > 20 cm), maturity stage, age (otoliths), and gonad measurements were collected for a random subset of pollock within each size group. Pollock and other fishes were measured to the nearest 1 mm

FL, or standard length (SL) for small specimens, with an electronic measuring board (Towler and Williams 2010). All lengths measured as SL were converted to FL using an SL to FL regression obtained from historic survey data when necessary. Other invertebrate organisms (e.g., jellyfish, squid) were measured to the nearest 1 mm length using accepted measurements for their class (e.g., jellyfish bell diameter, squid mantle length). Gonad maturity of pollock was determined by visual inspection and categorized as immature, developing, mature (hereafter, "pre-spawning"), spawning, or spent[3]. The ovary weight was determined for pre-spawning females. An electronic motion-compensating scale (Marel M60) was used to weigh individual pollock and selected ovaries to the nearest 2 g. Otoliths that were collected were stored in 50% glycerin/thymol/water solution and interpreted by AFSC Age and Growth Program researchers to determine fish ages. Trawl station information and biological measurements were electronically recorded using the MACE Program's custom Catch Logger for Acoustic Midwater Surveys (CLAMS) software.

Additional biological samples were collected for special projects. Whole fish specimens were collected for the FMA Observer Services Training Program (Brian Mason, brian.mason@noaa.gov) and for inclusion in eDNA reference databases (Krista Nichols, krista.nichols@noaa.gov). Pollock ovaries were collected from pre-spawning pollock to investigate interannual variation in fecundity of mature females, and from female pollock of all maturity stages for a histological study (Sandi Neidetcher, sandi.neidetcher@noaa.gov). Blood and tissue samples were also taken from pollock and Pacific cod (*Gadus macrocephalus*) to investigate the prevalence of antifreeze proteins (Chi-Hing Christina Cheng, c-cheng@illinois.edu).

Data Analysis

Pollock abundance was estimated by combining acoustic and trawl catch information. The analysis method employed here had three principal steps. First, backscatter was associated with the trawl catches from the nearest geographic haul locations within a stratum. Second, a correction was made for net selectivity (escapement from the midwater net, based on relationships derived from recapture nets; Williams et al. 2011). Third, backscatter was converted to estimates of abundance using the nearest-haul catch association (step 1) with

[3] Alaska Fisheries Science Center. 2021. Groundfish survey data codes and forms, Table 3. https://doi.org/10.25923/kp5e-1g02.

sample corrections (step 2) and the expected backscatter from each organism given species and size. Biomass was computed from abundance using the mean weight-at-length from all pollock specimens measured in the survey.

Processing of acoustic data

Although acoustic data were recorded at five frequencies, the results of this report and the survey time series are based on the 38 kHz data. The sounder-detected bottom was calculated by averaging the bottom detections for the five frequencies (Jones et al. 2011) and then visually examined to remove any bottom integrations. A minimum S_v threshold of –70 dB re 1 m^{-1} was applied to the 38 kHz acoustic data, which were then echo-integrated from 16 m below the surface to 0.5 m above the sounder-detected bottom. Data were averaged at 0.5 nmi horizontal by 10 m vertical resolution intervals and exported to a database.

Associating size and species composition with acoustic backscatter

Acoustic backscatter was assigned to strata based on the appearance and vertical distribution of the aggregations in the echogram. Strata containing backscatter not adequately sampled by trawls (e.g., the near-surface mixture of unidentifiable backscatter, backscatter with frequency response indicative of euphausiids or myctophids (De Robertis et al. 2010), or near-bottom backscatter "haystack" morphology indicative of some rockfishes were excluded from further analyses. Each trawl was associated with a stratum, and the backscatter at a given location was associated with the species and size composition of the geographically-nearest haul within that stratum (see De Robertis et al. 2017b for details). For example, small pollock can be found in shallow, dense schools with a diffuse layer of large pollock at deeper depths in the same area. In this case, the backscatter dominated by aggregations of small pollock would be assigned to a shallow stratum (A) and the backscatter dominated by large pollock layers would be assigned to a deep stratum (B). Hauls that sampled the shallow layer would be assigned to stratum A, and hauls that sampled the deeper layer would be assigned to stratum B. Backscatter was apportioned by species and size within a stratum using the geographically nearest-trawl's selectivity-corrected catch composition in that stratum and converted to abundance.

Accounting for catch from non-targeted scattering layers

As noted above, each trawl was associated with an acoustic stratum. However, trawls may capture animals while passing through non-targeted strata during the trawling process. For example, a trawl targeting a deep stratum may capture acoustically-relevant animals while passing through a shallower stratum during set and retrieval. Because trawls aggregate catch from all the strata sampled, animals from the shallow stratum could then be associated incorrectly with the deeper stratum during analysis. These animals should not be included in the catch that is applied to the deeper stratum.

To avoid incorrectly applying catch from different strata, Camtrawl images collected during LFS1421 trawls were used to identify catch depth and location in the water column. Camtrawl images were captured at a rate of approximately 1 s^{-1} and each image was tagged with collection time and depth. Analysts visually identified and counted animals present in every 100^{th} image (approximately one image per 1.5 minute of trawl time) using SEBASTES Stereo Image Analysis software (Williams et al. 2016). For every examined image, the analyst identified all visible fish to the lowest taxonomic level possible, and identified invertebrates to broad taxonomic group (e.g., 'jellyfish', 'squid', 'shrimp'). Images were then examined using custom Python applications to identify cases where the trawl retained catch from non-targeted layers. In rare, exceptional cases where it was evident that the trawl catch contained acoustically-relevant species and/or size classes from outside of the target stratum, these species and/or size class records were excluded during the analysis process from the trawl catch associated with the target stratum (see figs. 3 and 4 in Levine et al. 2024 for a summary of the review process).

Selectivity correction

Previous research has found that smaller pollock are less likely to be retained in large midwater trawls than larger pollock (Williams et al. 2011). To correct for species- and size-related differences in retention, trawl catch compositions were adjusted to that which would be expected from an unselective net. Trawl selectivity was estimated using correction functions developed from catch data collected by recapture nets mounted on the midwater trawl. Net selectivity corrections to trawl species and size composition estimates have been incrementally implemented to winter Shelikof Strait AT surveys conducted since 2008 based on the survey vessel, how backscatter was allocated to species, and the type of midwater net

used in the survey (Honkalehto et al. 2024., Lauffenburger et al. 2019, Stienessen et al. 2019, McCarthy et al. 2022). Trawl selectivity in the 2023 surveys was estimated for all species observed in the codend using correction functions developed from catch data collected by recapture nets mounted on the LFS1421 trawl during the 2020 and 2021 winter Shelikof Strait AT surveys (see appendix IV in Honkalehto et al. 2024). The counts and weights of fish and other taxa caught in the recapture nets were expanded to provide an estimate of escapement from the entire trawl. The catch of all species was corrected for the estimated probability of escapement by dividing the abundance of a given species and size class by the estimated probability of retention of that species and size class. The probability of retention was calculated using either species-specific trawl selectivity correction functions for the most abundant species or more generic selectivity functions for less abundant species that were pooled together (De Robertis et al. 2017b, Honkalehto et al. 2024). Thus, the 2023 survey estimates reflect adjustments to the trawl-derived estimates of species and size composition which incorporate the estimated escapement of all organisms from the catch (e.g., De Robertis et al. 2017a).

Abundance calculations

A series of target strength (TS, dB re 1 m^2; the expected backscatter from each organism) to length relationships from the literature (Appendix Table 1) were used along with size and species distributions from selectivity-corrected trawl catches to estimate the proportion of the observed acoustic scattering attributable to each of the species captured in the trawls (Appendix III). For species for which the TS-length relationship was derived using a different length measurement type than the one used for measuring the trawl catch specimens, an appropriate length conversion was applied (e.g., total length to fork length). Species-specific TS-length relationships from the literature were used for pollock, Pacific capelin, eulachon, Pacific herring, and for any species whose contribution to the total backscatter used in survey estimates was > 5%. Otherwise, species were assigned one of five group TS-length relationships: fishes with swim bladders, fishes without swim bladders, jellyfish, squid, and pelagic crustaceans (Appendix Table 1).

Biomass was computed from abundance using the mean weight-at-length from all pollock specimens included in the length-weight key, which in winter is typically all specimens that were lengthed and weighed in the survey trawl catches (Appendix III). When < 5 pollock

occurred within a 1-cm length interval, weight at that length interval was estimated from a linear regression of the natural logs of the length and weight data and corrected for a small bias due to back-transformation (Appendix III; Miller 1984, De Robertis and Williams 2008).

An age-length key and a proportion-at-age matrix were applied to the population numbers-at-length and biomass-at-length to estimate numbers and biomass at age (Appendix III; Jones et al. 2019). For population estimates at lengths where no otolith specimens were collected, the proportion-at-age was estimated using a Gaussian-model approach based on historical age-at-length data (2000–2014).

Processing of maturity data

Maturity data by haul were weighted by the local acoustically-estimated abundance of pollock (number of individuals > 30 cm FL). The 30 cm size criterion was selected as the approximate minimum size at which ≥ 5% of pollock are mature. The sum of the local abundance, A_h, assigned to the geographically-nearest haul was computed. A weight, W_h, was then assigned to each haul by dividing the local abundance A_h by the average abundance per haul $\overline{A}$:

$$W_h = \frac{A_h}{\overline{A}} \quad , \qquad \text{Eqn. 1}$$

where

$$\overline{A} = \frac{\sum_h A_h}{H} \quad , \qquad \text{Eqn. 2}$$

and H is the total number of hauls.

The percent of pollock, $PP_{sex,mat}$ > 40 cm by sex and maturity stage (immature, developing, pre-spawning, spawning, or spent) was computed for each haul and combined by survey area using a weighted average with W_h:

$$PP_{sex,mat} = \frac{\sum_h \left(N_{sex,mat,h} \cdot W_h\right)}{\sum_h W_h} \quad , \qquad \text{Eqn. 3}$$

where $N_{(sex,mat,h)}$ is the number of pollock > 40 cm by sex and maturity for each haul. The > 40 cm cutoff is used for consistency with reporting from past surveys.

For each haul, the numbers of female pollock considered mature (pre-spawning, spawning, or spent) and immature (immature or developing) were determined for each cm length bin. The length at 50% maturity ($L50$) was estimated for female pollock as a logistic regression using a weighted generalized linear model following Williams (2007) with the inclusion of the haul weights, W_h, into the model (function glm, R Core Team 2021).

The gonadosomatic index, GSI_h, (GSI: ovary weight/total body weight) was calculated for pre-spawning females in each haul and then a weighted average was computed for each survey area with W_h:

$$GSI = \frac{\sum_h (GSI_h \cdot W_h)}{\sum_h W_h} \quad . \qquad \text{Eqn. 4}$$

Relative estimation error

Transects were parallel and relative estimation errors for the acoustic-based estimates were derived using a one-dimensional (1-D) geostatistical method (Petitgas 1993, Williamson and Traynor 1996, Walline 2007). "Relative estimation error" is defined as the ratio of the square root of the 1-D estimation variance ($variance_{sum}$) to the biomass estimate (i.e., the sum of biomass over all transects, $biomass_{sum}$, kg):

$$Relative\ estimation\ error_{1-D} = \frac{\sqrt{variance_{sum}}}{biomass_{sum}} \quad . \qquad \text{Eqn. 5}$$

Because sampling resolution affects the variance estimate, and the 1-D method assumes equal transect spacing, estimation variance was determined separately in each area with unique transect spacing. Relative estimation error for an entire survey area (among n survey areas with different transect spacings) was computed by summing the estimation variance for each area j, taking the square root, and then dividing by the sum of the biomass over all areas, assuming independence among estimation errors for each survey area (Rivoirard et al. 2000):

$$Relative\ estimation\ error_{1-D\ survey} = \frac{\sqrt{\sum_{j=1}^{n} v\ ariance_{sum_j}}}{\sum_{j=1}^{n} b\ iomass_{sum_j}} \quad . \qquad \text{Eqn. 6}$$

Geostatistical methods were used to compute estimation error as a means to account for estimation uncertainty arising from the observed spatial structure in the fish distribution. These errors, however, quantify only across-transect sampling variability of the acoustic data

(Rivoirard et al. 2000). Other sources of error (e.g., target strength, trawl sampling) were not evaluated.

Spatial patterns analysis

To examine pollock horizontal distribution relative to prior surveys, geostatistical measures of the mean location (center of gravity, COG) and dispersion of the distribution around its COG (inertia) were calculated for each survey from 2008 to 2023 (Woillez et al. 2007). To account for interannual changes in survey coverage, COG and inertia were estimated using acoustic samples located within a standardized area of Shelikof Strait based on a minimum convex polygon that encompasses 95% of all samples collected between 2008 and 2023. The minimum convex polygon was estimated using the smoothed cross-validation bandwidth selector and kernel density estimator functions in the 'KS' R package (Duong 2022). COG and inertia were calculated using the 'RGeostats' R package (MINES ParisTech / ARMINES 2021).

Additional analyses

A 'no-selectivity' analysis was conducted for the Shelikof Strait estimate to evaluate the effect of the selectivity corrections used in the 'primary' Shelikof analysis on the numbers and biomass of pollock and other target species. The no-selectivity analysis was the same as the primary analysis described above, except that it did not include a selectivity correction (i.e., trawl selectivity S_l for each cm length class l of all species or species group was set to 1 (see Eqn. x, appendix IV in Jones et al. 2022).

Pollock vertical distribution patterns were examined using two metrics: 1) mean weighted depth (MWD) of pollock from the surface-referenced primary analysis, and 2) height above bottom (HAB) calculated from a 'bottom-referenced' analysis in which pollock vertical position was measured in terms of distance above the seafloor. The MWD in each along-track interval i is computed as:

$$MWD_i = \sum_j \left(\left(\frac{B_{i,j}}{\sum_j B_{i,j}} \right) d_{i,j} \right) \quad , \qquad \text{Eqn. 7}$$

where $B_{i,j}$ is observed biomass in 0.5 nmi along-track interval i and 10 m depth bin j, and d is the depth in meters of bin i from the sea surface. In contrast to the surface-referenced

primary analysis, the bottom-referenced analysis data were exported using Echoview in 10 m vertical bins referenced to the scrutinized line 0.5 m above the sounder-detected bottom. The HAB is computed in a similar fashion:

$$HAB_i = \sum_j \left(\left(\frac{B_{i,j}}{\sum_j B_{i,j}} \right) h_{i,j} \right) \quad , \qquad \text{Eqn. 8}$$

where the terms are as described above and h is the height in meters of bin i above the sounder-detected bottom. MWD and HAB were summarized for a given survey area by first summing biomass over all intervals i in the area and then computing the MWD and HAB using the equations above. The bottom-referenced analysis was generated for previous years to allow for inter-annual comparison of vertical distribution. All other parts of this analysis are the same as the primary analysis.

RESULTS AND DISCUSSION

Acoustic System Calibration

Pre-survey calibration measurements of the 38 kHz echosounder showed no notable differences in on-axis gain parameters or beam pattern characteristics confirming that the acoustic system was stable throughout the survey (Table 1). At 38 kHz, the integration gain differed by 0.03 dB across the two measurements. On-axis acoustic system gain, S_a correction values, and EK80 calibration utility 3 dB beamwidths and offset angles measured during the winter 2023 calibrations were averaged in the linear domain. These averaged values were used with the nominal sound speed and absorption values appropriate for the survey areas in the final parameter set for survey data analysis. The measured equivalent beam angle recorded on the 38 kHz transducer's specification sheet was adjusted (Bodholt 2002) using the sound speed assumed during survey conditions for data analysis (Table 1).

Shumagin Islands

Survey timing and extent

The 2023 winter AT survey of pre-spawning pollock in the Shumagin Islands was conducted between 15 and 17 February. The survey began in Stepovak Bay, proceeded southwest through Unga Strait, and then through West Nagai Strait. Due to poor weather conditions, the

Shumagin Trough area was surveyed between 19 and 21 February, after Pavlof Bay and Morzhovoi Bay (Appendix I). The entire survey area encompassed 6,448 km^2 (1,880 nmi^2). Acoustic backscatter was measured along 861.5 km (465.2 nmi) of transects spaced mainly 9.3 km (5 nmi) apart with spacing varying from 2.8 km to 9.3 km (1.5 to 5 nmi) in the survey area (Fig. 1). Bottom depths in the survey area ranged from 58 m to 221 m.

Environmental conditions

Sea surface temperatures (SST) measured in the Shumagin Islands in 2023 indicate relatively average thermal conditions during the survey. SST ranged from 3.4°C to 4.5°C as measured by the ship's flow-through instrumentation along acoustic transects and averaged 4.1°C (Fig. 2). The along-transect mean SST was 0.6°C warmer than observed during 2020 and 0.2°C warmer than the 2009-2020 historical mean (3.9°C). The average SST measured by the SBE 39 at all haul locations was 3.9°C (Table 2), which was 0.4°C warmer than the haul-based mean SST in 2020, 0.2°C warmer than the 2006-2020 mean, and 0.2°C warmer than the long-term 1994-2020 historical mean. Mean SST anomalies from both sources in 2023 were less than ± 0.5, indicating average conditions relative to the 2006-2020 period (Fig. 3). Mean temperature between the surface and deepest trawl (i.e., headrope) depth at all haul locations varied by approximately 1.2°C (Fig. 4).

Trawl catch summary

Biological data and specimens were collected in the Shumagin Islands from 8 LFS1421 hauls (Fig. 1, Table 2) targeted on backscatter. The lengths of an average of 257 randomly selected pollock were measured from each haul, with an average of 39 individuals more extensively sampled for at least one of the following: body weight, maturity, and age (Table 3). A total of 305 otoliths used to estimate pollock ages were collected in the Shumagin Islands, and a total of 2,053 pollock lengths were measured (Table 3). Pollock lengths ranged from 10 to 55 cm FL. Pollock and salmon shark (*Lamna ditropis*) were the most abundant species by weight in the LFS1421 hauls, contributing 98.2% and 1% of the catch by weight respectively (Table 4). Pollock and Pacific capelin were the most abundant species by numbers with 95.2% and 3.6% of total catch by numbers, respectively.

Pollock maturity

Male and female pollock observed in the Shumagin Islands were mostly in the pre-spawning maturity stage. The abundance-weighted maturity composition for males > 40 cm FL (n = 17) in the Shumagin Islands was 0% immature, 0% developing, 100% pre-spawning, 0% spawning, and 0% spent, and for females > 40 cm FL (n = 13) the abundance weighted maturity composition was 39% immature, 6% developing, 56% pre-spawning, 0% spawning, and 0% spent (Fig. 5A), which suggests that the timing of the survey relative to the spawning period was appropriate. The length at which 50% of female pollock were determined to be reproductively mature (i.e., pre-spawning, spawning, or spent) was 43 cm FL (Fig. 5B). Only five female pollock were examined for the gonadosomatic index, which averaged 0.11 ± 0.01 and all fish were within ± 1 standard deviation of the historic mean (Fig. 5C) from 2009 to 2020.

Distribution and abundance

Pollock were observed throughout the surveyed area and were most abundant between Popof and Unga islands, and in the Unga Strait areas (Fig. 6). Larger pollock (> 30 cm FL) were detected in all areas, but to a lesser extent in the outer Shumagin Trough. Smaller pollock (≤ 30 cm FL) were present primarily in the outer Shumagin Trough (92% by number) and in Unga Strait (4% by number). Most of the larger pollock (75% of the larger pollock biomass) were detected between depths of 75-155 m (Fig. 7A). The overall average depth for the larger pollock observed in 2023 (115 m) was deeper than the average depth observed for the larger pollock in 2020 (108 m) and more similar to the average depth in 2018 (119 m). The smaller pollock were similarly distributed, where the overall average depth (137 m) observed in 2023 was deeper than the average depth observed in 2020 (118 m) and more similar to what was observed in 2018 (140 m). Compared to the larger pollock, most smaller pollock (75% of the smaller pollock biomass) in 2023 were detected slightly deeper, between depths of 95-175 m (Fig. 7B). Results from the bottom referenced analysis indicated that about 13% of the larger pollock biomass was observed within 10 m of the seafloor, and 65% percent was within 50 m of the seafloor (Fig. 7C). Similarly, in 2020, 70% of the larger pollock biomass was within 50 m of the seafloor (Fig. 7C). Most of the smaller pollock were found within 50 m of the seafloor (82% in 2023, 60% in 2020 (Fig. 7D)).

Numerically, the pollock size composition in the Shumagin Islands was dominated by young fish (12 cm FL length mode). Pollock with lengths 10-16 cm FL, indicative of age-1 pollock, accounted for 70.5% of the numbers and 9% of the biomass of all pollock observed in the Shumagin Islands (Fig. 8). Pollock 17-24 cm FL, indicative of age-2s, accounted for 1.5% by numbers and 1.4% by biomass. Pollock ≥ 30 cm FL accounted for 26.2% of the numbers and 86.8% of the biomass.

A total of 550.1 million pollock weighing 48,867.94 t were estimated to be in the Shumagin Islands at the time of the survey. The 2023 biomass was 999.5% of that observed in 2020 (4,889 t) and 74.9% of the historic mean of 65.2 thousand tons (Table 5; Fig. 9). The 2023 survey biomass estimate is the largest in the Shumagin survey time series since 2015 (Table 5; Fig. 9). The relative estimation error of the 2023 biomass estimate based on the 1-D geostatistical analysis was 8.7%. The 2023 high abundance estimates for small pollock (10-16 cm FL) was consistent with several historical Shumagin Islands surveys (Fig. 10).

Pavlof Bay

Survey timing and extent

The 2023 winter AT survey of pre-spawning pollock in Pavlof Bay was conducted on 17 February. Acoustic backscatter was measured along 72.2 km (39 nmi) of transects spaced mainly 3.7 km (2 nmi) apart with spacing varying from 3.7 km to 6.1 km (2 to 3.3 nmi) in the survey area (Fig. 1). The entire survey area encompassed 294 km^2 (86 nmi^2). Bottom depths in the survey area ranged from 62 to 137 m.

Environmental conditions

Sea surface temperatures (SST) measured in Pavlof Bay in 2023 indicate relatively average thermal conditions during the survey. SST ranged from 3.1°C to 3.4°C as measured by the ship's flow-through instrumentation along acoustic transects and averaged 3.3°C (Fig. 2). The average SST measured by the SBE 39 at the haul location was 3.3°C (Table 2), which was 0.1°C cooler than the haul-based mean SST in 2018, and 0.1°C cooler than the haul-based mean SST for the years 2010-2018. Mean temperature between the surface and deepest trawl (i.e. headrope) depth at the haul location varied by approximately 0.3°C (Fig. 4).

Trawl catch summary

Biological data and specimens were collected in Pavlof Bay from one LFS1421 haul that targeted backscatter, where pollock was the only species captured in the net (Fig. 1, Table 6). The lengths of 430 randomly selected pollock were measured from the haul; lengths ranged from 10 to 62 cm FL, with 77 individuals more extensively sampled for at least one of the following: body weight, maturity, and age (Table 3). A total of 55 otoliths were collected to estimate pollock ages.

Pollock maturity

Pollock in Pavlof Bay were mostly in pre-spawning (males) or immature (females) maturity stages. However, maturity compositions were represented by relatively few fish > 40 cm and may not be a good indicator for whether the survey timing was appropriate or not. The maturity composition of males > 40 cm FL (n = 10) was 0% immature, 0% developing, 80% pre-spawning, 20% spawning, and 0% spent, while for the females > 40 cm FL (n = 4), 50% were immature, 0% developing, 25% pre-spawning, 25% spawning, and 0% spent (Fig. 11). The length at which 50% of female pollock was not computed due to insufficient data and no ovaries were sampled for the GSI.

Distribution and abundance

Pollock were observed throughout Pavlof Bay and were most abundant at the mouth of the Bay (Fig. 6). Small pollock (≤ 30 cm FL) were intermixed with larger pollock, and detected between depths of 65-105 m; hence, the violin plots for 2023 are the same for small and large pollock (Fig. 12A-B). The plots were presented to show the similarity in the depth distribution to the 2018 survey results. Pollock were observed within 45 m of the bottom and ranging up to 55 m off the bottom (Fig. 12C), computed from bottom-referenced analysis. About 34% of the pollock biomass was observed within 10 m of the seafloor, and 93% percent of biomass within 50 m of the seafloor (Fig. 12C). No bottom referenced analysis was completed for Pavlof Bay in 2018.

The pollock size composition in Pavlof Bay was variable with a primary length mode at 32 cm (Fig. 8). Pollock with lengths 10-16 cm FL, indicative of age-1 pollock, accounted for 2.5% of the numbers and 0.1% of the biomass of all pollock observed in Pavlof Bay, while

pollock ≥ 30 cm FL accounted for 89.9% and 96.6% of the numbers and biomass, respectively.

A total of 18.1 million pollock weighing 5,537 t were estimated to be in Pavlof Bay at the time of the survey. The 2023 biomass was 120.1% of that observed in 2018 (4,610 t) and 243.7% of the historic mean of 2.3 thousand tons (Table 5). The 2023 survey biomass estimate is the largest in the Pavlof Bay survey time series. The relative estimation error of the 2023 biomass estimate based on the 1-D geostatistical analysis was 13.6%.

Morzhovoi Bay

Survey timing and extent

The 2023 winter AT survey of pre-spawning pollock in Morzhovoi Bay was conducted on 18 February. The entire survey area encompassed 278 km^2 (81 nmi^2). Acoustic backscatter was measured along 70.7 km (38.2 nmi) of transects spaced mainly 3.7 km (2 nmi) apart with spacing varying from 3 to 5 km (1.6 to 2.7 nmi) in the survey area (Fig. 1). Bottom depths in the survey area ranged from 45 to 128 m.

Environmental conditions

Sea surface temperatures (SST) measured in Morzhovoi Bay in 2023 indicate relatively average thermal conditions during the survey. SST ranged from 3°C to 3.4°C as measured by the ship's flow-through instrumentation along acoustic transects and averaged 3.2°C (Fig. 2). The along-transect mean SST was 0.1°C cooler than observed during 2018 and 0.2°C warmer than the 2013-2018 historical mean (3.0°C). The average SST measured by the SBE 39 at the haul location was 3.1°C (Table 2), which was 0.1°C cooler than the haul-based SST in 2018, 0.4°C warmer than the 2006–2018 historical mean. Mean temperature between the surface and deepest trawl (i.e., headrope) depth at the haul location varied by approximately 0.2°C (Fig. 4).

Trawl catch summary

Biological data and specimens were collected in Morzhovoi Bay from one LFS1421 haul (Table 2, Fig. 1) targeted on backscatter. The lengths of 392 randomly selected pollock were measured for length, with individuals more extensively sampled for body weight, maturity,

and age (Table 3). The size range of pollock in Morzhovoi Bay ranged between 9 and 64 cm FL.

Pollock and Pacific cod were the most abundant species by weight in the haul, contributing 91.3% and 8.5% of the catch by weight, respectively (Table 7). Pollock and Pacific capelin (*Mallotus catervarius*) were the most abundant species by numbers with 82.6% and 16% of total catch by numbers, respectively.

Pollock maturity

Most of the pollock males observed in Morzhovoi Bay were in the spawning maturity stage, whereas most of the pollock females were equally represented in the pre-spawning and spawning maturity stages. Specifically, the maturity composition for males > 40 cm FL (n = 46) was 0% immature, 4% developing, 20% pre-spawning, 76% spawning, and 0% spent, while the maturity composition for females > 40 cm FL (n = 9) was 0% immature, 11% developing, 44% pre-spawning, 44% spawning, and 0% spent (Fig. 13A). Although the percent females in the spawning and spent maturity stages suggests that the timing of the survey relative to the spawning period was somewhat late, the maturity composition was represented by a small sample size. The length at which 50% of female pollock were determined was not computed due to insufficient data. The average GSI from three pre-spawning females was 0.14 ± 0 (Fig. 13B, mean $\pm$ standard deviation), which was similar to the 2018 estimate (0.15 ± 0) and the historical mean (0.13 ± 0) from 2010-2018.

Distribution and Abundance

Pollock were observed throughout the surveyed area and were most abundant to the southeast in the mouth of the Bay (Fig. 6). Small pollock ($\leq$ 30 cm FL) were caught intermixed with larger pollock and most of the fish (89%) were detected between depths of 55-95 m (Fig. 14A). About 43% of the pollock biomass was observed within 10 m of the seafloor, and 96% percent of biomass within 50 m of the seafloor (Fig. 14B, no bottom referenced analysis was completed in 2018).

The size composition of pollock in Morzhovoi Bay was variable with length modes at 12 cm, 44 cm, and 52 cm (Fig. 8). Pollock with lengths 9-16 cm FL, indicative of age-1 pollock, accounted for 19.4% of the numbers and 0.3% of the biomass of all pollock, while pollock $\geq$ 30 cm FL accounted for 79.9% and 99.5% of the numbers and biomass, respectively.

A total of 5.6 million pollock weighing 4,021 t were estimated to be in Morzhovoi Bay at the time of the survey. The 2023 biomass was 106.6% of that observed in 2018 (3,772 t) and 75.6% of the historic mean of 5.3 thousand tons (Table 5). The relative estimation error of the 2023 biomass estimate based on the 1-D geostatistical analysis was 5.4%.

Shelikof Strait

Survey timing and extent

The 2023 winter AT survey of pre-spawning pollock in Shelikof Strait was conducted between 4 and 11 March. The entire survey area encompassed 23,434 km^2 (6,832 nmi^2). Acoustic backscatter was measured along 1,663.9 km (898.5 nmi) of transects spaced mainly 13.9 km (7.5 nmi) apart, with spacing varying from 11.3 to 15.6 km (6.1 to 8.4 nmi) in the survey area (Fig. 15). Bottom depths in the survey area ranged from 46 to 326 m.

Environmental conditions

Sea surface temperatures (SST) measured in Shelikof Strait in 2023 indicate relatively average thermal conditions during the survey. SST ranged from 2.7°C to 4.5°C as measured by the ship's flow-through instrumentation along acoustic transects and averaged 3.7°C (Fig. 16). The along-transect mean SST was 0.3°C cooler than the mean SST observed during the 2022 survey, and the same as the 2006-2022 historical mean (3.7°C). The average SST measured by the SBE 39 at all haul locations was 3.5°C (Table 8), which was 0.5°C cooler than the haul-based mean SST in 2022 (4.0°C), the same as the 2006-2022 historical mean (3.5°C), and 0.2°C cooler than the long-term 1980-2022 historical mean at haul locations (3.7°C). Relative to the 2006-2022 period, mean SST anomalies from both sources in 2023 were near 0°C, indicating average conditions (Fig. 17). Mean temperature between the surface and deepest trawl (i.e. headrope) depth at all haul locations varied by approximately 2°C (Fig. 18).

Trawl catch summary

Biological data and specimens were collected in Shelikof Strait from 16 LFS1421 hauls (Table 8, Fig. 15) targeted on backscatter. The lengths of an average of 302 randomly selected pollock were measured from each haul, with an average of 39 individuals more extensively sampled for at least one of the following: body weight, maturity, and age

(Table 9). A total of 579 otoliths used to estimate pollock ages were collected in the Shelikof Strait, and a total of 4,535 pollock lengths were measured (Table 9). Pollock lengths ranged from 11 to 64 cm FL.

Pollock and magistrate armhook squid (*Berryteuthis magister*) were the most abundant species by weight in the LFS1421 hauls, contributing 82.2% and 6.2% of the total catch by weight respectively (Table 10). Eulachon (*Thaleichthys pacificus*) and northern smoothtongue (*Leuroglossus schmidti*) were the most abundant species by numbers with 31.4% and 19.8% of the total catch by numbers, respectively (Table 10).

Pollock maturity

While 81% of male pollock > 40 cm FL were in the spawning/spent maturity stages, less than 10% of the female pollock in Shelikof Strait were in the spawning/spent maturity stages, suggesting that the timing of the 2023 Shelikof Strait survey relative to the spawning period was appropriate. The maturity composition of females > 40 cm FL (n = 373) was 1% immature, 1% developing, 94% pre-spawning, 5% spawning, and 0% spent, while the maturity composition of males > 40 cm FL (n = 325) was 0% immature, 1% developing, 18% pre-spawning, 78% spawning, and 3% spent (Fig. 19A). The length at which 50% of female pollock were determined to be reproductively mature (i.e., pre-spawning, spawning, or spent) was 39.5 cm FL (Fig. 19B). The average GSI from 193 pre-spawning females was 0.13 $\pm$ 0.01 (Fig. 19C, mean $\pm$ standard deviation), which was within 1 standard deviation of the 2022 estimate (0.15 $\pm$ 0.03) and the historical mean (0.13 $\pm$ 0.03) from 2008 to 2022.

Distribution and abundance

Pollock were detected throughout the Strait. Pollock (> 30 cm FL) were detected in moderate density layers near the seafloor (Fig. 20). Pollock were more concentrated on the Alaska Peninsula side of the Strait with high densities centered off Cape Kekurnoi where large numbers of pre-spawning fish have been observed during most previous Shelikof surveys. Pollock (≤ 30 cm FL) were found mixed with larger pollock rather than separated in a different layer. The COG for pollock biomass shifted 17.5 km to the east and 29.7 km to the north from the 2022 distribution (McGowan et al., 2024), continuing a 24.9 km shift to the west and 8.4 km shift to the south from the historical mean COG between 2008 and 2022 (Fig. 21).

Generally, most pollock were detected between depths of 185-285 m (Fig. 22A-B). Larger pollock (> 30 cm FL) depth distributions in 2023 were similar to the distributions observed in 2021-2022, whereas the smaller pollock (≤ 30 cm FL) were more variable in 2021-2022. The HAB analysis indicated that all pollock were primarily observed within 55 m of the seafloor in 2023, which was similar for the larger pollock in 2021-2022 but more variable for the smaller pollock 2021-2022 (Fig. 22C-D).

A total of 287.4 million pollock weighing 258,109.5 t were estimated to be in Shelikof Strait at the time of the survey (Tables 11, 12). The 2023 biomass decreased 29.4% from that observed in 2022 (365,409 t) and was 36.9% of the historical mean of 699.8 thousand tons (Table 11, Fig. 23). The 2023 survey biomass estimate is the lowest since 2009 (Fig. 23). The relative estimation error of the 2023 biomass estimate based on the 1-D geostatistical analysis was 4.8% (Table 11).

Pollock in Shelikof Strait were primarily composed of fish > 30 cm FL. The modal length at 48 cm was the dominant length by weight (Table 13, Fig. 24), and the population was primarily composed of 5 and 11 year-old fish from the 2018 and 2012 year classes respectively. These ages accounted for 30% and 23% of total biomass, respectively (Table 14, Fig. 25). In 2021, age-1 pollock were particularly numerous but, as age-3 in 2023, these fish represented only 2.8% of the population by number and were a minor component of the biomass (1.1%) (Tables 12 - 15, Figs. 24, 25). This is a notable decline in numbers and biomass of the 2021 year class from the 2022 survey (McGowan et al. 2024), when they were numerous as age-2s (Tables 14, 15, Figs. 26, 27). In addition, very few age-1 pollock (< 17 cm FL, 2022 year class) were observed in 2023 (Figs. 24, 25). Pollock that were age-12 and older in 2023 were shorter and lighter than those from previous surveys conducted in 2008–2022 (Fig. 28).

Effects of net selectivity corrections and estimated strength of 2022 year class

There were relatively minor effects in pollock abundance by not invoking a selectivity correction. The no-selectivity analysis generated an overall increase of 2.1% by numbers (to 293 million) and an increase of 2.3% by weight (to 263,977 t) for pollock in the Shelikof Strait area compared to the primary analysis (i.e., “selectivity corrected”, Fig. 29). Escapement corrections for smaller organisms changes the relative proportions between the smaller organisms and the larger organisms, giving more emphasis to the corrected smaller

organisms thereby decreasing the numbers and biomass for the larger pollock in the biomass estimate.

Historic population trends in Shelikof Strait as observed by winter pre-spawning AT surveys track the strong year classes well through time starting from relatively small sizes and young ages (Figs. 26, 27). McKelvey (1996) showed that there was a strong relationship between the estimated number of age-1 pollock from the winter Shelikof Strait survey and year-class strength for GOA pollock. The McKelvey index is based on data that did not include a correction for escapement of age-1 pollock, therefore, the 2023 non-selectivity based estimate (Analysis 2) was used to classify the strength of the 2022 year class (age-1 pollock observed in 2023) in the context of the McKelvey index. This estimate was < 1 million age-1 pollock, which is considered a low or weak year class based on the McKelvey index.

Chirikof Shelfbreak

Survey timing and extent

The 2023 winter AT survey of pre-spawning pollock in Chirikof shelfbreak was conducted between 12 and 15 March. The entire survey area encompassed 3,745 km^2 (1,092 nmi^2). Acoustic backscatter was measured along 329.3 km (177.8 nmi) of transects spaced 11.1 km (6 nmi) apart (Fig. 15). Bottom depths in the survey area ranged from 77 m to 1291 m.

Environmental conditions

Sea surface temperatures (SST) measured at Chirikof shelfbreak in 2023 indicate relatively average thermal conditions during the survey. SST ranged from 4.1°C to 4.8°C as measured by the ship's flow-through instrumentation along acoustic transects and averaged 4.5°C (Fig. 16). The along-transect mean SST was 1.1°C cooler than observed during 2019 and 0.1°C warmer than the 2006-2019 historical mean (4.5°C). The average SST measured by the SBE 39 at all haul locations was 4.5°C (Table 8), which was 1.1°C cooler than the haul-based mean SST in 2019, and 0.1°C warmer than the long-term 2002-2019 historical mean. Mean temperature between the surface and deepest trawl (i.e., headrope) depth at all haul locations varied by approximately 0.8°C (Fig. 18).

Trawl catch summary

Biological data and specimens were collected in Chirikof shelfbreak from 6 LFS1421 hauls (Tables 8, 9; Fig. 15) targeted on backscatter. The lengths of an average of 202 randomly selected pollock were measured from each haul, with individuals more extensively sampled for at least one of the following: body weight, maturity, and age (Table 9). A total of 185 otoliths to estimate pollock ages were collected in the Chirikof shelfbreak area and 1,209 pollock lengths were measured (Table 9). Pollock lengths ranged from 30 to 62 cm FL. Only one small pollock (30 cm) was captured in the Chirikof shelfbreak area.

Pacific ocean perch (*Sebastes alutus*) and pollock were the most abundant species by weight in the LFS1421 hauls, contributing 64.1% and 34.5% of the total catch by weight, respectively (Table 16). Euphausiids (family Euphausiidae) and Pacific ocean perch were the most abundant species by numbers with 55% and 22% of the total catch by numbers, respectively (Table 16).

Pollock maturity

Ten percent of the Chirikof shelfbreak female pollock > 40 cm FL were in the spawning/spent maturity stages, which suggests that the timing of the 2023 Chirikof shelfbreak survey relative to the spawning period was marginally appropriate (< 10% is ideal). The maturity composition of females > 40 cm FL (n = 109) was 2% immature, 19% developing, 70% pre-spawning, 10% spawning, and 0% spent, while the maturity composition of males > 40 cm FL (n = 84) was 3% immature, 4% developing, 8% pre-spawning, 80% spawning, and 5% spent (Fig. 30A). The length at which 50% of female pollock were determined to be reproductively mature (i.e., pre-spawning, spawning, or spent) was 39.7 cm FL (Fig. 30B). The average GSI from 46 pre-spawning females was 0.12 ± 0.01 (Fig. 30C, mean $\pm$ standard deviation), which was within 1 standard deviation of the 2019 estimate (0.14 ± 0.02) and the historical mean (0.14 ± 0.01) from 2008 to 2019.

Distribution and Abundance

Large pollock (defined as > 30 cm FL) were detected across the Chirikof shelfbreak area (Fig. 20). As in previous years large pollock were often caught intermixed with Pacific ocean perch and in similar schooling aggregations.

A total of 69.6 million pollock weighing 39,874.7 t were estimated to be at the Chirikof shelfbreak at the time of the survey (Table 11). The 2023 biomass increased 302.5% from that observed in 2019 (9,907 t) and was 119.7% of the historical mean of 33.3 thousand tons (Table 11). The 2023 survey biomass estimate is the highest since 2013, while the relative estimation error of the 2023 biomass estimate based on the 1-D geostatistical analysis was 11.5%, which is the lowest reported in the Chirikof shelfbreak time series since 2008 (Table 11). Most all of the pollock in the Chirikof shelfbreak area were > 30 cm FL; pollock measuring 44 cm FL were most abundant by number and weight (Fig. 24).

Marmot Bay

Survey timing and extent

The 2023 winter AT survey of pre-spawning pollock in Marmot Bay was conducted between 15 and 17 March. The entire survey area encompassed 1,010 km^2 (294 nmi^2). Acoustic backscatter was measured along 341.1 km (184.2 nmi) of transects spaced mainly 3.7 km (2 nmi) apart, with spacing varying from 1.9 to 3.7 km (1 to 2 nmi) in the survey area (Fig. 15). Bottom depths in the survey area ranged from 78 to 279 m.

Environmental conditions

Sea surface temperatures (SST) measured in Marmot Bay in 2023 indicate relatively average thermal conditions during the survey. SST ranged from 3.7°C to 4.4°C as measured by the ship's flow-through instrumentation along acoustic transects and averaged 4°C (Fig. 16). The along-transect mean SST was 0.2°C cooler than observed during 2021 and 0.6°C cooler than the 2009–2021 historical mean (4.6°C). The average SST measured by the SBE 39 at all haul locations was 3.8°C (Table 8), which was 0.2°C cooler than the haul-based mean SST in 2021, and 0.3°C cooler than the 2007-2021 historical mean. Mean temperature between the surface and deepest trawl (i.e. headrope) depth at all haul locations varied by approximately 0.3°C (Fig. 18).

Trawl catch summary

Biological data and specimens were collected in Marmot Bay from 5 LFS1421 hauls (Tables 8, 9, Fig. 15) targeted on backscatter. The lengths of an average of 386 randomly selected pollock were measured from each haul, with an average of 42 individuals more

extensively sampled for at least one of the following: body weight, maturity, and age (Table 9). A total of 212 otoliths used to estimate pollock ages were collected in the Marmot Bay area and a total of 1,930 pollock lengths were measured (Table 9). Pollock lengths ranged from 10 to 62 cm FL.

Pollock and Pacific cod were the most abundant species by weight in the LFS1421 hauls, contributing 99.1% and 0.3% of the total catch by weight, respectively (Table 17). Pollock and smelt were the most abundant species by numbers with 86.8% and 5.8% of the total catch by numbers, respectively (Table 17).

Pollock maturity

Most female pollock > 40 cm FL in Marmot Bay were in the pre-spawning stage of maturity and substantially fewer were spawning or spent, which suggests that the timing of the 2023 Marmot Bay survey relative to the spawning period was appropriate. The maturity composition of females > 40 cm FL (n = 44) was 8% immature, 26% developing, 58% pre-spawning, 0% spawning, and 8% spent, while the maturity composition of males > 40 cm FL (n = 27) was 47% immature, 0% developing, 0% pre-spawning, 47% spawning, and 7% spent (Fig. 32B). The length at which 50% of female pollock were determined to be reproductively mature (i.e., pre-spawning, spawning, or spent) was 46.1 cm FL (Fig. 32B). The average GSI from 12 pre-spawning females was 0.11 ± 0.02 (Fig. 32C, mean $\pm$ standard deviation), which was within 1 standard deviation of the 2021 estimate (0.10 ± 0.02) and the historical mean (0.13 ± 0.01) from 2009 to 2021.

Distribution and Abundance

Pollock were detected throughout Marmot Bay, with the largest aggregations concentrated in the northeast portion of the inner Bay and in the Spruce Gully area. Pollock were observed in inner Marmot Bay as low-density, near-bottom backscatter layers of mixed sizes, periodically topped with very dense midwater schools at ~50 m depths comprising mostly of pollock < 30 cm FL. Near bottom, mixed size, backscatter layers were somewhat denser in Spruce Gully, with diffuse near-surface backscatter comprising the smaller pollock (Fig. 20). Small pollock were also observed in outer Marmot Bay.

Most pollock > 30 cm FL (86% of large pollock biomass) were detected between depths of 45-225 m (Fig. 33A). Most of the pollock ≤ 30 cm FL (87% of small pollock biomass) were

between depths of 45-125 m (Fig. 33B). The 'bottom-referenced' analysis indicated that large and small pollock were observed within 145 m of the seafloor (Fig. 33C, D), and were shallower than the distributions observed in 2021.

A total of 62.6 million pollock weighing 9,284.4 t were estimated to be in Marmot Bay at the time of the survey (Table 11). The 2023 biomass increased 25.5% from that observed in 2021 (7,401 t) and was 63.7% of the historical mean of 14.6 thousand tons (Table 11). The 2023 survey biomass estimate is the highest since 2018, while the relative estimation error of the 2023 biomass estimate based on the 1-D geostatistical analysis was 8.3 (Table 11).

The length composition in Marmot Bay consisted of small and large pollock. Presumed age-1 pollock (modal length ~12 cm FL, 2022 year class) dominated in terms of numbers (57%) and accounted for 3.9% of the biomass. Presumed age-2 pollock (modal length ~25 cm FL, 2021 year class) accounted for 18% of the total numbers and 14% of the biomass. Large pollock > 30 cm FL dominated in terms of weight, accounting for 79% of total biomass in Marmot Bay (Fig. 24).

ACKNOWLEDGMENTS

The authors would like to thank the officers and crew of the NOAA ship *Oscar Dyson* for their dedication and contribution to the successful completion of this work. Thanks also to AFSC scientists for their invaluable assistance with fish processing, data collection, and data analysis.

CITATIONS

Bodholt, H. 2002. The effect of water temperature and salinity on echo sounder measurements. ICES Symposium on Acoustics in Fisheries, Montpellier, France, 10–14 June 2002.

Bodholt, H., and H. Solli. 1992. Split beam techniques used in Simrad EK500 to measure target strength. Pages 16–31 *In* World Fisheries Congress. May 1992, Athens, Greece.

De Robertis, A., D. R. McKelvey, and P. H. Ressler. 2010. Development and application of an empirical multifrequency method for backscatter classification. Can. J. Fish. Aquat. Sci. 67:1459–1474.

De Robertis, A., and K. Taylor. 2014. *In situ* target strength measurements of the scyphomedusa *Chrysaora melanaster*. Fish. Res. 153:18–23.

De Robertis, A., K. Taylor, K. Williams, and C. D. Wilson. 2017a. Species and size selectivity of two midwater trawls used in an acoustic survey of the Alaska Arctic. Deep Sea Res. Part II 135:40–50.

De Robertis, A., K. Taylor, C. D. Wilson, and E. V. Farley. 2017b. Abundance and distribution of Arctic cod (*Boreogadus saida*) and other pelagic fishes over the U.S. continental shelf of the northern Bering and Chukchi Seas. Deep Sea Res. Part II 135:51–65.

De Robertis, A., and K. Williams. 2008. Weight-length relationships in fisheries studies: The standard allometric model should be applied with caution. Trans. Am. Fish. Soc. 137:707–719.

Demer, D. A., L. Berger, M. Bernasconi, E. Bethke, K. Boswell, D. Chu, R. Domokos, A. Dunford, S. Fässler, S. Gauthier, L. T. Hufnagle, J. M. Jech, N. Bouffant, A. Lebourges-Dhaussy, X. Lurton, G. J. Macaulay, Y. Perrot, T. Ryan, S. Parker-Stetter, S. Stienessen, T. Weber, and N. Williamson. 2015. Calibration of acoustic instruments. ICES Coop. Res. Rep. 326. 133p.

Demer, D. A., and S. G. Conti. 2005. New target-strength model indicates more krill in the Southern Ocean. ICES J. Mar. Sci. 62:25–32.

Duong, T. 2022. Ks: Kernel smoothing. R package version 1.13.4. https://CRAN.R-project.org/package=ks

Foote, K. G. 1987. Fish target strengths for use in echo integrator surveys. J. Acoust. Soc. Am. 82:981–987.

Foote, K. G., H. P. Knudson, G. Vestnes, and E. J. Simmonds. 1987. Calibration of acoustic instruments for fish density estimation: A practical guide. ICES Coop. Res. Rep. 144:69.

Foote, K. G., and J. J. Traynor. 1988. Comparisons of walleye pollock target strength estimates determined from *in situ* measurements and calculations based on swimbladder form. J. Acoust. Soc. Am. 83:9–17.

Gauthier, S., and J. K. Horne. 2004. Acoustic characteristics of forage fish species in the Gulf of Alaska and Bering Sea based on Kirchhoff-approximation models. Can. J. Fish. Aquat. Sci. 61:1839–1850.

Guttormsen, M. A., and C. D. Wilson. 2009. *In situ* measurements of capelin (*Mallotus villosus*) target strength in the North Pacific Ocean. ICES J. Mar. Sci. 66:258–263.

Honkalehto, T., A. McCarthy, M. Levine, D. Jones, and K. Williams. 2024. Results of the acoustic-trawl survey of walleye pollock (*Gadus chalcogrammus*) in Shelikof Strait and Marmot Bay March 2021 (DY-202102). AFSC Processed Rep. 2024-09, 68 p. Alaska Fish. Sci. Cent., NOAA, Natl. Mar. Fish. Serv., 7600 Sand Point Way NE, Seattle WA 98115.

Jech, J. M., K. G. Foote, D. Chu, and L. C. Hufnagle. 2005. Comparing two 38-kHz scientific echosounders. ICES J. Mar. Sci. 62:1168–1179.

Jones, D. T., A. De Robertis, and N. J. Williamson. 2011. Statistical combination of multi-frequency sounder-detected bottom lines reduces bottom integrations. U.S. Dep. Commer., NOAA Tech Memo. NMFS-AFSC-219:13 p.

Jones, D. T., N. E. Lauffenburger, K. Williams, and A. De Robertis. 2019. Results of the acoustic-trawl survey of walleye pollock (*Gadus chalcogrammus*) in the Gulf of Alaska, June-August 2017 (DY2017-06). AFSC Processed Rep. 2019-08, 110 p. Alaska Fish. Sci. Cent., NOAA, Natl. Mar. Fish. Serv., 7600 Sand Point Way NE, Seattle WA 98115.

Jones, D. T., M. Levine, K. Williams, and A. De Robertis. 2022. Results of the acoustic-trawl survey of walleye pollock (*Gadus chalcogrammus*) in the Gulf of Alaska, May-August 2019 (DY2019-06). AFSC Processed Rep. 2022-07, 118 p. Alaska Fish. Sci. Cent., NOAA, Natl. Mar. Fish. Serv., 7600 Sand Point Way NE, Seattle WA 98115.

Kang, D., T. Mukai, K. Iida, D. Hwang, and J.-G. Myoung. 2005. The influence of tilt angle on the acoustic target strength of the Japanese common squid (*Todarodes pacificus*). ICES J. Mar. Sci. 62:779–789.

Lauffenburger, N., K. Williams, and D. Jones. 2019. Results of the acoustic-trawl surveys of walleye pollock (*Gadus chalcogrammus*) in the Gulf of Alaska, March 2019 (SH2019-04). AFSC Processed Rep. 2019-10, 76 p. Alaska Fish. Sci. Cent., NOAA, Natl. Mar. Fish. Serv., 7600 Sand Point Way NE, Seattle WA 98115.

Levine, M., D. Jones, and D. McGowan. 2024. Results of the acoustic-trawl survey of walleye pollock (*Gadus chalcogrammus*) in the Gulf of Alaska, June-July 2021 (DY2021-04). AFSC Processed Rep. 2024-07, 100 p. Alaska Fish. Sci. Cent., NOAA, Natl. Mar. Fish. Serv., 7600 Sand Point Way NE, Seattle WA 98115.

MacLennan, D. N., P. G. Fernandes, and J. Dalen. 2002. A consistent approach to definitions and symbols in fisheries acoustics. ICES J. Mar. Sci. 59:365–369.

McCarthy, A., M. Levine, and D. Jones. 2022. Results of the acoustic-trawl surveys of walleye pollock (*Gadus chalcogrammus*) in the Shumagin Islands and Shelikof Strait, February and March 2020 (DY-202001 and DY-202003). AFSC Processed Rep. 2022-08, 78 p. Alaska Fish. Sci. Cent., NOAA, Natl. Mar. Fish. Serv., 7600 Sand Point Way NE, Seattle WA 98115.

McGowan, D., D. Jones, M. Levine, and A. McCarthy. 2024. Results of the acoustic-trawl survey of walleye pollock (*Gadus chalcogrammus*) in the Shelikof Strait, March 2022 (DY2022-04). AFSC Processed Rep. 2024-04, 66 p. Alaska Fish. Sci. Cent., NOAA, Natl. Mar. Fish. Serv., 7600 Sand Point Way NE, Seattle WA 98115.

McKelvey, D. R. 1996. Juvenile walleye pollock, *Theragra chalcogramma*, distribution and abundance in Shelikof Strait—what can we learn from acoustic surveys. Ecology of juvenile walleye pollock, *Theragra chalcogramma*. U.S. Dep. Commer., NOAA Tech. Rep. NMFS 126.

Miller, D. M. 1984. Reducing transformation bias in curve fitting. Am. Stat. 38:124–126.

MINES ParisTech / ARMINES. 2021. RGeostats: The Geostatistical R Package. MINES ParisTech / ARMINES; Free download from: http://cg.ensmp.fr/rgeostats, Fontainebleau, France.

Ona, E. 2003. An expanded target-strength relationship for herring. ICES J. Mar. Sci. 60:493–499.

Ona, E., and R. B. Mitson. 1996. Acoustic sampling and signal processing near the seabed: The deadzone revisited. ICES J. Mar. Sci. 53:677–690.

Petitgas, P. 1993. Geostatistics for fish stock assessments: A review and an acoustic application. ICES J. Mar. Sci. 50:285–298.

R Core Team. 2021. R: A language and environment for statistical computing. R Foundation for Statistical Computing, Vienna, Austria.

Rivoirard, J., J. Simmonds, K. G. Foote, P. Fernandes, and N. Bez. 2000. Geostatistics for estimating fish abundance. Blackwell Science Ltd, Oxford, UK. 206 p.

Simmonds, E. J., and D. N. MacLennan. 2005. Fisheries acoustics: Theory and practice. 2nd edition. Blackwell Science Ltd, Oxford, UK. 473 p.

Simrad. 2018. Reference manual for Simrad EK80 scientific echo sounder application. Strandpromenenaden 50, Box 111, N-3191 Horten, Norway.

Stienessen, S. C., N. Lauffenburger, and A. De Robertis. 2019. Results of the acoustic-trawl surveys of walleye pollock (*Gadus chalcogrammus*) in the Gulf of Alaska, February-March 2018 (DY2018-01 and DY2018-03). AFSC Processed Rep. 2019-05, 109 p. Alaska Fish. Sci. Cent., NOAA, Natl. Mar. Fish. Serv., 7600 Sand Point Way NE, Seattle WA 98115.

Towler, R., and K. Williams. 2010. An inexpensive millimeter-accuracy electronic length measuring board. Fish. Res. 106:107–111.

Traynor, J. J. 1996. Target-strength measurements of walleye pollock (*Theragra chalcogramma*) and Pacific whiting (*Merluccius productus*). ICES J. Mar. Sci. 53:253–258.

Walline, P. D. 2007. Geostatistical simulations of eastern Bering Sea walleye pollock spatial distributions, to estimate sampling precision. ICES J. Mar. Sci. 64:559–569.

Williams, K. 2007. Evaluation of the macroscopic staging method for determining maturity of female walleye pollock *Theragra chalcogramma* in Shelikof Strait, Alaska. Alaska Fish. Res. Bull. 12:252–263.

Williams, K., A. E. Punt, C. D. Wilson, and J. K. Horne. 2011. Length-selective retention of walleye pollock, *Theragra chalcogramma*, by midwater trawls. ICES J. Mar. Sci. 68:119–129.

Williams, K., C. N. Rooper, and R. Towler. 2010. Use of stereo camera systems for assessment of rockfish abundance in untrawlable areas and for recording pollock behavior during midwater trawls. Fish. Bull., U.S. 108:352–362.

Williams, K., R. Towler, P. Goddard, R. Wilborn, and C. Rooper. 2016. Sebastes Stereo Image Analysis Software. AFSC Processed Rep. 2016-03, 42 p. Alaska Fish. Sci. Cent., NOAA, Natl. Mar. Fish. Serv., 7600 Sand Point Way NE, Seattle WA 98115.

Williamson, N. J., and J. J. Traynor. 1996. Application of a one-dimensional geostatistical procedure to fisheries acoustic surveys of Alaskan pollock. ICES J. Mar. Sci. 53:423–428.

Woillez, M., J.-C. Poulard, J. Rivoirard, P. Petitgas, and N. Bez. 2007. Indices for capturing spatial patterns and their evolution in time, with application to European hake (*Merluccius merluccius*) in the Bay of Biscay. ICES J. Mar. Sci. 64:537–550.

TABLES

Table 1. -- Simrad EK80 38 kHz acoustic system description and settings used during the 2023 winter acoustic-trawl surveys. These include environmental parameters and results from standard sphere acoustic system calibrations conducted in association with the survey and final values used to calculate biomass and abundance data. The collection settings column contains 12 February 2023 EK80 calibration utility results. Other columns are a combination of on-axis and EK80 calibration utility results (see Methods and Results and Discussion sections of text for details).

2023	Survey collection settings	12 February Uyak Bay Kodiak Is.	13 March Kaiugnak Bay Kodiak Is.	Final analysis settings
Echosounder	Simrad EK80	--	--	Simrad EK80
Transducer	ES38-7 s/n 324	--	--	ES38-7 s/n 324
Frequency (kHz)	38.00	--	--	38.00
Transducer depth (m)	9.15	--	--	9.15
Pulse length (ms)	1.024	--	--	1.024
Transmitted power (W)	2000	--	--	2000
Angle sensitivity along	18.00	--	--	18.00
Angle sensitivity athwart	18.00	--	--	18.00
2-way beam angle (dB re 1 steradian)	-20.70	--	--	-20.52
Gain (dB)	27.17	27.09	27.12	27.11
S_a correction (dB)	-0.04	-0.04	-0.04	-0.04
Integration gain (dB)	27.13	27.05	27.08	27.06
3 dB beamwidth along	6.42	6.42	6.48	6.45
3 dB beamwidth athwart	6.54	6.54	6.53	6.54
Angle offset along	-0.03	-0.03	-0.04	-0.04
Angle offset athwart	0.07	0.07	0.06	0.07
Post-processing S_v threshold (dB re 1 m^{-1})	-70.00	--	--	-70.00
Standard sphere TS (dB re 1 m^2)		-42.17	-42.25	
Sphere range from transducer (m)		24.68	24.95	
Absorption coefficient (dB m^{-1})	0.00986	0.00984	0.00997	0.00986
Sound velocity (ms^{-1})	1466.0	1466.0	1463.4	1466.0
Water temp at transducer (°C)	4.0	4.66	3.97	4.0

Note: Gain and beam pattern terms are defined in the Operator Manual for Simrad EK80 Scientific Echosounder Application, which is available from Simrad Strandpromenaden 50, Box 111, N-3191 Horten, Norway.
-- symbol indicates the same values for the system settings and final analysis are also applicable for the various calibrations.

Table 2. -- Trawl stations and catch data summary from the 2023 acoustic-trawl survey of walleye pollock in the Shumagin Islands, Pavlof Bay, and Morzhovoi Bay areas.

Haul	Area	Gear	Date	Time	Duration	Start Position		Depth (m)		Temp (°C)		walleye pollock		Other
No.		Type[a]	(GMT)	(GMT)	(mins)	Lat. (N)	Long. (W)	Headrope[b]	Bottom	Headrope	Surface[c]	(kg)	Number	(kg)
1	Shumagin Islands	LFS1421	15-Feb	22:52	2.6	55.4301	-160.5865	75	132	4.5	3.5	1,084.0	4,368	0.1
2	Shumagin Islands	LFS1421	16-Feb	03:10	2.7	55.5719	-160.2627	132	188	5.2	3.5	2,810.0	12,408	0.0
3	Shumagin Islands	LFS1421	16-Feb	06:35	11.9	55.7514	-159.7807	78	127	4.7	3.5	1,277.8	3,459	4.0
4	Shumagin Islands	LFS1421	16-Feb	23:51	0.3	55.2299	-160.4004	-	174	-	3.8	3,898.2	12,737	1.8
5	Shumagin Islands	LFS1421	17-Feb	03:27	14.3	55.2237	-160.1812	184	219	4.4	4.0	812.9	2,273	9.1
6	Pavlof Bay	LFS1421	17-Feb	22:28	14.2	55.2979	-161.7458	91	117	3.6	3.3	3,600.0	10,727	-
7	Morzhovoi Bay	LFS1421	18-Feb	22:58	19.0	54.9173	-162.9745	89	113	3.3	3.1	384.4	512	36.5
8	Shumagin Islands	LFS1421	20-Feb	01:21	26.7	55.2747	-159.1149	160	188	5.5	4.3	182.2	13,157	6.9
9	Shumagin Islands	LFS1421	20-Feb	05:40	4.1	55.1932	-158.8498	161	201	5.5	4.3	122.5	9,297	129.7
10	Shumagin Islands	LFS1421	20-Feb	23:50	10.8	55.0887	-158.6212	178	209	5.6	4.4	99.8	7,573	31.6

[a]LFS1421 = LFS1421 midwater trawl.

[b]Headrope depth obtained from SBE temperature logger. In hauls without SBE temperature logger records, depth was obtained from scientist notes when possible.

[c]Average temperature measured from an SBE temperature logger.

Table 3. -- Numbers of walleye pollock measured and biological samples collected during the winter 2023 acoustic-trawl survey of Shumagin Islands, Pavlof Bay, and Morzhovoi Bay areas.

Haul no.	Area name	Catch lengths	Weights	Maturities	Otoliths	Ovary weights	Ovaries collected
1	Shumagin Islands	303	49	49	49	1	19
2	Shumagin Islands	326	51	51	51	2	7
3	Shumagin Islands	316	50	50	50	4	9
4	Shumagin Islands	349	55	55	50	-	6
5	Shumagin Islands	415	83	58	56	4	6
6	Pavlof Bay	430	77	57	55	-	4
7	Morzhovoi Bay	392	77	57	55	3	6
8	Shumagin Islands	148	70	50	25	-	-
9	Shumagin Islands	104	33	14	19	-	-
10	Shumagin Islands	92	19	-	5	-	-
Total		2,875	564	441	415	14	57

Table 4. -- Catch by species and numbers of length and weight measurements taken from 8 LFS1421 hauls during the 2023 acoustic-trawl survey of walleye pollock in Shumagin Islands.

		Catch				Measurements	
Species name	Scientific name	Weight (kg)	%	Number	%	Length	Weight
walleye pollock	*Gadus chalcogrammus*	10,287.3	98.2	65,272	95.2	2,053	410
salmon shark	*Lamna ditropis*	106.0	1.0	1	< 0.1	1	1
big skate	*Beringraja binoculata*	25.6	0.2	1	< 0.1	1	1
Pacific capelin	*Mallotus catervarius*	22.3	0.2	2,494	3.6	116	42
Pacific cod	*Gadus macrocephalus*	10.5	0.1	4	< 0.1	4	4
Chinook salmon	*Oncorhynchus tshawytscha*	7.7	< 0.1	6	< 0.1	5	5
eulachon	*Thaleichthys pacificus*	4.7	< 0.1	157	0.2	48	26
arrowtooth flounder	*Atheresthes stomias*	3.8	< 0.1	8	< 0.1	8	8
squid unid.	Cephalopoda (class)	2.3	< 0.1	335	0.5	46	23
Alaskan pink shrimp	*Pandalus eous*	0.2	< 0.1	106	0.2	11	-
Pacific herring	*Clupea pallasii*	0.2	< 0.1	6	< 0.1	4	4
isopod unid.	Isopoda (order)	< 0.1	< 0.1	90	0.1	-	-
smelt unid.	Osmeridae (family)	< 0.1	< 0.1	55	< 0.1	14	-
Total		10,470.6		68,535		2,311	524

Table 5. -- Estimates of walleye pollock biomass (thousands of metric tons) and relative estimation error for the Shumagin Islands, Sanak Trough, Morzhovoi Bay, and Pavlof Bay areas. Estimates for 2009-2023 reflect selectivity corrections for escapement of small fish. Blank values indicate no survey or estimation error was completed within a given area and year.

Year	Shumagin Islands		Sanak Trough		Morzhovoi Bay		Pavlof Bay	
	Biomass	Est. error	Biomass	Est. error	Biomass	Est. error	Biomass	Est. error
1994	112.0[1]							
1995	290.1							
1996	117.7[2]							
1997								
1998								
1999								
2000								
2001	119.6							
2002	135.6	27.1%						
2003	67.7	17.2%	80.5	21.6%				
2004								
2005	52.0	11.4%	65.5	7.4%				
2006	37.3	10.1%	127.2	10.4%	11.7	15.1%		
2007	20.0	8.6%	60.3	5.7%	2.5	15.1%		
2008	30.6	9.8%	19.8	6.7%				
2009	55.4	10.8%	31.4	17.4%				
2010	18.2	11.6%	27.0	11.6%	1.8		0.2	
2011								
2012	15.5	5.2%	24.3	15.6%				
2013	63.0	17.3%	13.3	5.1%	2.1	11.6%		
2014	35.5	18.2%	7.3	9.0%				
2015	61.3	17.1%	17.9	10.0%				
2016	20.8	7.2%	3.6	6.9%	11.5	12.0%	2.1	14.7%
2017	29.8	9.8%	0.8	19.6%	3.9	6.5%	2.1	9.5%
2018	17.4	8.3%	1.3	12.2%	3.8	23.0%	4.6	19.9%
2019								
2020	4.9	12.2%						
2021								
2022								
2023	48.9	8.7%			4.0	5.4%	5.5	13.6%

[1]Survey conducted after peak spawning had occurred.

[2]Partial survey.

Table 6. -- Catch by species and numbers of length and weight measurements taken from 1 LFS1421 haul during the 2023 acoustic-trawl survey of walleye pollock in Pavlof Bay.

		Catch				Measurements	
Species name	Scientific name	Weight (kg)	%	Number	%	Length	Weight
walleye pollock	*Gadus chalcogrammus*	3,600.0	100.0	10,727	100.0	430	77
Total		3,600.0		10,727		430	77

Table 7. -- Catch by species and numbers of length and weight measurements taken from 1 LFS1421 haul during the 2023 acoustic-trawl survey of walleye pollock in Morzhovoi Bay.

		Catch				Measurements	
Species name	Scientific name	Weight (kg)	%	Number	%	Length	Weight
walleye pollock	*Gadus chalcogrammus*	384.4	91.3	512	82.6	392	77
Pacific cod	*Gadus macrocephalus*	35.6	8.5	7	1.1	7	7
Pacific capelin	*Mallotus catervarius*	0.7	0.2	99	16.0	35	10
jellyfish unid.	Scyphozoa (class)	0.1	< 0.1	-	< 0.1	-	-
squid unid.	Cephalopoda (class)	< 0.1	< 0.1	2	0.3	2	-
Total		420.9		620		436	94

Table 8. -- Trawl stations and catch data summary from the 2023 acoustic-trawl survey of walleye pollock in the Shelikof Strait, Chirikof shelfbreak, and Marmot Bay areas.

Haul	Area	Gear	Date	Time	Duration	Start Position		Depth (m)		Temp (°C)		walleye pollock		Other
No.		Type[a]	(GMT)	(GMT)	(mins)	Lat. (N)	Long. (W)	Headrope[b]	Bottom	Headrope	Surface[c]	(kg)	Number	(kg)
1	Shelikof Strait	LFS1421	5-Mar	19:01	30.1	58.2194	-153.3396	196	204	5.6	3.9	612.9	787	1,018.8
2	Shelikof Strait	LFS1421	6-Mar	06:12	12.6	58.0652	-154.1971	237	264	5.5	3.0	995.3	1,073	233.3
3	Shelikof Strait	LFS1421	6-Mar	12:38	20.1	57.7892	-154.2018	193	216	5.5	3.5	1,198.5	1,267	528.7
4	Shelikof Strait	LFS1421	6-Mar	17:33	12.8	57.9463	-154.6131	190	237	5.5	3.2	592.3	722	142.7
5	Shelikof Strait	LFS1421	7-Mar	02:31	7.0	57.7737	-154.9537	249	293	5.5	3.6	2,016.8	2,400	79.8
6	Shelikof Strait	LFS1421	7-Mar	06:51	5.8	57.7267	-155.2183	250	288	5.4	2.7	2,596.9	3,332	106.3
7	Shelikof Strait	LFS1421	7-Mar	17:06	5.2	57.4865	-155.4826	266	298	5.4	3.1	1,343.3	1,601	99.5
8	Shelikof Strait	LFS1421	8-Mar	02:23	4.2	57.3574	-155.5840	254	285	5.4	3.4	4,318.8	3,886	149.6
9	Shelikof Strait	LFS1421	8-Mar	09:04	5.2	57.2348	-155.5257	240	268	5.4	3.1	703.4	704	113.3
10	Shelikof Strait	LFS1421	8-Mar	20:01	18.1	57.0092	-155.9204	247	259	5.5	3.5	287.5	274	76.0
11	Shelikof Strait	LFS1421	9-Mar	04:06	5.8	56.8895	-155.8453	273	304	5.4	3.4	1,051.6	994	48.1
12	Shelikof Strait	LFS1421	9-Mar	18:13	21.6	56.6612	-156.0276	262	299	5.4	3.6	853.9	739	265.5
13	Shelikof Strait	LFS1421	10-Mar	01:49	20.2	56.5199	-156.0445	243	274	5.6	4.0	568.4	610	195.3
14	Shelikof Strait	LFS1421	10-Mar	08:07	30.0	56.4253	-156.1815	239	269	5.6	3.9	506.7	565	68.9
15	Shelikof Strait	LFS1421	11-Mar	02:17	45.6	55.8846	-156.2311	188	220	5.6	4.0	46.0	64	15.0
16	Shelikof Strait	LFS1421	11-Mar	18:40	16.1	55.4851	-156.2029	188	207	5.6	4.3	-	-	682.6
17	Chirikof shelfbreak	LFS1421	12-Mar	05:26	33.5	55.8880	-154.8582	194	409	5.6	4.7	128.9	236	9.0
18	Chirikof shelfbreak	LFS1421	12-Mar	11:16	8.4	56.0045	-154.5449	246	365	5.6	4.5	259.3	480	23.4
19	Chirikof shelfbreak	LFS1421	12-Mar	19:53	20.6	55.9221	-153.8892	353	562	4.7	4.6	244.6	468	213.1
20	Chirikof shelfbreak	LFS1421	13-Mar	03:21	12.1	56.1002	-153.7155	234	271	5.7	4.6	3.2	4	1,084.8
21	Chirikof shelfbreak	LFS1421	14-Mar	20:28	34.5	56.2494	-152.8483	279	510	5.0	4.2	362.4	613	45.6
22	Chirikof shelfbreak	LFS1421	15-Mar	02:15	3.4	56.3584	-152.5030	242	514	5.1	4.4	22.7	31	563.3
23	Marmot Bay	LFS1421	15-Mar	23:50	36.8	58.0270	-152.5011	120	201	4.0	3.7	1,771.4	8,078	5.7
24	Marmot Bay	LFS1421	16-Mar	05:23	10.0	58.0210	-152.3634	175	247	4.0	3.8	1,016.4	1,886	7.8
25	Marmot Bay	LFS1421	16-Mar	10:21	6.2	57.9816	-152.2886	209	285	4.0	3.8	1,301.9	2,665	12.7
26	Marmot Bay	LFS1421	16-Mar	18:19	11.9	57.9342	-151.9660	111	208	4.3	3.8	75.1	5,604	9.2
27	Marmot Bay	LFS1421	17-Mar	02:29	30.0	58.0644	-151.7696	125	166	4.2	4.1	162.2	4,823	4.8

[a]LFS1421 = LFS1421 midwater trawl

[b]Headrope depth obtained from SBE temperature logger. In hauls without SBE temperature logger records, depth was obtained from scientist notes when possible

[c]Average temperature measured from an SBE temperature logger.

Table 9. -- Numbers of walleye pollock measured and biological samples collected during the winter 2023 acoustic-trawl survey of Shelikof Strait, Chirikof shelfbreak, and Marmot Bay areas.

Haul no.	Area name	Catch lengths	Weights	Maturities	Otoliths	Ovary weights	Ovaries collected
1	Shelikof Strait	323	50	50	35	25	18
2	Shelikof Strait	352	51	51	35	15	16
3	Shelikof Strait	301	50	50	35	32	9
4	Shelikof Strait	346	50	50	35	13	7
5	Shelikof Strait	329	50	50	35	4	5
6	Shelikof Strait	326	52	50	37	3	3
7	Shelikof Strait	341	50	50	34	12	4
8	Shelikof Strait	294	49	49	34	5	5
9	Shelikof Strait	316	49	49	34	7	7
10	Shelikof Strait	274	50	50	35	27	12
11	Shelikof Strait	298	51	51	36	3	5
12	Shelikof Strait	304	51	51	39	27	5
13	Shelikof Strait	319	50	50	45	9	15
14	Shelikof Strait	348	51	51	46	3	10
15	Shelikof Strait	64	64	64	64	9	12
17	Chirikof shelfbreak	236	50	50	45	3	11
18	Chirikof shelfbreak	295	50	50	45	15	-
19	Chirikof shelfbreak	341	50	50	30	4	2
20	Chirikof shelfbreak	4	4	4	4	-	1
21	Chirikof shelfbreak	302	50	50	30	20	3
22	Chirikof shelfbreak	31	31	31	31	6	11
23	Marmot Bay	589	48	43	45	2	15
24	Marmot Bay	437	53	53	50	6	12
25	Marmot Bay	482	53	40	44	4	10
26	Marmot Bay	144	69	49	25	1	-
27	Marmot Bay	278	145	118	48	12	14
Total		7,674	1,371	1,304	976	267	212

Table 10. -- Catch by species and numbers of length and weight measurements taken from 16 LFS1421 hauls during the 2023 acoustic-trawl survey of walleye pollock in Shelikof Strait.

		Catch				Measurements	
Species name	Scientific name	Weight (kg)	%	Number	%	Length	Weight
walleye pollock	*Gadus chalcogrammus*	17,692.3	82.2	19,018	19.7	4,535	768
magistrate armhook squid	*Berryteuthis magister*	1,339.5	6.2	4,945	5.1	397	153
eulachon	*Thaleichthys pacificus*	1,198.0	5.6	30,388	31.4	368	159
Pacific ocean perch	*Sebastes alutus*	677.9	3.2	1,035	1.1	93	26
Berry armhook squid	*Gonatus berryi*	225.1	1.0	597	0.6	-	-
northern smoothtongue	*Leuroglossus schmidti*	200.0	0.9	19,168	19.8	419	149
squid unid.	Cephalopoda (class)	68.7	0.3	11,836	12.2	352	94
Chinook salmon	*Oncorhynchus tshawytscha*	49.9	0.2	41	<0.1	39	39
smooth lumpsucker	*Aptocyclus ventricosus*	34.3	0.2	26	<0.1	26	26
Pacific glass shrimp	*Pasiphaea pacifica*	12.6	<0.1	8,755	9.1	104	13
big skate	*Beringraja binoculata*	7.7	<0.1	1	<0.1	1	1
northern sea nettle	*Chrysaora melanaster*	2.9	<0.1	13	<0.1	11	10
arrowtooth flounder	*Atheresthes stomias*	2.0	<0.1	2	<0.1	2	2
rougheye rockfish	*Sebastes aleutianus*	1.5	<0.1	2	<0.1	2	2
lanternfish unid.	Myctophidae (family)	1.0	<0.1	312	0.3	29	20
Pacific capelin	*Mallotus catervarius*	0.6	<0.1	163	0.2	6	6
eelpout unid.	Zoarcidae (family)	0.5	<0.1	23	<0.1	1	1
Pacific lamprey	*Lampetra tridentata*	0.4	<0.1	15	<0.1	13	13
moon jelly	*Aurelia labiata*	0.4	<0.1	<0.1	<0.1	-	-
salmon unid.	Oncorhynchus (genus)	0.3	<0.1	1	<0.1	1	1
sablefish	*Anoplopoma fimbria*	0.2	<0.1	1	<0.1	1	1
isopod unid.	Isopoda (order)	<0.1	<0.1	76	<0.1	-	-
Pacific herring	*Clupea pallasii*	<0.1	<0.1	1	<0.1	1	1
amphipod unid.	Amphipoda (order)	<0.1	<0.1	211	0.2	-	-
fish larvae unid.	Actinopterygii (class)	<0.1	<0.1	41	<0.1	3	3
egg yolk jelly	*Phacellophora camtschatica*	<0.1	<0.1	<0.1	<0.1	-	-
euphausiid unid.	Euphausiacea (order)	<0.1	<0.1	47	<0.1	-	-
blackmouth eelpout	*Lycodapus fierasfer*	<0.1	<0.1	1	<0.1	1	1
Total		21,515.8		96,719		6,405	1,489

Table 11. -- Estimates of walleye pollock biomass (thousands of tons) and relative estimation error for the Shelikof Strait, Chirikof shelfbreak, and Marmot Bay areas. Estimates for 2008-2023 reflect selectivity corrections for escapement of small fish. Blank values indicate no survey or estimation error was completed within a given area and year.

Year	Shelikof Strait		Chirikof shelfbreak		Marmot Bay	
	Biomass	Est. error	Biomass	Est. error	Biomass	Est. error
1981	2,785.7					
1982						
1983	2,278.1					
1984	1,757.1					
1985	1,175.2					
1986	585.7					
1987						
1988	301.7					
1989	290.5				2.4	
1990	374.7					
1991	380.3					
1992	713.4	3.6%				
1993	435.8	4.6%				
1994	492.6	4.5%				
1995	763.6	4.5%				
1996	777.2	3.7%				
1997	583.0	3.7%				
1998	504.8	3.8%				
1999						
2000	448.6	4.6%				
2001	432.7	4.5%				
2002	256.7	6.9%	82.1	12.2%		
2003	317.3	5.2%	31.0	20.7%		
2004	330.8	9.2%	30.0	20.4%		
2005	356.1	4.1%	77.0	20.7%		
2006	293.6	4.0%	69.0	11.0%		
2007	180.9	5.8%	37.0	6.7%	3.6	5.0%
2008	197.5	5.6%	21.9	9.6%		
2009	257.9	5.9%	0.4	32.3%	20.2	
2010	421.4	2.6%	9.4	15.0%		
2011						
2012	327.6	7.9%	21.2	16.4%		
2013	796.4	5.3%	63.2	31.4%	19.9	4.1%
2014	829.0	4.7%			14.5	9.4%
2015	859.0	4.3%	11.7	14.2%	22.5	3.1%
2016	666.8	6.5%			36.8	8.8%[1]
2017	1,465.1	4.3%	2.5	24.0%	13.1	7.9%
2018	1,321.2	3.9%			13.5	7.5%[1]
2019	1,281.1	6.6%	9.9	17.7%	6.3	7.9%
2020	459.4	2.9%				
2021	527.0	2.9%			7.4	5.8%
2022	365.4	10.3%				
2023	258.1	4.8%	39.9	11.5%	9.3	8.3%

[1]During these years, outer Marmot Bay was surveyed in a zig-zag pattern, rather than parallel transects. Inner Marmot Bay was surveyed with parallel transects. Relative estimation error was determined by combining estimation of error for biomass within the inner Bay (1-D) and outer Bay (2-D).

Table 12. -- Numbers-at-length estimates (millions of fish) from acoustic-trawl surveys of walleye pollock in the Shelikof Strait area. Numbers from 2008 to 2023 reflect selectivity corrections for escapement of small fish.

Length	2008	2009	2010	2012	2013	2014	2015	2016	2017	2018	2019	2020	2021	2022	2023
5	0	0	0	0	0	0	0	0	0	0	0	0	0	0	0
6	0	0	0	0	0	0	0	0	0	0	0	0	0	0	0
7	0	0	0	0	0	0	0	0	0	0	0	0	0	0	0
8	0	0	4.5	0	0	15.4	<1	0	0	0	14.9	0	11.0	3.1	0
9	8.4	7.6	10.4	<1	454.9	44.6	0	0	1.3	77.1	115.7	0	246.1	<1	0
10	26.6	76.8	51.3	10.3	750.9	275.7	7.6	0	57.4	556.5	1799.9	<1	1386.2	<1	0
11	175.0	243.4	70.8	36.4	3789.1	433.0	5.5	0	134.1	756.8	3103.3	<1	2737.9	<1	<1
12	417.0	319.8	75.9	71.8	3096.5	382.4	4.7	0	308.5	375.4	1906.8	2.8	2135.8	2.4	<1
13	451.1	130.3	43.5	78.1	834.6	190.2	4.5	0	185.9	40.7	341.1	4.7	931.7	2.0	0
14	281.7	45.7	11.4	35.8	255.7	44.4	2.6	0	40.2	9.4	78.6	5.2	215.3	1.1	0
15	94.7	2.1	1.6	12.6	70.9	10.7	<1	0	16.8	2.4	0	2.0	59.5	<1	0
16	9.7	1.1	<1	3.3	22.1	5.0	<1	0	<1	1.2	<1	1.2	6.7	<1	0
17	1.7	0	<1	0	6.9	40.5	<1	0	0	0	5.8	<1	0	4.3	0
18	<1	4.9	<1	0	<1	104.7	<1	0	0	<1	37.4	<1	0	11.8	0
19	2.5	6.3	9.2	9.4	<1	461.0	<1	0	0	3.6	172.2	<1	0	41.7	0
20	3.3	70.6	15.4	54.4	1.4	995.0	1.6	0	<1	5.6	432.7	9.2	<1	56.9	0
21	11.0	166.3	34.4	151.3	3.0	942.7	8.6	0	0	16.3	437.5	19.8	<1	41.8	0
22	20.6	324.5	62.4	189.6	9.1	501.0	16.2	<1	0	26.3	291.5	24.0	<1	22.5	0
23	56.8	273.5	86.1	195.8	8.1	308.6	14.8	0	<1	27.9	166.1	17.0	<1	8.0	0
24	96.6	168.8	49.5	132.7	11.8	115.5	18.3	<1	<1	23.2	76.1	11.7	1.6	3.1	<1
25	53.2	75.6	26.7	65.8	15.3	46.3	15.5	<1	<1	19.0	40.5	19.0	3.5	2.2	0
26	27.6	19.2	16.3	33.2	21.4	16.1	33.8	<1	0	7.8	14.8	23.3	2.7	<1	<1
27	25.7	10.8	7.8	10.8	9.3	4.2	86.0	<1	0	7.9	4.2	44.4	1.8	<1	<1
28	22.8	12.6	9.2	6.3	9.4	3.7	172.0	<1	<1	4.1	6.2	53.4	2.9	<1	<1
29	16.8	5.4	28.6	<1	7.5	<1	274.3	<1	0	0	16.0	77.4	4.4	<1	<1
30	7.0	6.7	56.6	4.4	22.2	<1	296.4	1.9	0	1.2	19.9	53.3	7.2	<1	<1
31	32.0	8.5	91.5	<1	33.9	<1	244.2	3.2	0	<1	24.5	43.5	10.5	<1	<1
32	46.2	12.0	109.6	4.8	39.3	2.0	193.6	10.7	0	<1	31.8	23.1	15.4	<1	<1
33	49.2	24.7	91.4	3.2	66.6	3.6	128.9	22.0	<1	<1	17.9	16.7	17.3	1.1	<1
34	24.8	23.6	66.8	3.0	74.9	2.3	68.3	50.7	1.1	0	14.1	16.8	21.0	2.0	<1
35	40.2	18.8	32.2	4.3	112.3	3.0	50.0	91.1	<1	0	6.7	9.5	21.1	2.5	1.2
36	18.6	15.3	25.8	4.4	102.8	3.8	26.6	139.3	4.8	0	2.1	14.2	27.9	6.4	1.3
37	32.3	8.2	14.0	2.9	103.1	5.1	19.3	209.6	9.0	1.2	5.1	10.2	31.2	12.5	1.3
38	4.0	11.3	10.6	2.5	56.5	7.6	13.4	274.3	56.3	1.8	2.1	5.6	28.0	22.2	2.3
39	2.4	14.5	7.7	2.2	39.8	13.2	10.9	271.5	130.6	10.2	1.6	4.4	23.5	24.0	3.2
40	14.9	8.8	8.5	4.0	21.5	24.4	8.0	204.9	352.4	45.3	1.5	3.3	19.8	32.6	5.7
41	5.9	12.9	8.5	5.5	13.7	37.5	5.0	138.2	530.2	101.3	5.0	2.3	14.9	30.9	10.3
42	4.3	15.1	9.8	9.0	10.3	51.8	5.8	76.3	578.5	202.3	34.3	7.8	15.1	28.7	16.2
43	5.0	13.9	10.2	15.8	8.2	55.8	9.5	40.2	544.0	305.4	102.9	15.1	12.0	22.4	16.0
44	3.1	13.7	10.9	13.6	9.9	52.1	13.0	22.2	326.5	371.2	177.4	34.3	9.4	21.3	23.3
45	3.4	11.6	14.1	17.6	4.4	37.2	20.2	13.0	169.8	351.5	245.3	67.1	16.7	19.6	20.7
46	3.0	8.6	13.2	20.0	5.7	25.2	30.6	10.1	80.9	258.9	244.9	78.3	31.9	18.6	23.0
47	1.4	5.2	11.2	20.0	8.7	14.8	33.1	7.0	46.4	191.2	221.6	74.7	29.5	25.2	17.3
48	<1	4.5	11.3	22.0	12.3	13.0	38.8	7.4	24.0	117.6	169.1	62.0	43.0	27.7	21.8
49	<1	2.8	10.5	19.6	14.2	11.6	33.8	8.8	8.9	62.6	122.9	40.9	45.6	29.4	14.4
50	<1	2.9	12.0	19.6	13.9	15.3	26.5	6.4	6.8	30.7	68.2	33.0	38.0	26.6	17.6
51	<1	2.6	10.5	16.5	23.0	16.2	25.6	4.3	3.5	29.3	35.2	20.4	29.0	21.6	12.1
52	<1	3.5	9.1	12.2	18.1	31.5	21.2	5.4	2.6	9.8	25.3	13.2	28.2	18.8	13.6
53	1.3	2.3	6.0	10.6	21.2	28.3	24.1	2.7	<1	9.5	10.4	5.6	24.1	15.7	9.9
54	1.8	2.4	7.2	9.7	28.6	33.4	23.0	2.8	2.8	3.7	5.3	4.9	16.9	15.4	11.7
55	2.0	1.7	7.9	7.4	21.6	28.7	28.4	2.3	4.5	6.8	4.7	2.9	14.1	13.4	8.7
56	1.2	2.2	5.9	6.8	26.9	36.0	25.5	2.7	4.5	1.8	<1	1.4	8.6	8.9	9.4
57	<1	1.6	4.9	6.9	18.9	24.7	23.2	2.7	<1	<1	<1	<1	5.7	5.9	7.0
58	1.4	1.2	6.2	5.2	17.2	19.3	20.2	1.2	2.0	0	<1	<1	4.3	2.2	6.0
59	1.5	1.2	5.6	3.1	16.5	12.5	15.4	<1	<1	0	<1	<1	3.1	2.5	3.0
60	1.3	1.2	3.3	3.5	18.6	9.6	14.3	1.3	<1	<1	<1	<1	<1	<1	2.7

Length	2008	2009	2010	2012	2013	2014	2015	2016	2017	2018	2019	2020	2021	2022	2023
61	2.6	1.2	5.2	1.5	7.9	9.0	8.3	<1	<1	0	<1	<1	<1	<1	1.3
62	<1	1.1	3.8	<1	8.8	6.8	6.9	<1	<1	<1	0	<1	<1	<1	1.5
63	<1	1.0	3.3	1.2	11.1	1.2	3.8	<1	<1	0	0	<1	0	<1	<1
64	<1	<1	3.8	<1	2.7	2.9	1.6	0	0	0	0	0	<1	<1	<1
65	<1	<1	3.3	<1	1.7	1.2	2.1	0	0	0	0	0	<1	0	<1
66	<1	<1	2.5	<1	2.5	1.0	<1	0	0	0	0	0	0	0	0
67	<1	<1	2.4	<1	<1	<1	<1	0	0	0	0	0	0	0	<1
68	<1	<1	1.3	<1	<1	<1	<1	0	0	0	0	0	0	0	0
69	<1	<1	<1	0	0	0	<1	0	0	0	0	0	0	0	0
70	0	<1	<1	<1	<1	<1	0	0	0	0	0	0	0	0	0
71	0	<1	<1	0	<1	0	0	0	0	0	0	0	0	0	0
72	0	0	<1	0	0	0	0	0	0	0	0	0	0	0	0
73	0	0	0	0	<1	0	0	0	0	0	0	0	0	0	0
74	0	0	0	0	<1	<1	0	0	0	0	0	0	0	0	0
75	0	0	0	0	0	0	0	0	0	0	0	0	0	0	0
76	0	<1	0	0	0	0	0	0	0	0	0	0	0	0	0
Total	2120.4	2235.7	1338.7	1385.4	10401.5	5584.3	2188.2	1636.9	3638.7	4076.3	10664.6	985.0	8364.7	666.6	287.4

Table 13. -- Biomass-at-length estimates (thousands of metric tons) from acoustic-trawl surveys of walleye pollock in the Shelikof Strait area. Biomass from 2008 to 2023 reflects selectivity corrections for escapement of small fish.

Length	2008	2009	2010	2012	2013	2014	2015	2016	2017	2018	2019	2020	2021	2022	2023
5	0	0	0	0	0	0	0	0	0	0	0	0	0	0	0
6	0	0	0	0	0	0	0	0	0	0	0	0	0	0	0
7	0	0	0	0	0	0	0	0	0	0	0	0	0	0	0
8	0	0	<1	0	0	<1	<1	0	0	0	<1	0	<1	<1	0
9	<1	<1	<1	<1	1.7	<1	0	0	<1	<1	<1	0	1.2	<1	0
10	<1	<1	<1	<1	4.6	1.7	<1	0	<1	3.6	11.5	<1	8.8	<1	0
11	1.7	2.1	<1	<1	29.5	4.3	<1	0	1.0	6.2	25.5	<1	22.1	<1	<1
12	4.6	3.4	<1	<1	29.4	4.0	<1	0	3.0	3.9	18.9	<1	21.1	<1	<1
13	6.8	1.7	<1	1.1	10.1	2.5	<1	0	2.3	<1	4.3	<1	11.4	<1	0
14	4.9	<1	<1	<1	3.8	<1	<1	0	<1	<1	1.1	<1	3.3	<1	0
15	2.1	<1	<1	<1	1.3	<1	<1	0	<1	<1	0	<1	1.1	<1	0
16	<1	<1	<1	<1	<1	<1	<1	0	<1	<1	<1	<1	<1	<1	0
17	<1	0	<1	0	<1	1.3	<1	0	0	0	<1	<1	0	<1	0
18	<1	<1	<1	0	<1	3.9	<1	0	0	<1	1.4	<1	0	<1	0
19	<1	<1	<1	<1	<1	20.3	<1	0	0	<1	7.5	<1	0	1.8	0
20	<1	3.8	<1	3.1	<1	49.4	<1	0	<1	<1	22.0	<1	<1	2.7	0
21	<1	10.4	2.1	9.4	<1	54.5	<1	0	0	1.1	25.3	1.2	<1	2.3	0
22	1.6	23.1	4.3	13.5	<1	34.2	1.1	<1	0	1.9	19.1	1.7	<1	1.4	0
23	4.7	21.7	6.8	16.0	<1	23.3	1.2	0	<1	2.3	12.7	1.3	<1	<1	0
24	9.2	15.3	4.6	12.0	1.1	10.1	1.6	<1	<1	2.1	6.7	1.1	<1	<1	<1
25	5.9	7.5	2.7	6.5	1.5	4.6	1.7	<1	<1	2.0	4.1	1.9	<1	<1	0
26	3.6	2.4	1.9	3.9	2.5	1.9	4.0	<1	0	<1	1.7	2.7	<1	<1	<1
27	3.6	1.5	1.1	1.5	1.2	<1	11.3	<1	0	1.1	<1	5.8	<1	<1	<1
28	3.7	2.0	1.4	<1	1.4	<1	25.4	<1	<1	<1	<1	7.8	<1	<1	<1
29	3.1	<1	4.9	<1	1.3	<1	44.2	<1	0	0	2.5	12.6	<1	<1	<1
30	1.4	1.3	10.8	<1	4.3	<1	53.6	<1	0	<1	3.8	9.7	1.4	<1	<1
31	7.3	1.8	19.1	<1	7.3	<1	49.3	<1	0	<1	4.7	8.7	2.2	<1	<1
32	11.8	2.7	25.0	1.1	9.3	<1	43.2	2.3	0	<1	7.2	5.1	3.6	<1	<1
33	14.1	6.1	23.0	<1	17.6	<1	32.4	5.3	<1	<1	4.5	4.2	4.3	<1	<1
34	7.8	6.5	18.4	<1	21.8	<1	18.5	13.4	<1	0	4.0	4.6	6.0	<1	<1
35	13.8	5.7	9.7	1.3	36.4	<1	14.9	26.5	<1	0	2.2	2.9	6.6	<1	<1
36	6.9	5.1	8.8	1.5	35.4	1.3	8.9	44.2	1.5	0	<1	4.7	9.6	2.0	<1
37	13.2	3.1	5.2	1.1	40.1	1.9	7.0	72.4	3.1	<1	2.1	3.7	11.9	4.5	<1
38	1.8	4.6	4.3	<1	24.0	3.0	5.5	102.8	20.6	<1	<1	2.2	11.4	8.7	<1
39	1.2	6.5	3.6	<1	17.8	5.7	4.8	108.5	51.3	4.1	<1	1.9	10.3	9.9	1.4
40	8.1	4.3	4.2	1.9	13.0	11.6	4.0	88.3	150.1	20.0	<1	1.6	9.6	14.5	2.6
41	3.5	7.0	4.7	2.9	7.5	19.2	2.7	64.0	243.8	47.6	2.5	1.1	8.0	14.9	5.2
42	2.6	8.7	5.8	5.0	6.0	28.6	3.3	37.5	283.7	99.7	18.8	4.2	8.7	15.2	8.6
43	3.4	8.7	6.5	9.6	5.1	33.0	5.7	21.6	280.7	164.4	59.6	8.9	7.4	12.6	9.3
44	2.2	9.4	7.5	8.7	6.7	33.3	8.4	12.7	181.0	215.3	108.3	21.8	6.4	13.0	14.7
45	2.7	8.6	10.8	12.4	3.2	25.6	14.5	7.8	100.0	214.3	159.7	44.8	12.2	12.9	14.2
46	2.5	6.7	10.9	15.1	4.5	18.4	23.6	6.5	52.3	168.7	170.0	54.3	25.3	13.6	17.4
47	1.2	4.5	9.7	16.0	7.4	11.6	27.2	4.7	32.2	132.0	165.7	58.4	24.6	19.8	13.7
48	<1	4.2	10.5	18.4	11.1	11.0	33.9	5.6	18.0	89.1	136.1	51.8	36.9	22.9	18.8
49	<1	2.9	10.7	18.5	13.8	10.5	31.6	7.2	7.7	49.8	108.4	37.5	41.2	26.6	13.3
50	<1	3.3	12.7	20.0	15.1	14.8	27.0	5.4	6.2	24.8	63.8	31.2	37.3	25.1	17.3
51	<1	3.0	12.2	17.8	25.8	17.4	27.4	3.7	3.1	28.4	35.7	21.4	30.9	22.9	12.4
52	<1	4.6	11.3	14.1	22.1	36.6	23.9	5.1	2.6	9.4	25.9	14.3	32.2	21.3	15.1
53	1.8	3.3	8.0	12.5	27.7	35.9	29.3	2.8	<1	9.7	12.3	6.9	29.2	19.7	11.9
54	2.5	3.6	9.9	12.2	39.7	42.9	29.5	3.0	3.0	4.0	6.2	6.2	21.2	19.6	14.8
55	3.2	2.8	11.7	10.2	30.0	39.5	37.6	2.5	5.2	7.7	6.3	4.2	19.0	18.9	11.9
56	2.0	3.7	9.3	10.1	41.2	52.3	36.6	2.9	5.4	2.2	<1	2.0	11.4	13.6	13.8
57	<1	2.7	8.6	10.1	30.2	38.0	34.6	3.0	<1	<1	1.3	1.1	8.8	8.9	11.0
58	2.6	2.2	11.0	9.1	29.8	31.2	32.3	1.5	2.7	0	<1	<1	7.1	3.4	9.5
59	2.8	2.6	10.3	5.4	29.5	20.6	25.2	1.1	1.1	0	<1	<1	5.7	4.1	5.4
60	2.7	2.6	6.4	6.3	35.7	18.4	25.0	1.6	<1	<1	<1	<1	1.6	1.3	5.0

Length	2008	2009	2010	2012	2013	2014	2015	2016	2017	2018	2019	2020	2021	2022	2023
61	5.5	2.5	10.5	2.8	15.8	16.2	15.4	<1	<1	0	<1	1.4	1.5	1.7	2.5
62	1.6	2.4	7.9	1.6	18.6	13.6	13.2	1.0	<1	<1	0	<1	1.4	1.1	3.1
63	2.2	2.4	7.4	2.5	24.6	2.5	7.2	<1	<1	0	0	<1	0	<1	<1
64	1.4	1.7	8.8	2.0	6.4	6.2	3.4	0	0	0	0	0	<1	<1	1.1
65	2.2	<1	8.4	1.3	4.2	2.8	4.7	0	0	0	0	0	<1	0	<1
66	<1	2.7	6.4	<1	6.5	2.4	1.9	0	0	0	0	0	0	0	0
67	<1	1.5	6.7	<1	<1	<1	<1	0	0	0	0	0	0	0	<1
68	<1	1.3	3.7	<1	1.5	<1	<1	0	0	0	0	0	0	0	0
69	<1	<1	1.5	0	0	0	<1	0	0	0	0	0	0	0	0
70	0	<1	2.9	<1	1.7	<1	0	0	0	0	0	0	0	0	0
71	0	<1	1.8	0	3.1	0	0	0	0	0	0	0	0	0	0
72	0	0	1.6	0	0	0	0	0	0	0	0	0	0	0	0
73	0	0	0	0	1.3	0	0	0	0	0	0	0	0	0	0
74	0	0	0	0	<1	<1	0	0	0	0	0	0	0	0	0
75	0	0	0	0	0	0	0	0	0	0	0	0	0	0	0
76	0	<1	0	0	0	0	0	0	0	0	0	0	0	0	0
Total	197.5	257.9	421.4	327.6	796.4	829.0	859.0	666.8	1465.1	1321.2	1281.1	459.4	527.0	365.4	258.1

Table 14. -- Biomass-at-age estimates (thousands of metric tons) from acoustic-trawl surveys of walleye pollock in the Shelikof Strait area. Numbers from 2008 to 2023 reflect selectivity corrections for escapement of small fish.

Age	2008	2009	2010	2012	2013	2014	2015	2016	2017	2018	2019	2020	2021	2022	2023
1	20.6	8.5	2.4	3.0	81.3	14.2	<1	0	7.7	14.8	61.9	<1	69.3	<1	<1
2	29.5	88.1	23.6	67.3	14.9	204.3	9.3	<1	0	12.6	102.1	5.9	7.0	9.9	<1
3	75.3	27.7	129.0	7.9	229.0	4.8	310.4	23.6	3.3	<1	34.3	59.3	30.2	10.3	2.8
4	30.2	49.0	55.4	53.5	31.6	161.4	40.4	565.8	57.2	5.1	3.0	22.4	74.4	72.8	26.6
5	8.8	42.0	83.2	98.6	72.6	58.5	152.6	24.2	1287.5	89.4	4.2	7.5	37.8	68.4	77.2
6	1.6	10.4	35.5	53.5	140.7	78.3	75.2	25.2	70.4	1099.2	183.5	19.2	6.3	23.3	30.6
7	4.7	4.7	20.5	35.6	92.8	141.5	84.4	13.3	29.7	58.1	830.3	55.4	11.0	2.0	6.7
8	14.7	1.7	10.6	5.5	75.5	81.2	103.9	4.1	8.4	41.7	42.5	155.4	65.2	15.9	1.9
9	8.8	10.3	11.5	1.5	19.2	39.9	46.6	8.3	<1	0	9.7	93.5	141.2	32.1	4.1
10	2.7	12.3	20.9	<1	10.3	26.2	16.4	2.0	<1	0	9.3	29.9	66.3	98.1	29.1
11	<1	2.8	20.4	<1	9.9	11.7	8.3	0	0	0	<1	6.5	16.3	28.9	59.9
12	0	<1	8.2	<1	1.5	1.5	5.9	0	0	0	<1	4.3	2.0	2.3	12.4
13	0	0	0	0	3.4	4.1	1.5	0	0	0	0	0	0	1.4	5.1
14	0	0	0	0	8.7	0	<1	0	0	0	0	0	0	0	<1
15	0	0	0	0	5.0	1.4	1.8	0	0	0	0	0	0	0	<1
16	0	0	0	0	0	0	1.5	0	0	0	0	0	0	0	0
17	0	0	0	0	0	0	0	0	0	0	0	0	0	0	0
18	0	0	0	0	0	0	0	0	0	0	0	0	0	0	0
Total	197.5	257.9	421.4	327.6	796.4	829.0	859.0	666.8	1465.1	1321.2	1281.1	459.4	527.0	365.4	258.1

Table 15. -- Numbers-at-age estimates (millions of fish) from acoustic-trawl surveys of walleye pollock in the Shelikof Strait area. Numbers from 2008 to 2023 reflect selectivity corrections for escapement of small fish.

Age	2008	2009	2010	2012	2013	2014	2015	2016	2017	2018	2019	2020	2021	2022	2023
1	1465.9	826.7	270.5	248.3	9282.1	1397.8	25.6	0	745.0	1819.4	7361.3	17.6	7730.1	11.1	<1
2	289.0	1125.9	299.1	848.7	116.7	3544.0	97.7	1.9	0	142.6	1671.7	81.4	36.7	193.3	1.4
3	272.8	106.6	538.7	28.5	659.3	15.8	1565.2	78.2	9.2	1.6	155.5	345.3	94.2	27.9	8.0
4	63.4	93.9	82.9	79.8	50.0	269.5	71.4	1451.8	126.4	9.9	6.1	72.2	150.7	132.7	41.2
5	11.4	57.0	76.3	107.1	62.6	81.2	172.4	43.4	2576.4	165.9	6.6	15.5	55.4	111.9	106.9
6	1.2	9.7	27.7	42.1	102.5	61.0	71.6	33.5	126.0	1804.6	261.7	27.0	7.3	26.9	34.5
7	2.5	2.8	11.2	25.0	58.0	106.6	60.7	15.5	32.0	85.7	1127.5	68.5	12.5	2.4	5.6
8	8.0	<1	5.1	3.7	42.7	54.6	70.9	3.6	8.9	46.7	53.9	192.8	64.0	13.5	1.3
9	4.6	4.8	5.0	<1	10.4	26.0	30.2	7.4	<1	0	11.1	116.8	133.9	30.7	3.5
10	1.3	5.8	10.3	<1	4.8	16.7	10.5	1.7	<1	0	9.0	37.2	63.4	86.6	23.3
11	<1	1.3	8.8	<1	4.6	7.7	5.4	0	0	0	<1	8.0	14.3	26.3	46.6
12	0	<1	3.2	<1	<1	<1	3.4	0	0	0	<1	2.7	2.2	1.9	9.7
13	0	0	0	0	1.4	2.1	<1	0	0	0	0	0	0	1.5	4.2
14	0	0	0	0	4.0	0	<1	0	0	0	0	0	0	0	<1
15	0	0	0	0	2.0	<1	1.3	0	0	0	0	0	0	0	<1
16	0	0	0	0	0	0	<1	0	0	0	0	0	0	0	0
17	0	0	0	0	0	0	0	0	0	0	0	0	0	0	0
18	0	0	0	0	0	0	0	0	0	0	0	0	0	0	0
Total	2120.4	2235.7	1338.7	1384.6	10401.5	5584.3	2188.2	1636.9	3624.5	4076.3	10664.6	985.0	8364.7	666.6	287.4

Table 16. -- Catch by species and numbers of length and weight measurements taken from 6 LFS1421 hauls during the 2023 acoustic-trawl survey of walleye pollock in Chirikof shelfbreak area.

		Catch				Measurements	
Species name	Scientific name	Weight (kg)	%	Number	%	Length	Weight
Pacific ocean perch	*Sebastes alutus*	1,897.9	64.1	2,599	22.0	390	126
walleye pollock	*Gadus chalcogrammus*	1,021.1	34.5	1,832	15.5	1,209	235
rougheye rockfish	*Sebastes aleutianus*	15.3	0.5	11	<0.1	11	11
giant grenadier	*Coryphaenoides pectoralis*	6.1	0.2	2	<0.1	2	2
dusky rockfish	*Sebastes variabilis*	6.1	0.2	6	<0.1	6	6
shortraker rockfish	*Sebastes borealis*	5.8	0.2	2	<0.1	2	2
lanternfish unid.	Myctophidae (family)	2.6	<0.1	365	3.1	103	33
squid unid.	Cephalopoda (class)	0.9	<0.1	151	1.3	52	34
smooth lumpsucker	*Aptocyclus ventricosus*	0.8	<0.1	1	<0.1	1	1
northern sea nettle	*Chrysaora melanaster*	0.6	<0.1	2	<0.1	2	2
arrowtooth flounder	*Atheresthes stomias*	0.5	<0.1	1	<0.1	1	1
Pacific glass shrimp	*Pasiphaea pacifica*	0.5	<0.1	266	2.3	33	-
northern smoothtongue	*Leuroglossus schmidti*	0.4	<0.1	26	0.2	11	11
euphausiid unid.	Euphausiacea (order)	0.4	<0.1	6,494	55.0	-	-
magistrate armhook squid	*Berryteuthis magister*	0.4	<0.1	1	<0.1	1	1
jellyfish unid.	Scyphozoa (class)	0.3	<0.1	<0.1	<0.1	-	-
moon jelly	*Aurelia* sp.	0.2	<0.1	1	<0.1	-	-
unsorted shab		0.1	<0.1	<0.1	<0.1	-	-
viperfish unid.	Stomiidae (family)	<0.1	<0.1	27	0.2	19	15
Pacific lamprey	*Lampetra tridentata*	<0.1	<0.1	1	<0.1	1	1
northern pearleye	*Benthalbella dentata*	<0.1	<0.1	2	<0.1	2	2
helmet jelly.	*Periphylla* sp.	<0.1	<0.1	8	<0.1	3	-
isopod unid.	Isopoda (order)	<0.1	<0.1	3	<0.1	-	-
salp unid.	Thaliacea (class)	<0.1	<0.1	1	<0.1	-	-
Total		2,960.2		11,802		1,849	483

Table 17. -- Catch by species and numbers of length and weight measurements taken from 5 LFS1421 hauls during the 2023 acoustic-trawl survey of walleye pollock in Marmot Bay area.

		Catch				Measurements	
Species name	Scientific name	Weight (kg)	%	Number	%	Length	Weight
walleye pollock	*Gadus chalcogrammus*	4,327.0	99.1	23,056	86.8	1,930	368
Pacific cod	*Gadus macrocephalus*	11.8	0.3	3	<0.1	3	3
eulachon	*Thaleichthys pacificus*	9.9	0.2	247	0.9	80	22
Pacific capelin	*Mallotus catervarius*	6.5	0.1	1,390	5.2	51	26
smooth lumpsucker	*Aptocyclus ventricosus*	4.0	<0.1	4	<0.1	4	4
Chinook salmon	*Oncorhynchus tshawytscha*	1.8	<0.1	1	<0.1	1	1
Pacific herring	*Clupea pallasii*	1.8	<0.1	275	1.0	40	16
arrowtooth flounder	*Atheresthes stomias*	1.2	<0.1	1	<0.1	1	1
squid unid.	Cephalopoda (class)	1.1	<0.1	8	<0.1	3	3
northern sea nettle	*Chrysaora melanaster*	1.0	<0.1	4	<0.1	4	4
smelt unid.	Osmeridae (family)	0.8	<0.1	1,533	5.8	46	-
Alaskan pink shrimp	*Pandalus eous*	<0.1	<0.1	17	<0.1	17	-
blackmouth eelpout	*Lycodapus fierasfer*	<0.1	<0.1	3	<0.1	3	3
isopod unid.	Isopoda (order)	<0.1	<0.1	3	<0.1	-	-
poacher unid.	Agonidae (family)	<0.1	<0.1	2	<0.1	2	-
Total		4,367.1		26,547		2,185	451

FIGURES

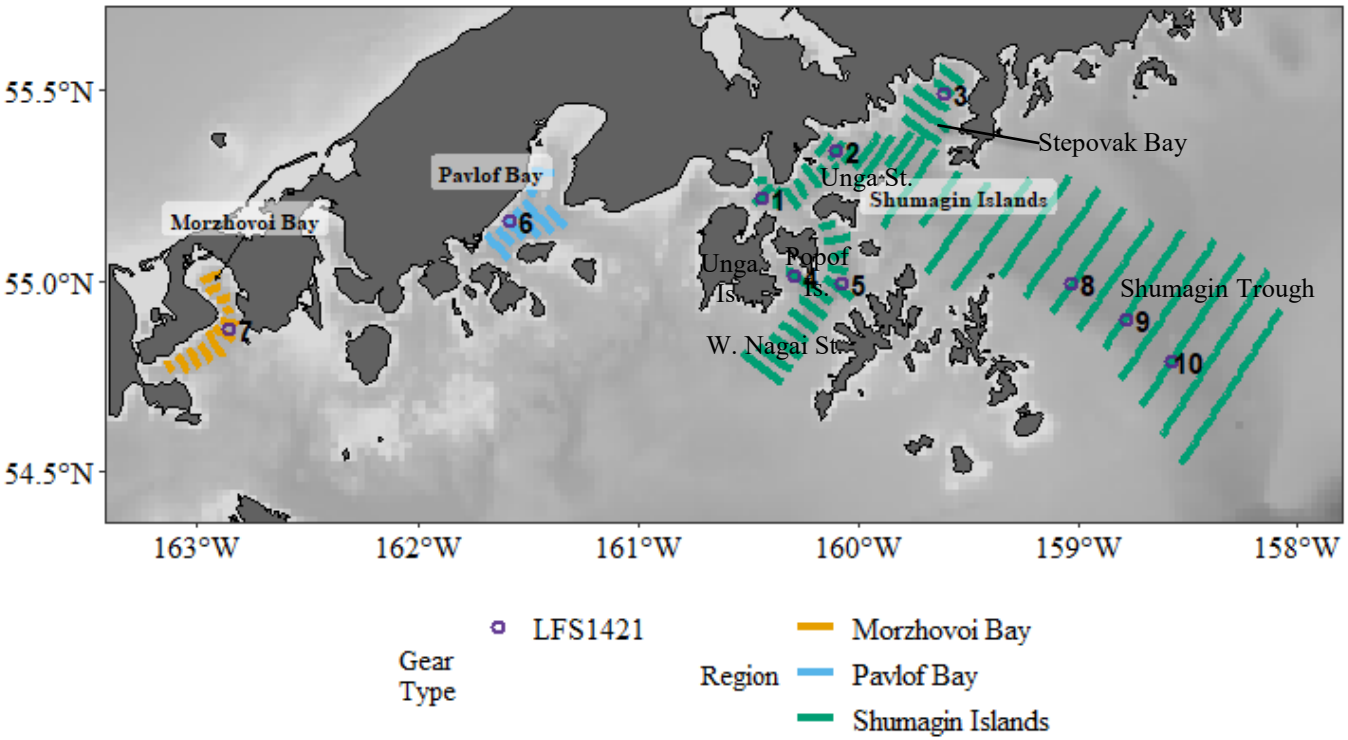

Figure 1. -- Transect lines and locations of trawl hauls during the winter 2023 acoustic-trawl survey of walleye pollock in the Shumagin Islands, Pavlof Bay, and Morzhovoi Bay areas. Labeled areas are referenced in the text and hauls are numbered.

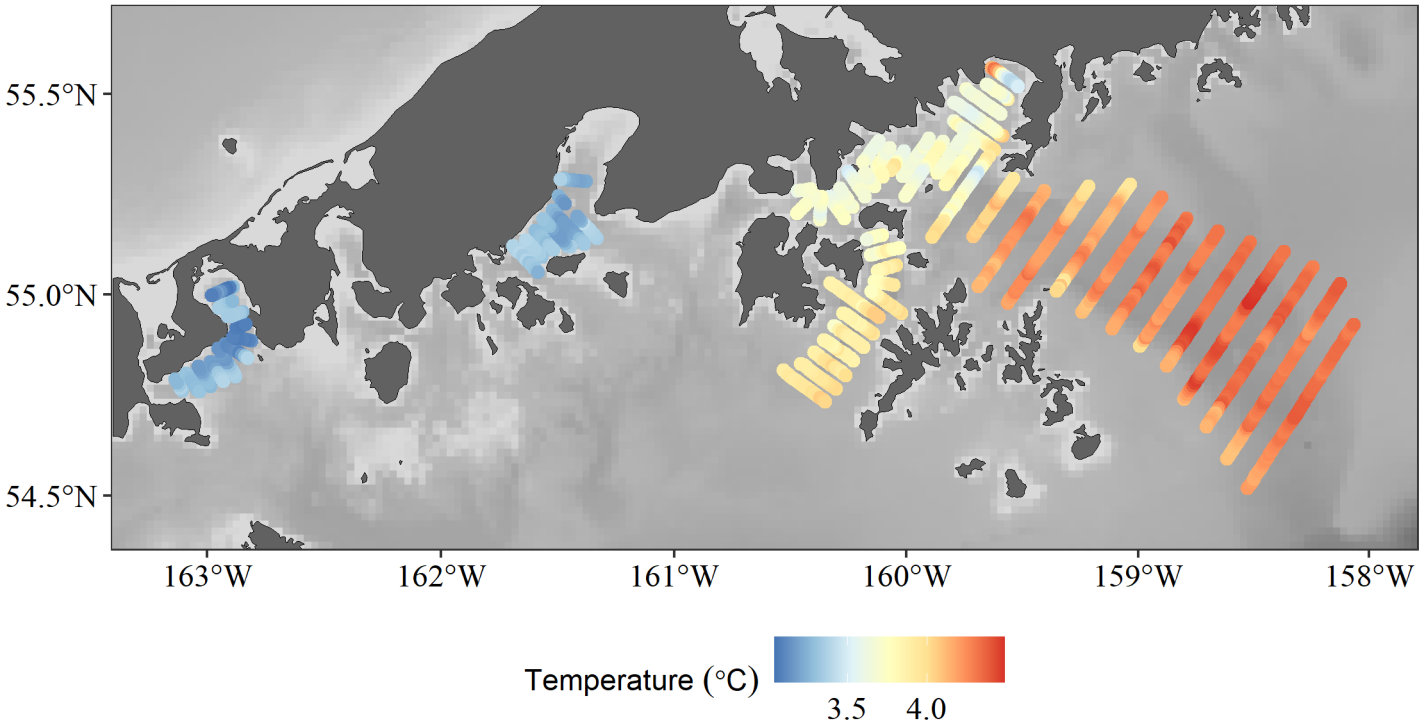

Figure 2. -- Surface water temperatures (°C) recorded at 5-second intervals during the winter 2023 acoustic-trawl survey of the Shumagin Islands, Pavlof Bay, and Morzhovoi Bay areas.

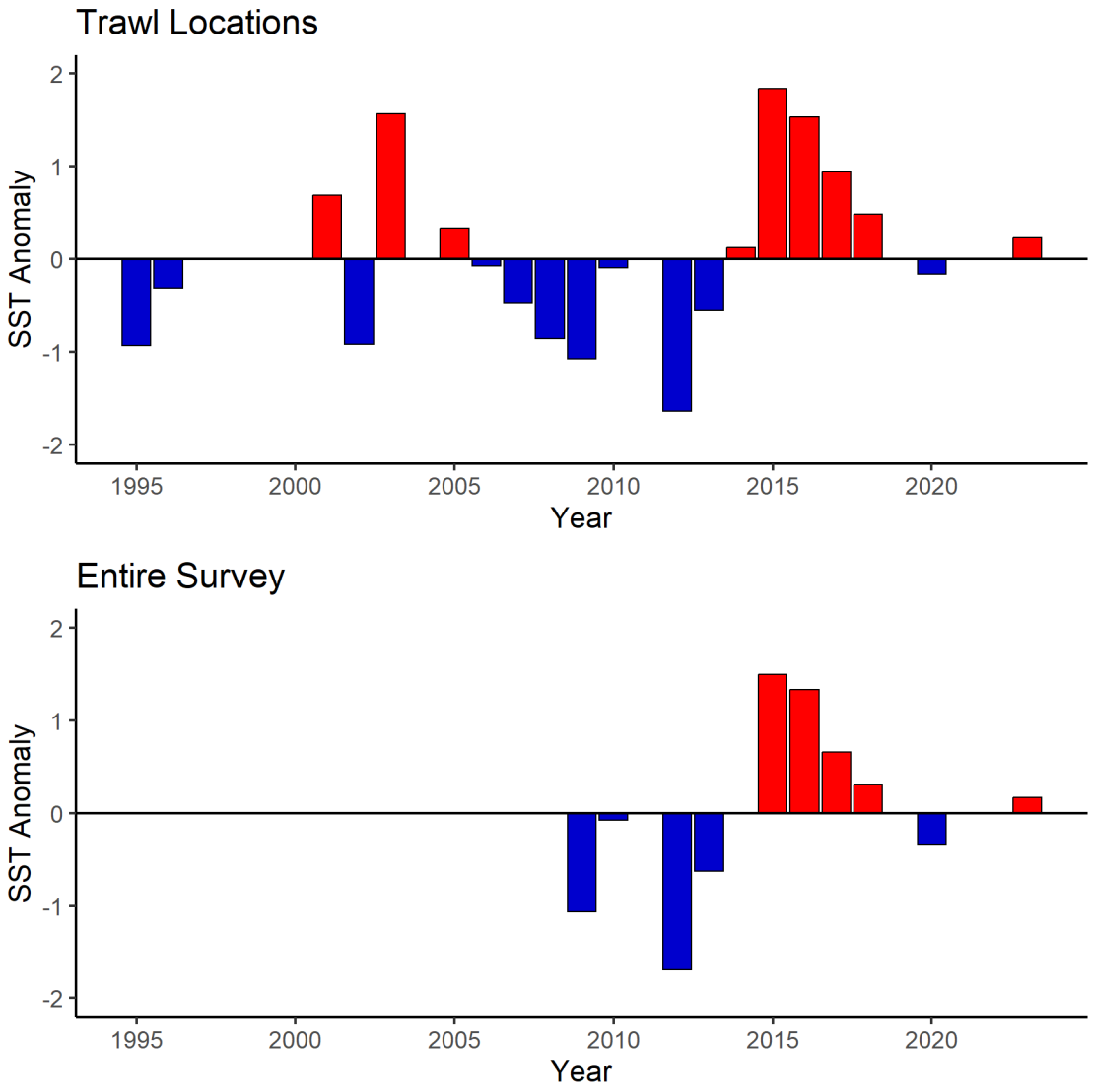

Figure 3. -- Sea surface temperature (SST, °C) anomalies recorded at trawl locations (upper panel) and from the ship's flow-through system for the entire survey (lower panel) in the Shumagin Islands. SST anomalies for each temperature source are centered and scaled by their respective mean temperature and standard deviation from the 2006-2022 period. Positive and negative anomalies are indicated by red and blue bars, respectively.

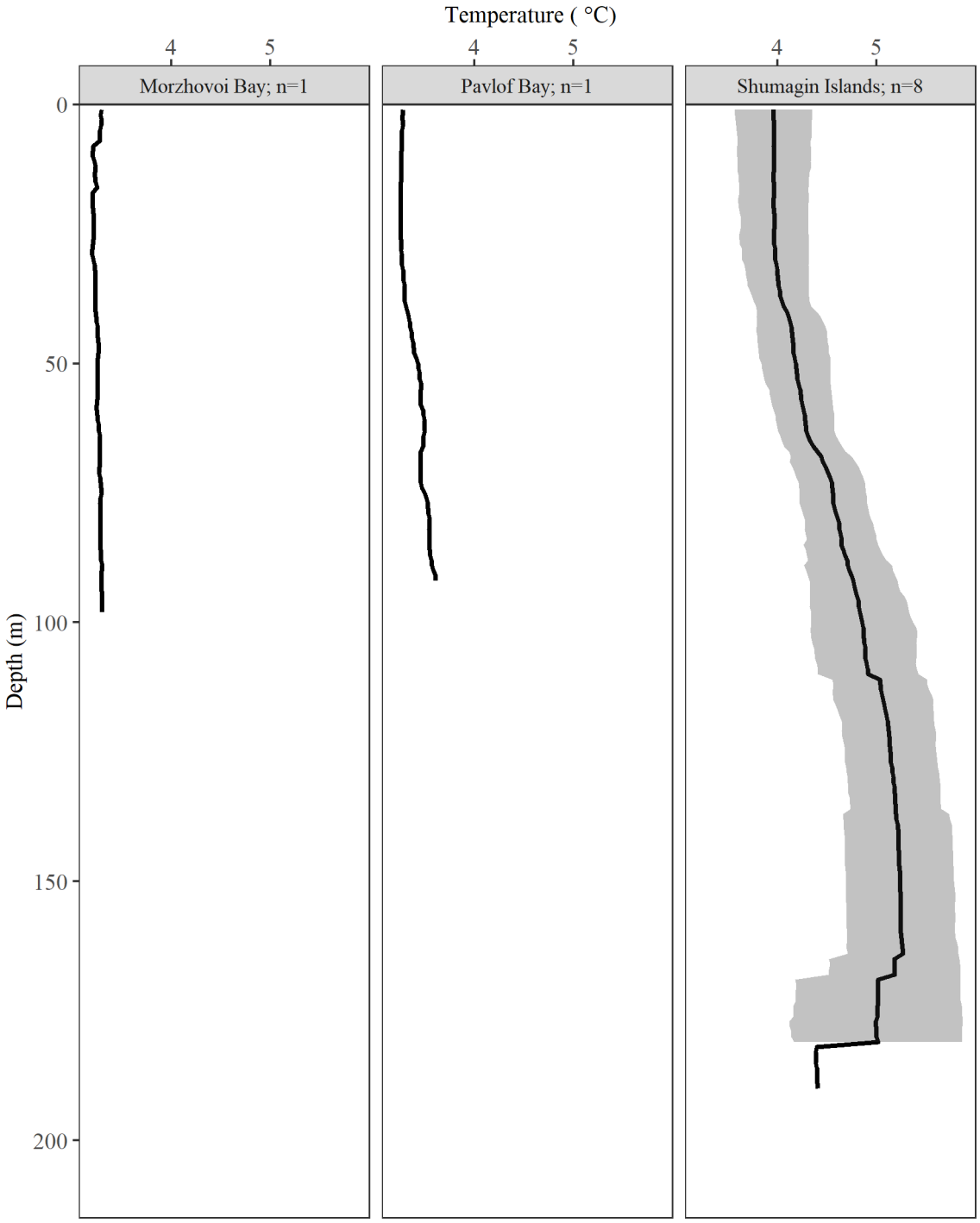

Figure 4. -- Mean water temperature (°C; solid line) by 1-m depth intervals measured at trawl locations during the 2023 acoustic-trawl survey of walleye pollock in the Shumagin Islands area. The shaded area represents one standard deviation. Number of trawls per area shown with area name.

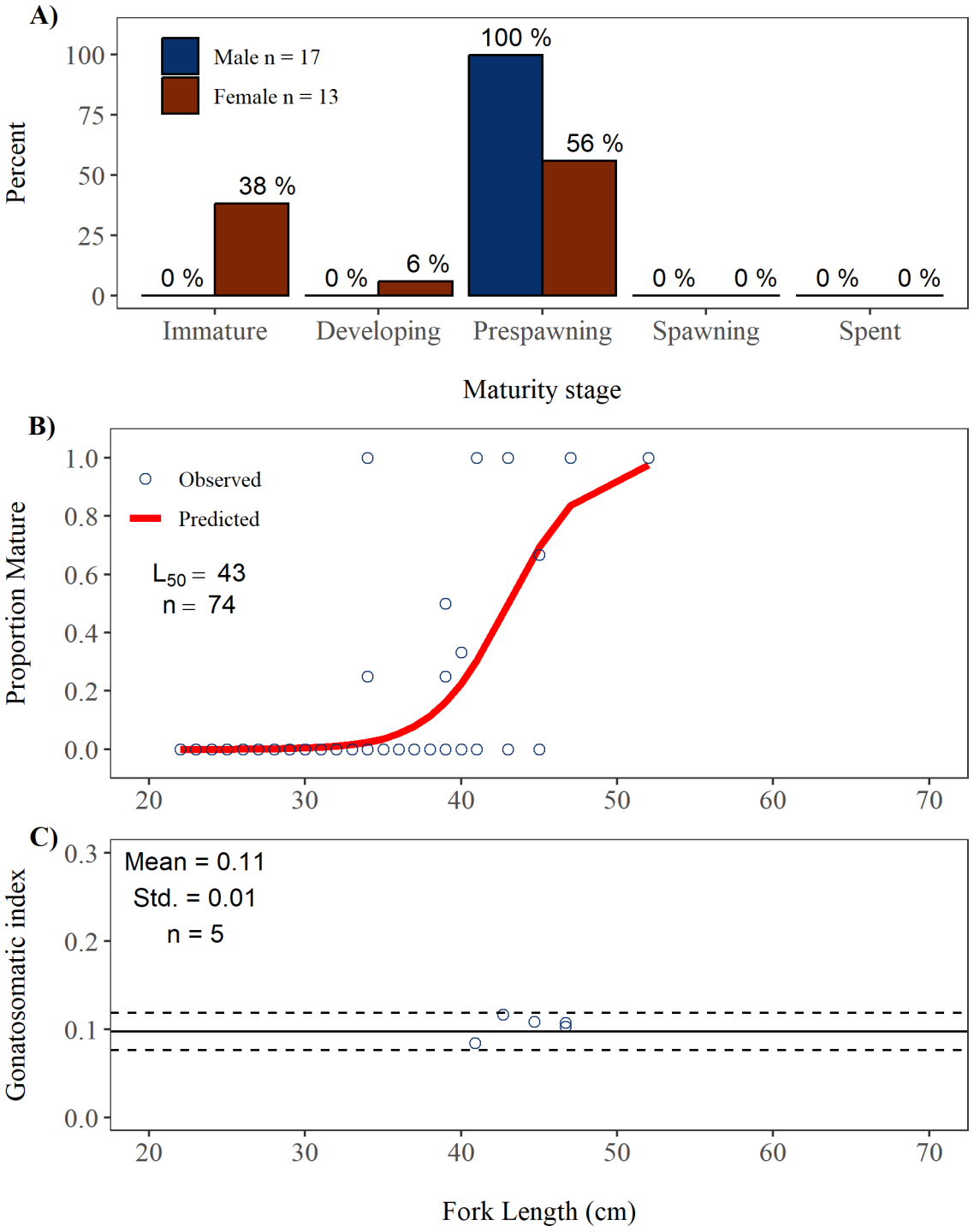

Figure 5. -- Walleye pollock maturity in the Shumagin Islands. A) Maturity composition for male and female walleye pollock > 40 cm FL within each stage; B) proportion mature (i.e., pre-spawning, spawning, or spent) by 1-cm size group for female walleye pollock; C) gonadosomatic index for females > 40 cm FL (with historic survey mean ± 1 standard deviation (Std.)). All maturity quantities are weighted by local pollock abundance.

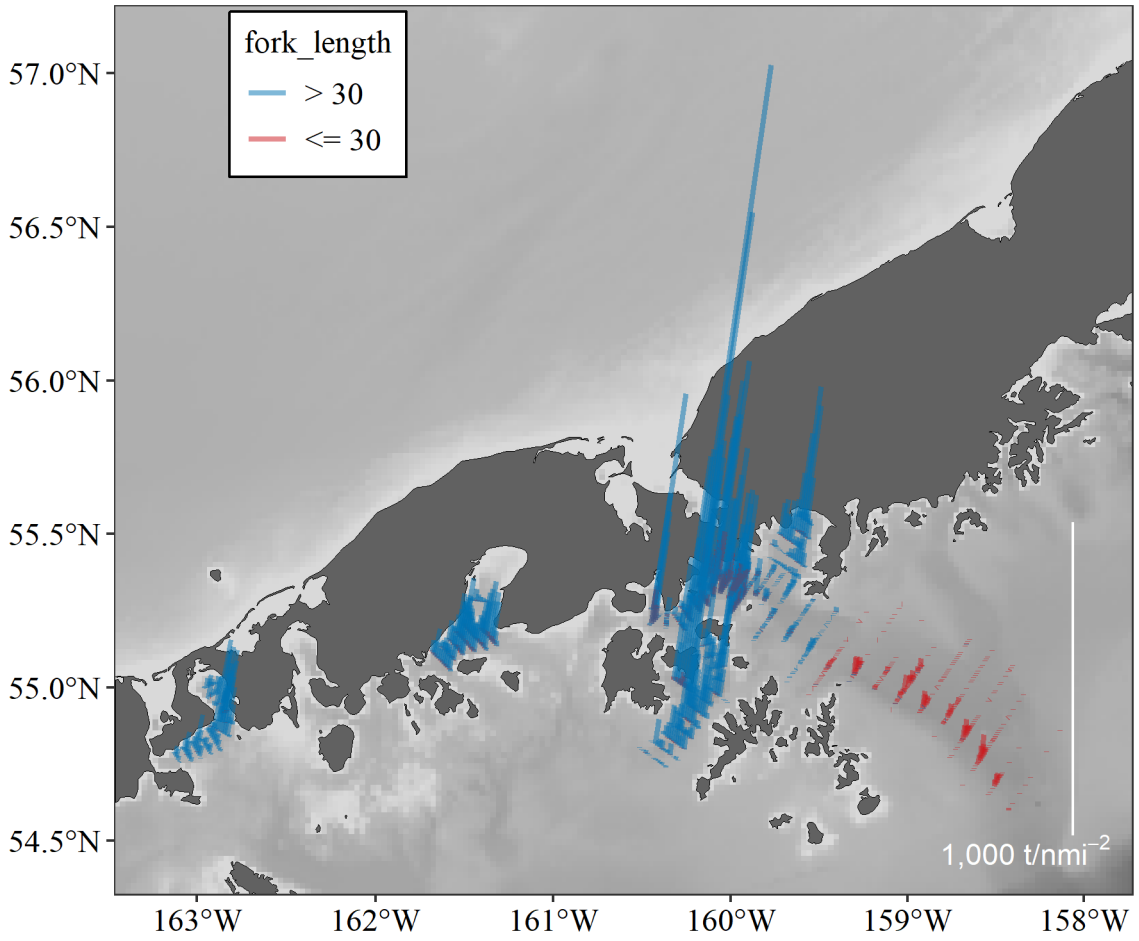

Figure 6. – Biomass per unit area (tnmi^{-2}) attributed to walleye pollock (vertical lines) along tracklines surveyed during the winter acoustic-trawl survey of the Shumagin Islands, Pavlof Bay, and Morzhovoi Bay areas.

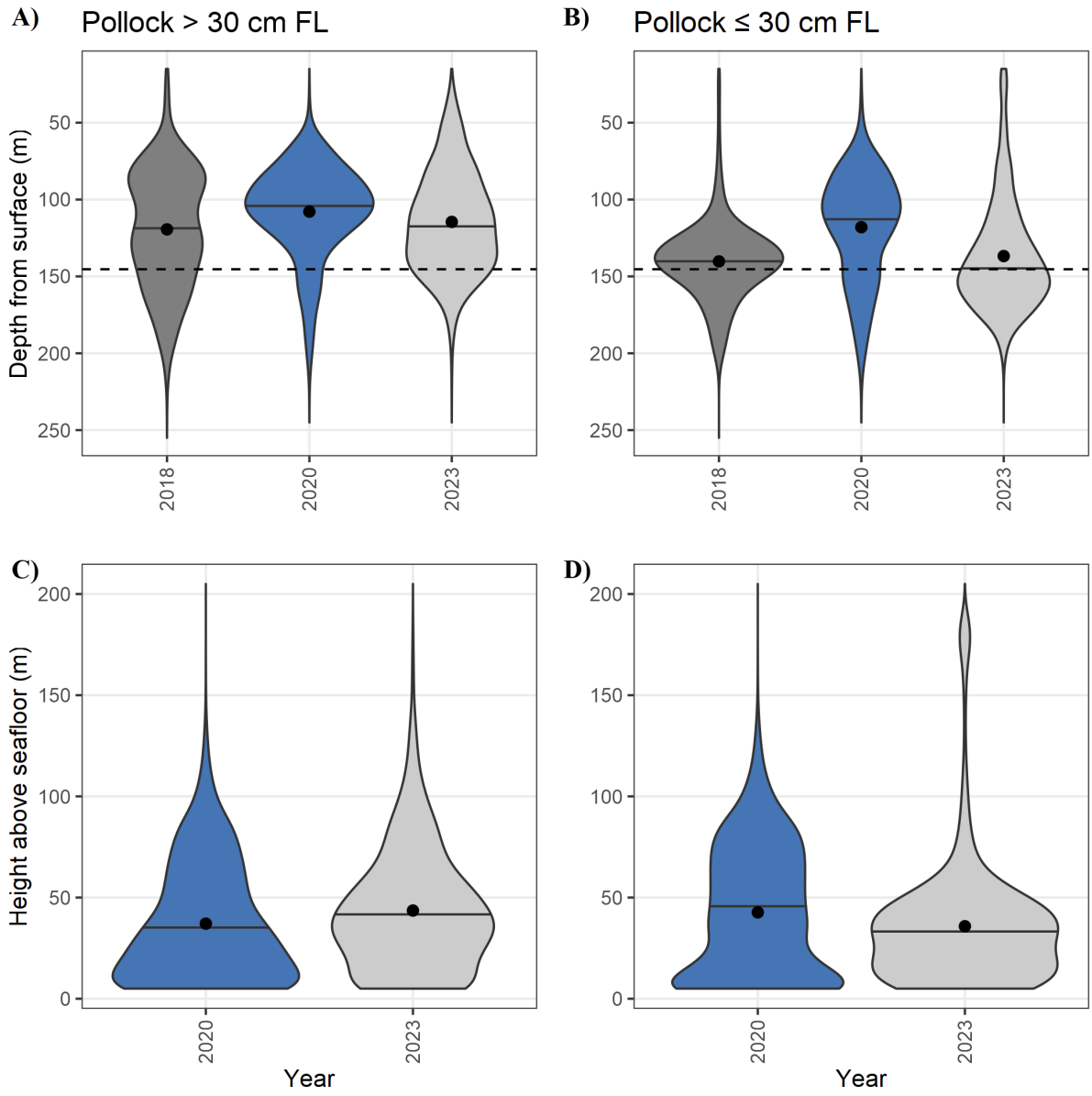

Figure 7. -- Estimated biomass distributions of large pollock (> 30 cm FL) and small pollock (≤ 30 cm FL) depth (A and B) and height (C and D) above the seafloor in the Shumagin Islands 2023 acoustic-trawl survey. Depth is referenced to the surface and height is referenced to the bottom. Data were averaged in 10 m depth bins. Mean bottom depth for 2023 is shown in A and B (dashed line). Plots show the probability density of pollock distribution, with median pollock depth noted by black horizontal lines, and the mean weighted pollock depth indicated by black points.

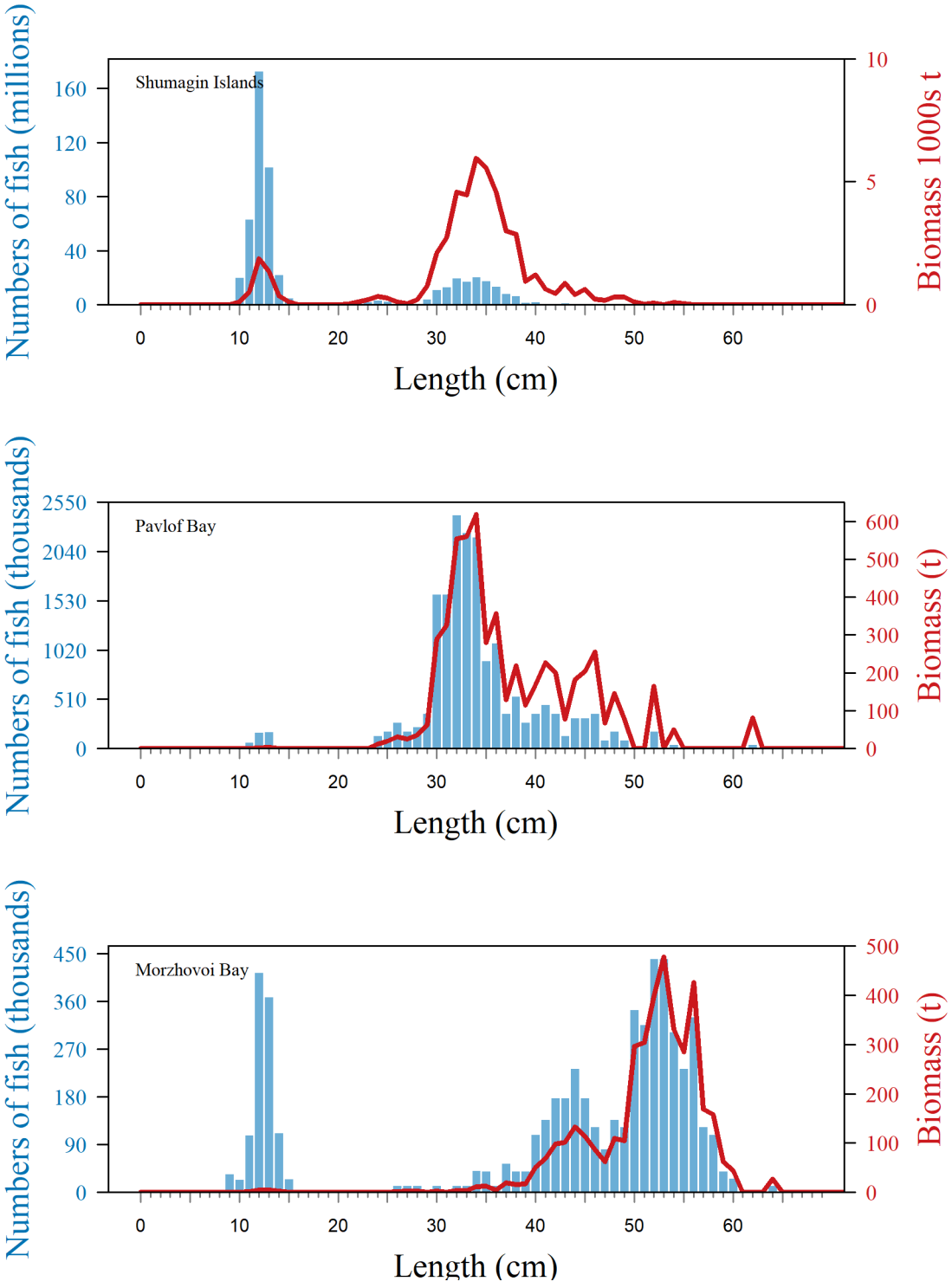

Figure 8. -- Length distribution of numbers of walleye pollock shown with blue bars and biomass estimates in red line for the 2023 acoustic-trawl survey of Shumagin Islands, Pavlof Bay, and Morzhovoi Bay.

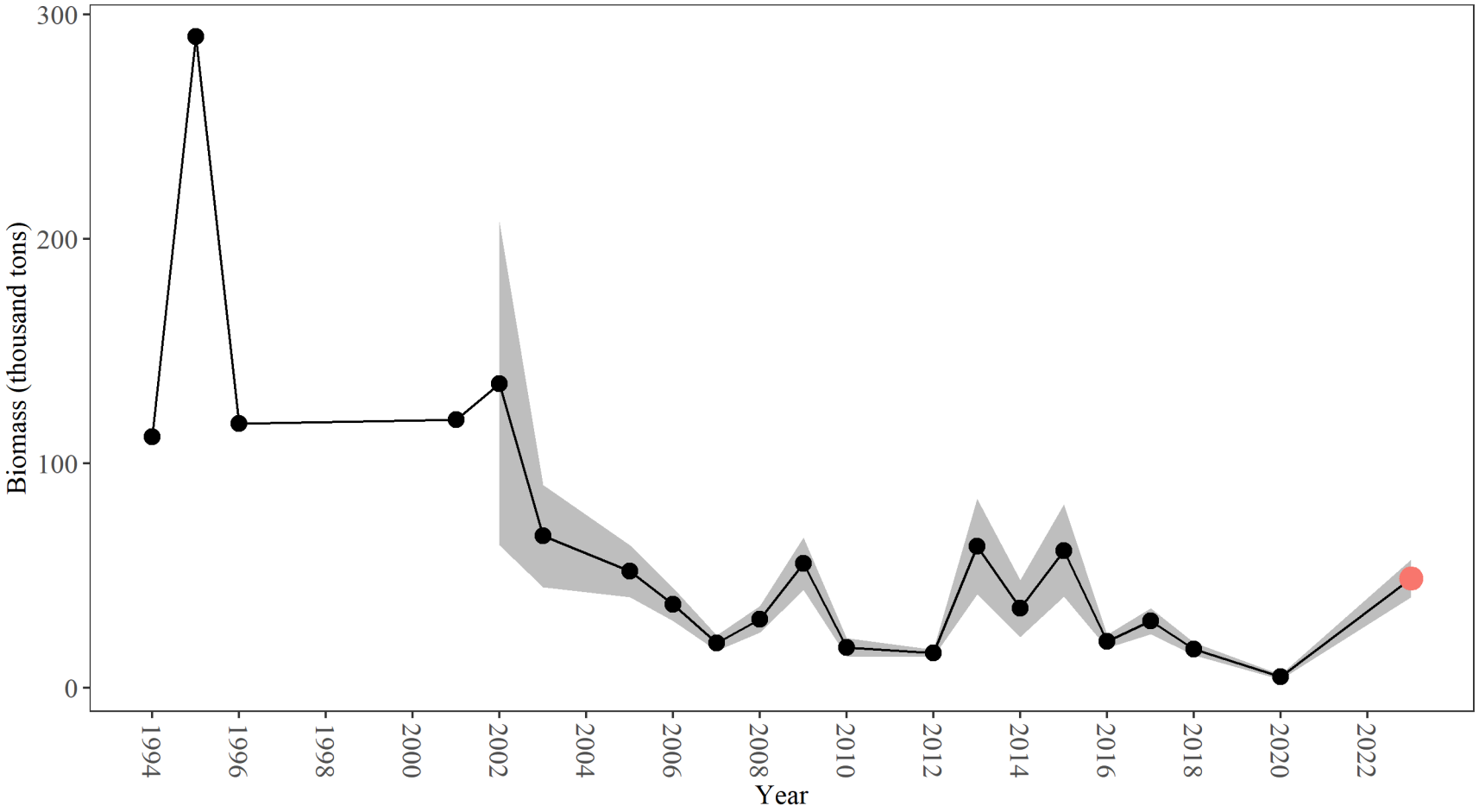

Figure 9. -- Summary of age-1+ pollock biomass estimates (thousands of tons) for Shumagin Islands based on acoustic-trawl surveys from 1994 to 2023 (except 1997-2000, 2004, 2011, 2019, 2021 and 2022). Estimates for 2009-2023 include selectivity corrections for small fish escapement (see text for explanation). Current survey estimate in red, and shaded area indicates 1-D geostatistical 95% confidence intervals for 2002-2023.

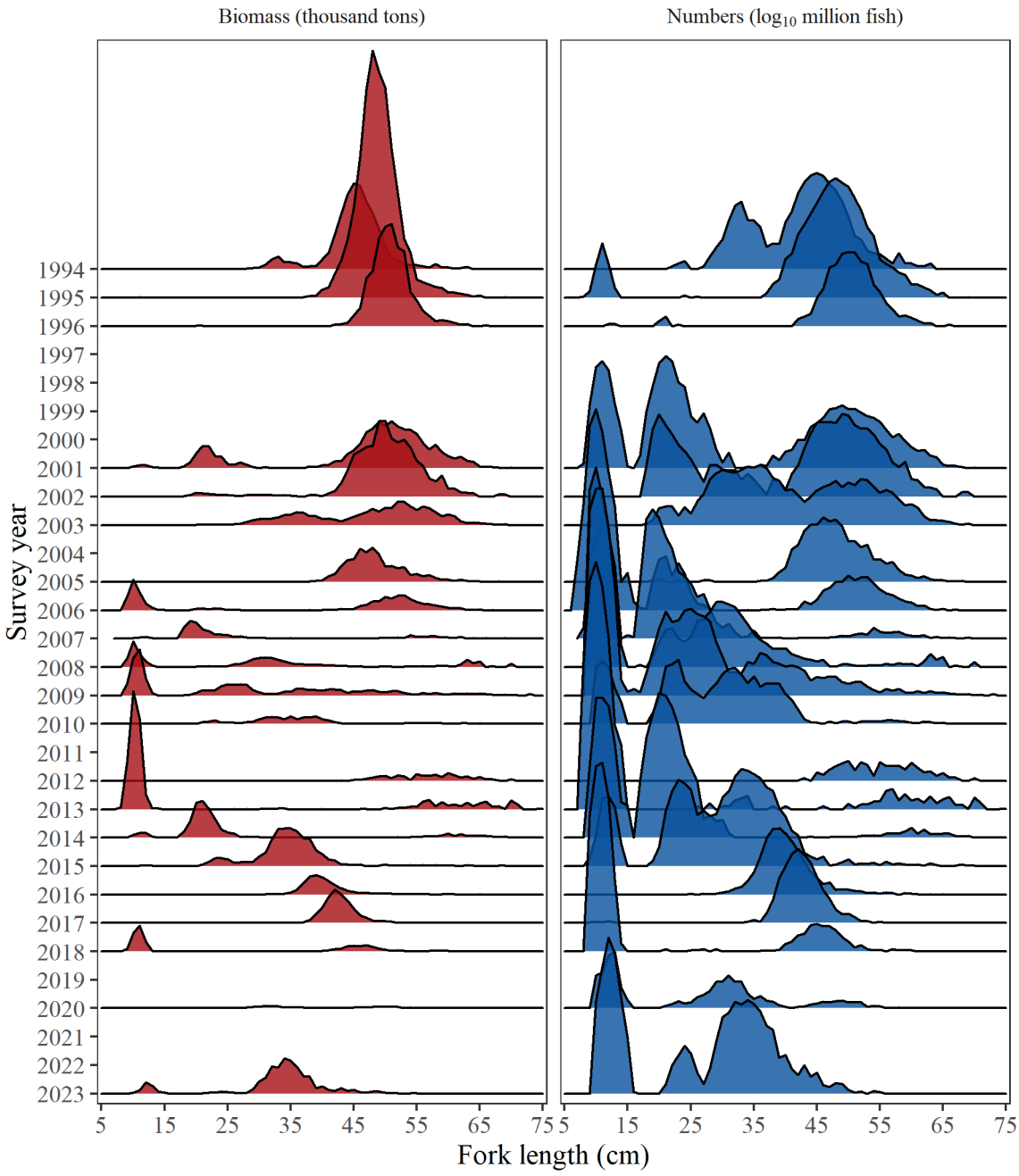

Figure 10. -- Time series of walleye pollock population size composition by weight (left panel, thousand tons) and numbers (right panel, $\log_{10}$(million fish)) from acoustic-trawl surveys of the Shumagin Islands since 1994. Estimates for 2009-2023 include selectivity corrections for small fish escapement (see text for explanation).

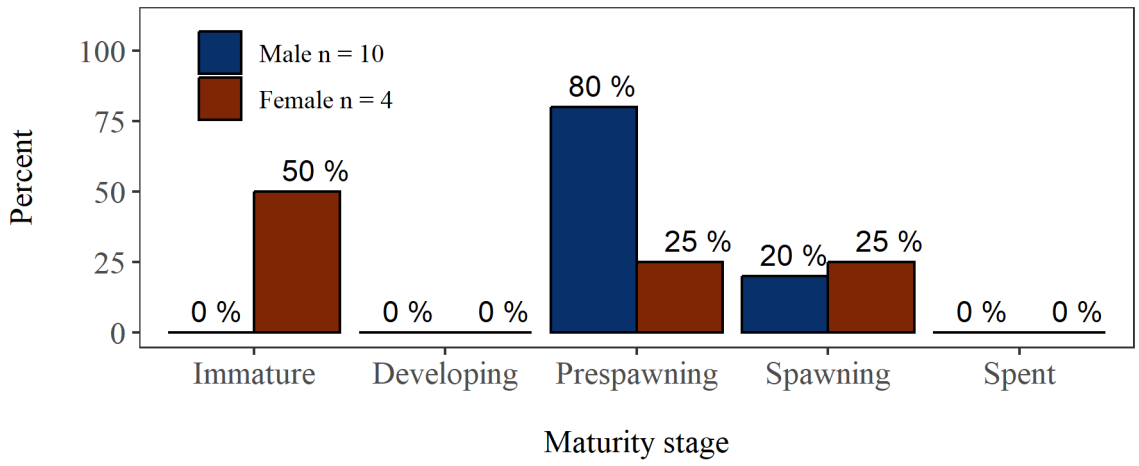

Figure 11. -- Walleye pollock maturity composition in Pavlof Bay for male and female pollock > 40 cm FL within each stage. All maturity quantities were weighted by local pollock abundance.

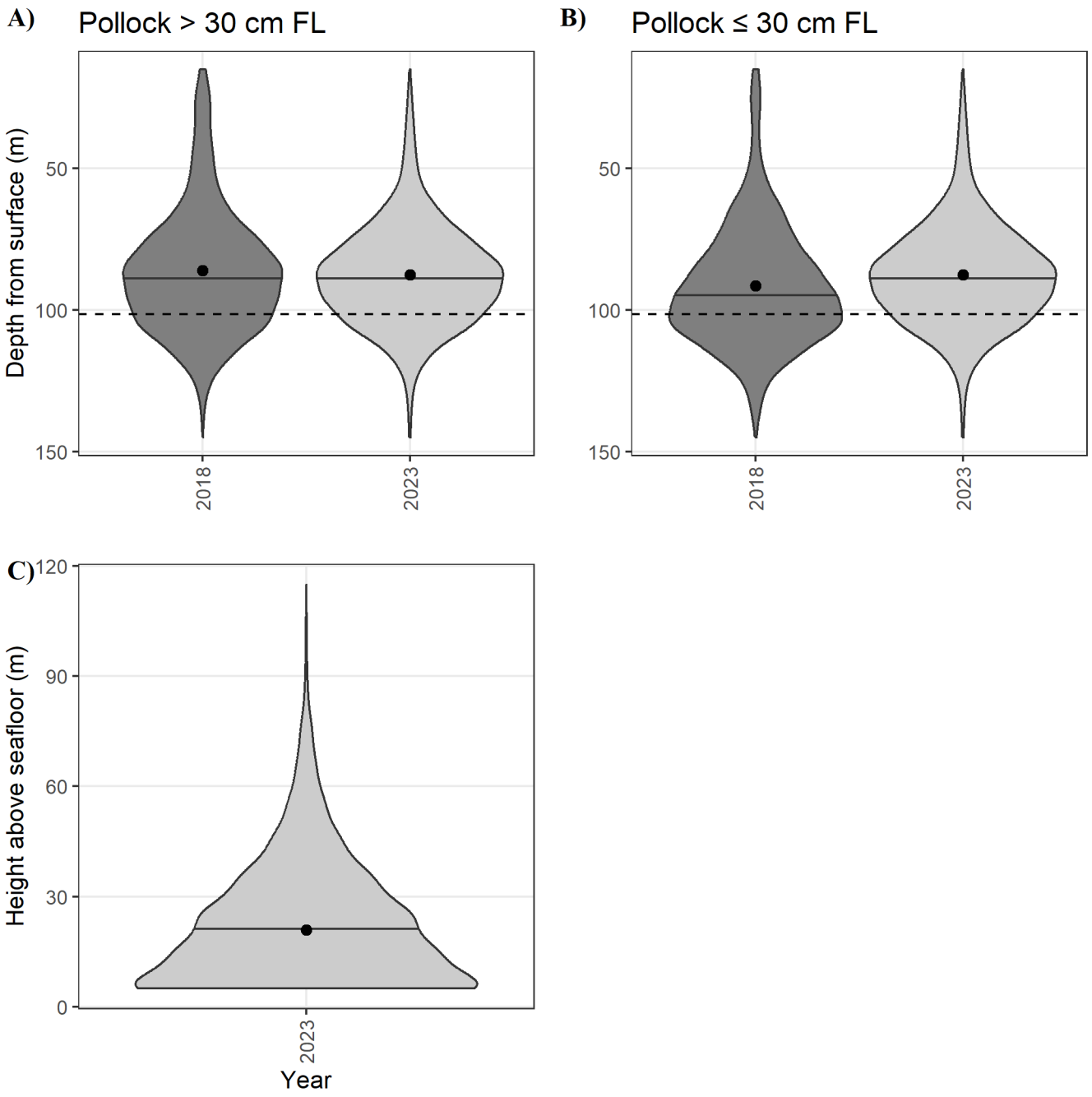

Figure 12. -- Estimated biomass distributions of large pollock (> 30 cm FL) and small pollock (≤ 30 cm FL) depth (A-B) and height (C) above the seafloor in the Pavlof Bay 2023 acoustic-trawl survey. Depth is referenced to the surface and height is referenced to the bottom. Data were averaged in 10 m depth bins. Mean bottom depth for 2023 is shown in A and B (dashed line). Plots show the probability density of pollock distribution, with median pollock depth noted by black horizontal lines, and the mean weighted pollock depth indicated by black points.

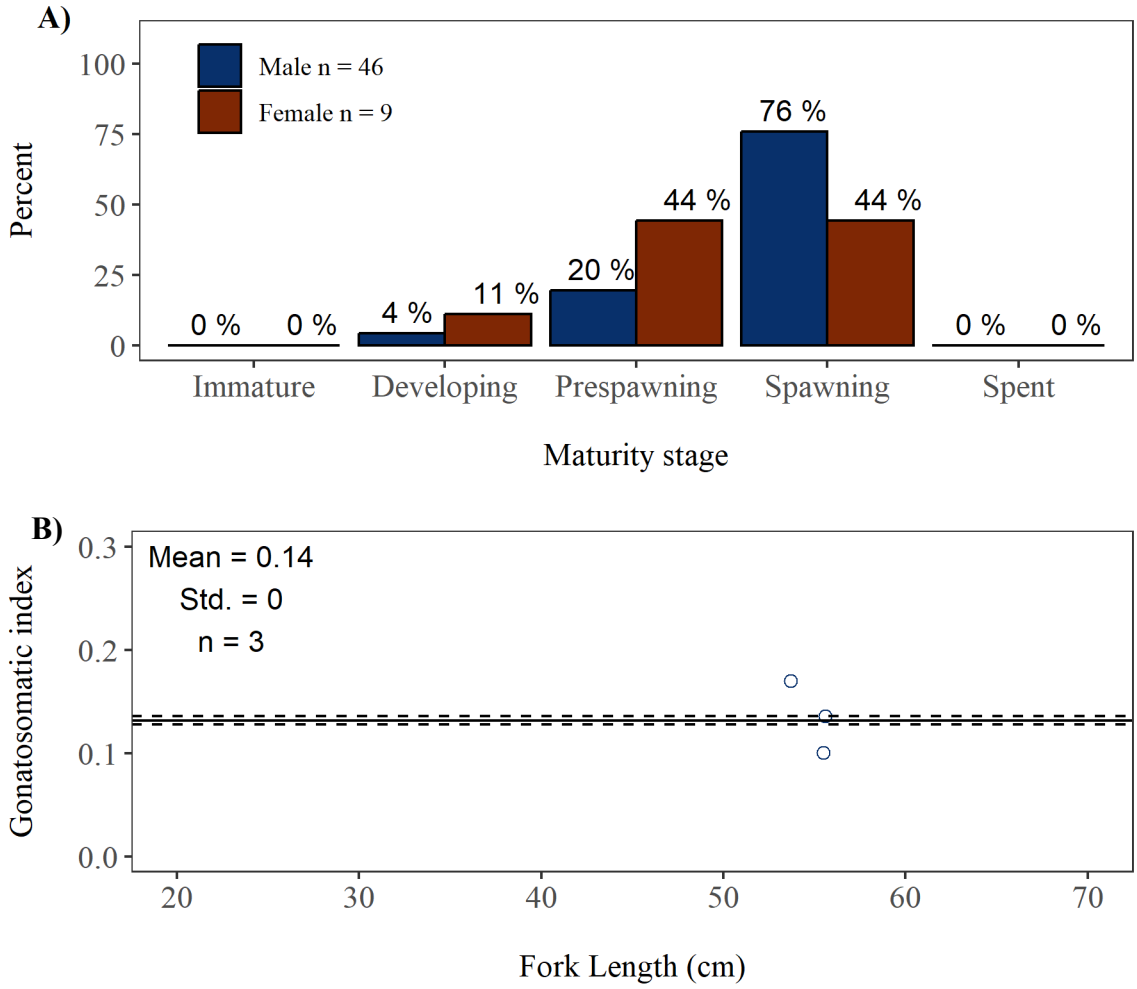

Figure 13. -- Walleye pollock maturity in Morzhovoi Bay. A) Maturity composition for male and female walleye pollock > 40 cm FL within each stage; B) gonadosomatic index for females > 40 cm FL (with historic survey mean ± 1 standard deviation (Std.). All maturity quantities were weighted by local pollock abundance.

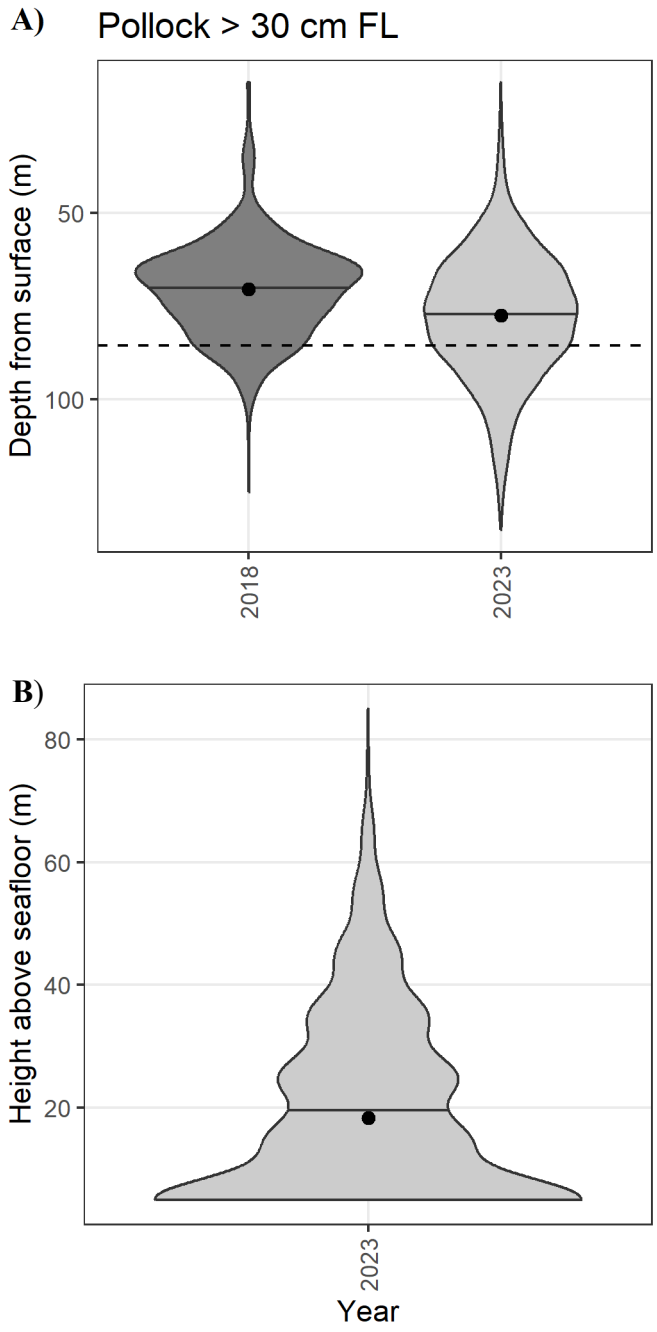

Figure 14. -- Estimated biomass distributions of pollock depth A) and height above the B) seafloor in the Morzhovoi Bay 2023 acoustic-trawl survey. Depth is referenced to the surface and height is referenced to the bottom. Data were averaged in 10 m depth bins. Mean bottom depth for 2023 is shown in A) (dashed line). Plots show the probability density of pollock distribution, with median pollock depth noted by black horizontal lines, and the mean weighted pollock depth indicated by black points.

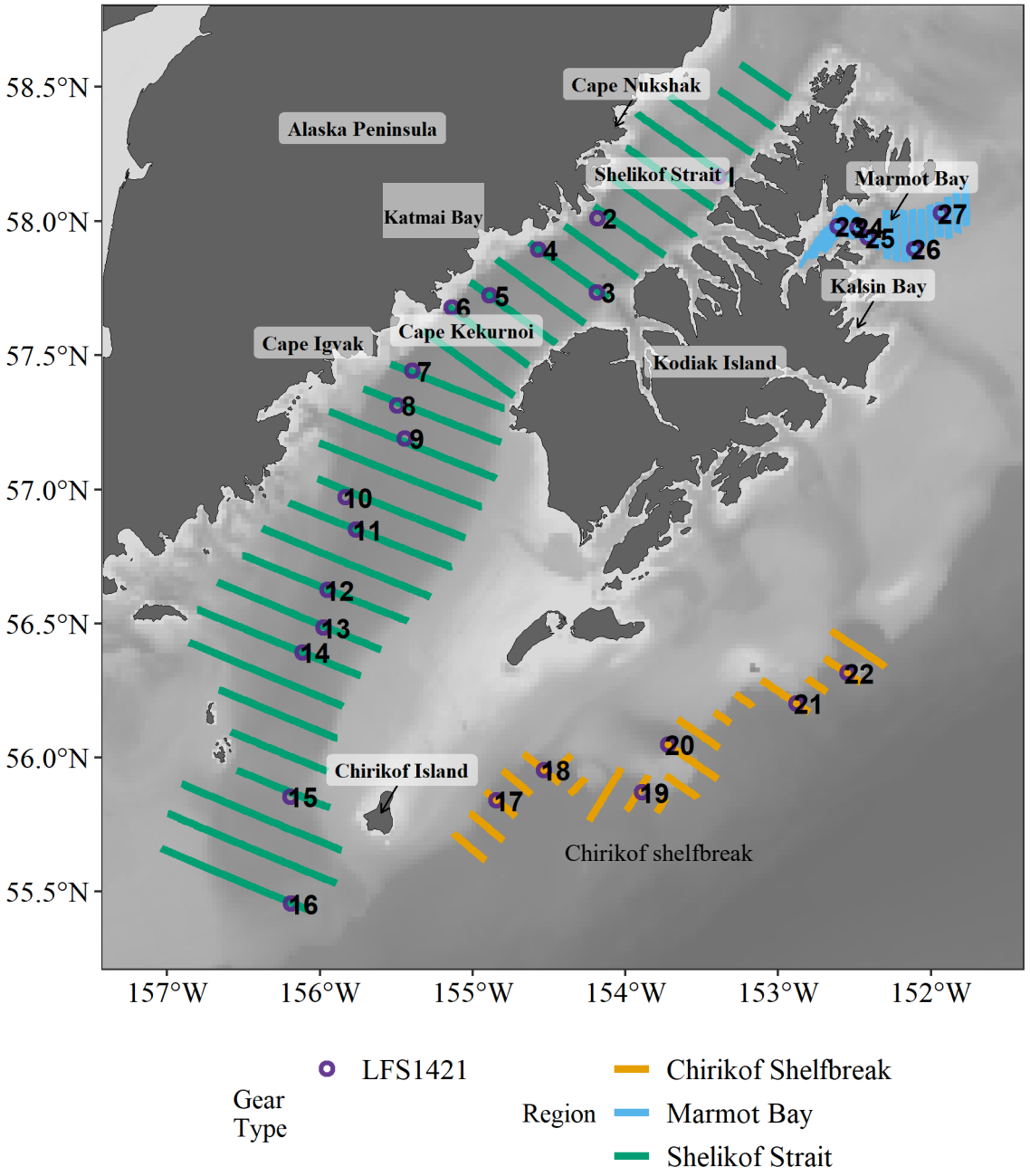

Figure 15. -- Transect lines and locations of trawl hauls during the winter 2023 acoustic-trawl survey of pollock in the Shelikof Strait, Chirikof shelfbreak, and Marmot Bay areas. Labeled areas are referenced in the text and hauls are numbered.

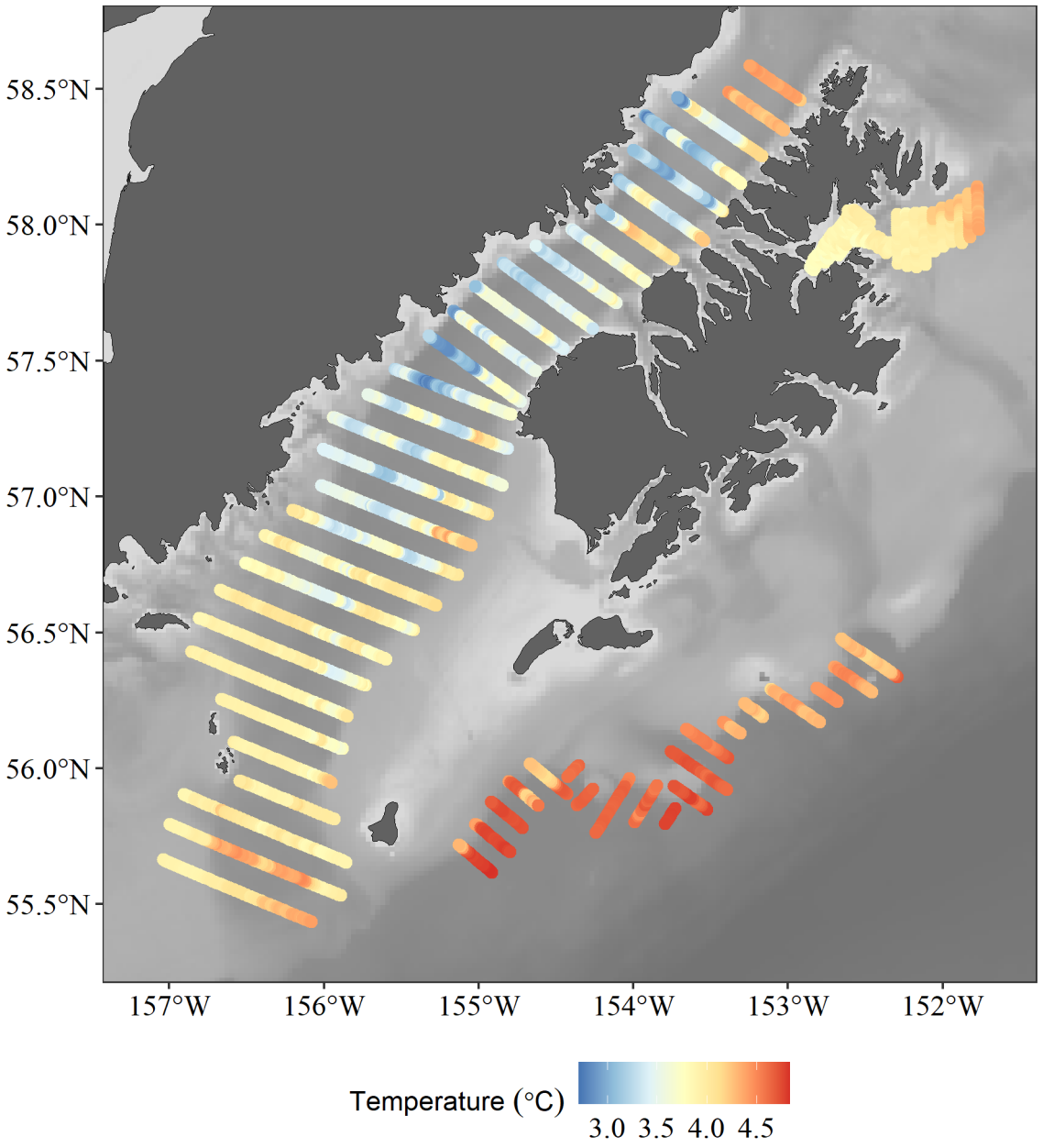

Figure 16. -- Surface water temperatures (°C) recorded at 5-second intervals during the winter 2023 acoustic-trawl survey of the Shelikof Strait, Chirikof shelfbreak, and Marmot Bay areas.

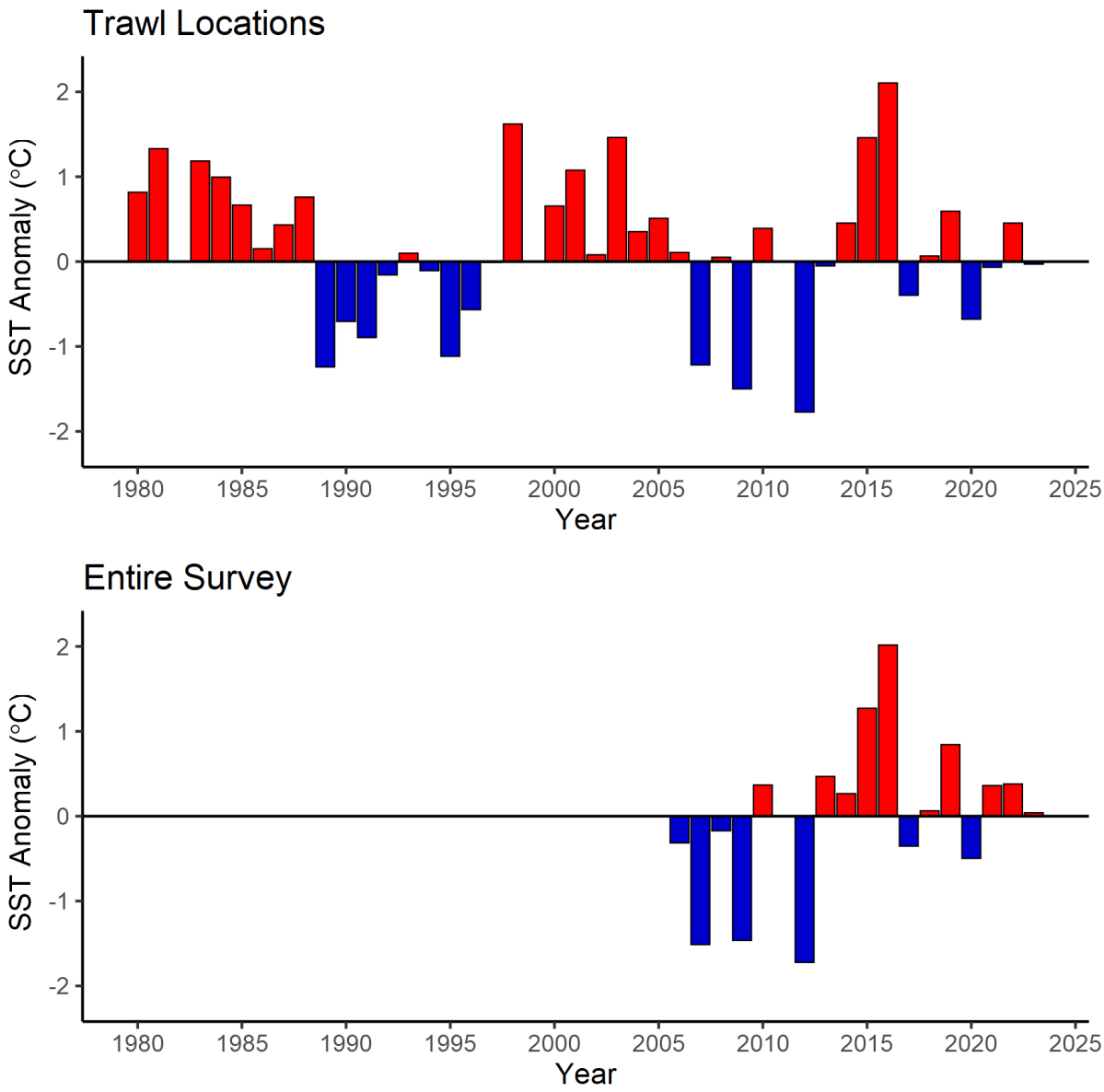

Figure 17. -- Sea surface temperature (SST, °C) anomalies recorded at trawl locations (upper panel) and from the ship's flow-through system for the entire survey (lower panel) in Shelikof Strait. SST anomalies for each temperature source are centered and scaled by their respective mean temperature and standard deviation from the 2006-2022 period. Positive and negative anomalies are indicated by red and blue bars, respectively.

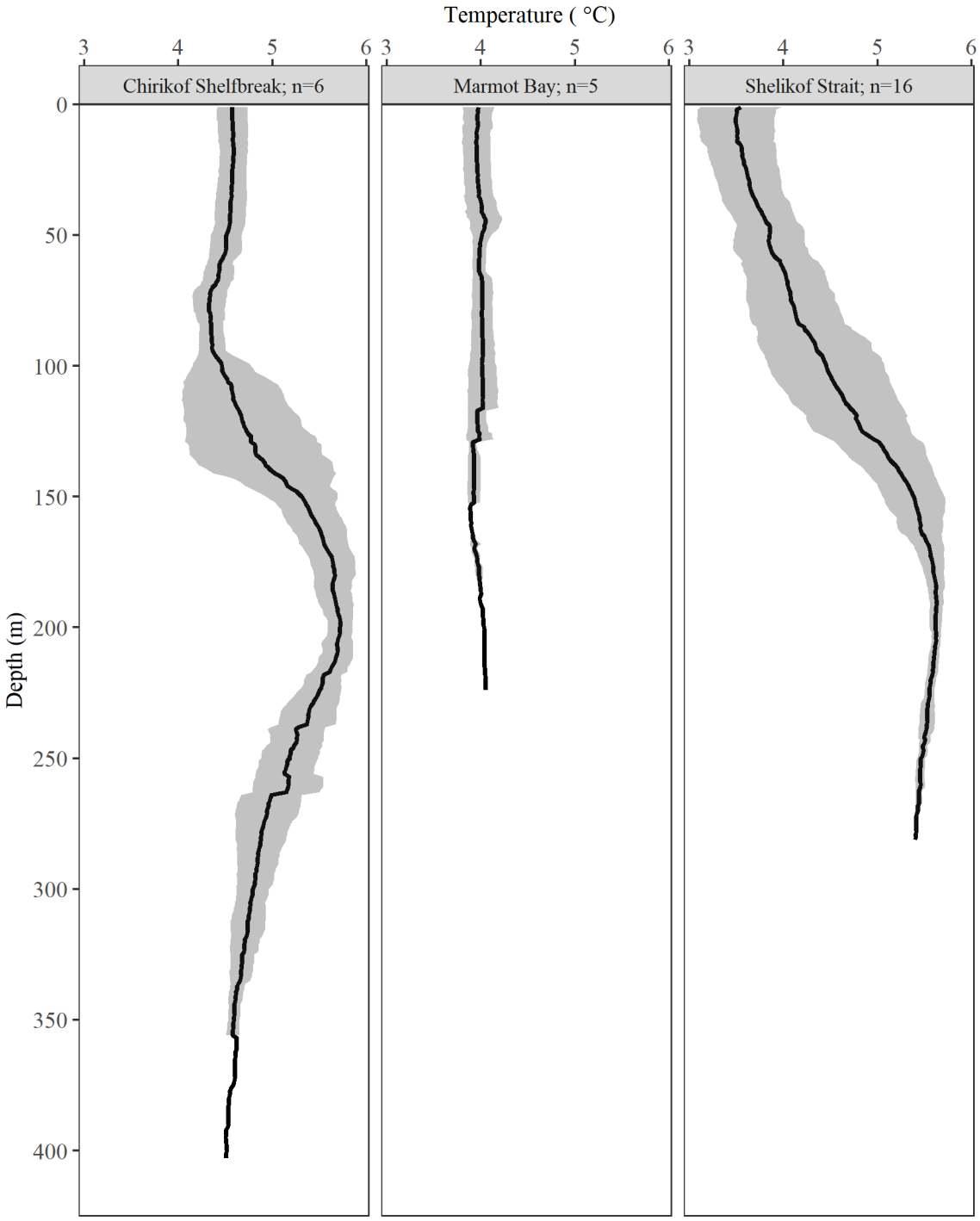

Figure 18. -- Mean water temperature (°C; solid line) by 1-m depth intervals measured at trawl locations during the 2023 acoustic-trawl survey of walleye pollock in the Shelikof Strait area. The shaded area represents one standard deviation. Number of trawls per area shown with area name.

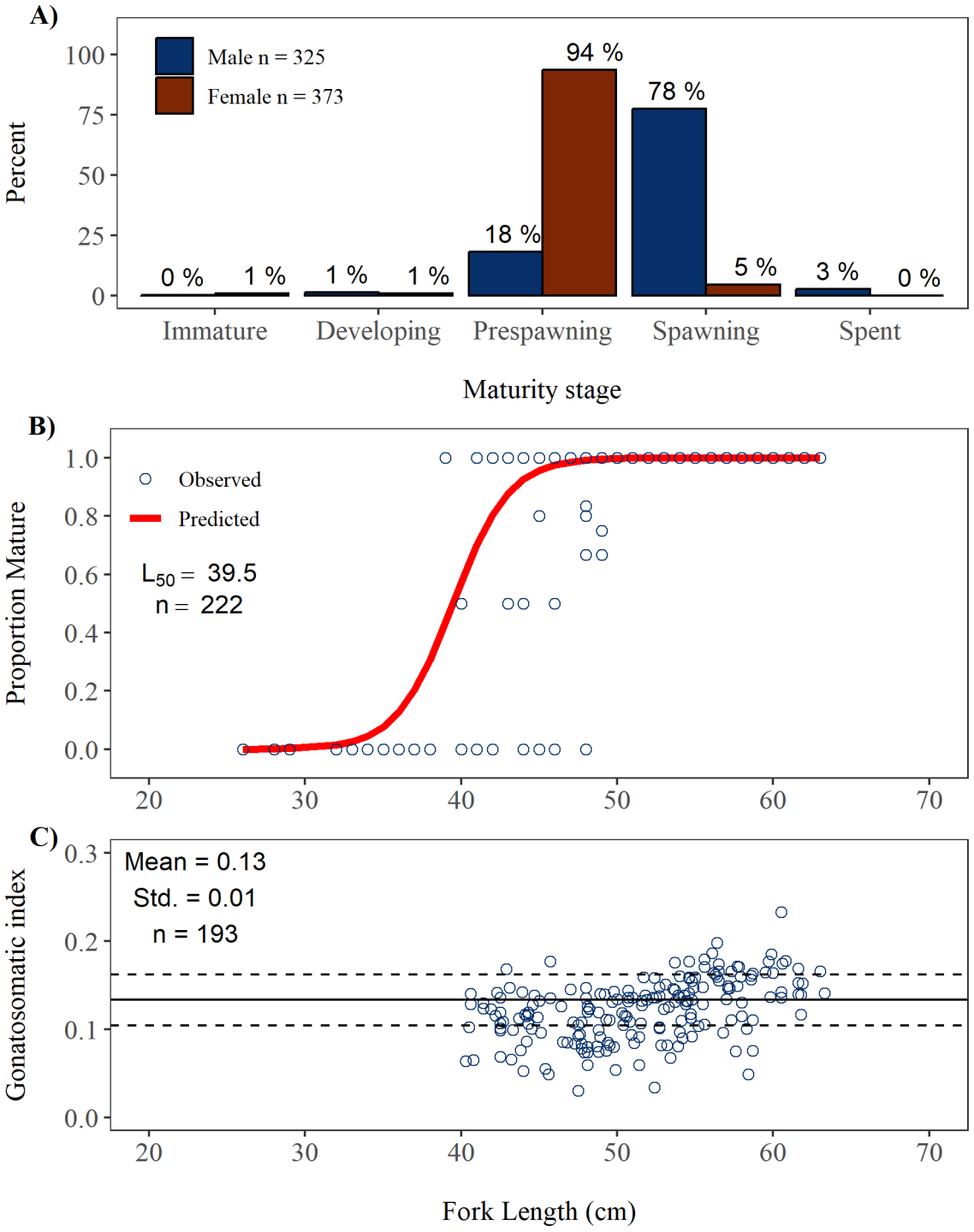

Figure 19. -- Pollock maturity in Shelikof Strait. A) Maturity composition for male and female pollock > 40 cm fork length (FL) within each stage; B) proportion mature (i.e., pre-spawning, spawning, or spent) by 1-cm size group for female pollock; C) gonadosomatic index for females > 40 cm FL (with historic survey mean ± 1 standard deviation (Std.)). All maturity quantities are weighted by local pollock abundance.

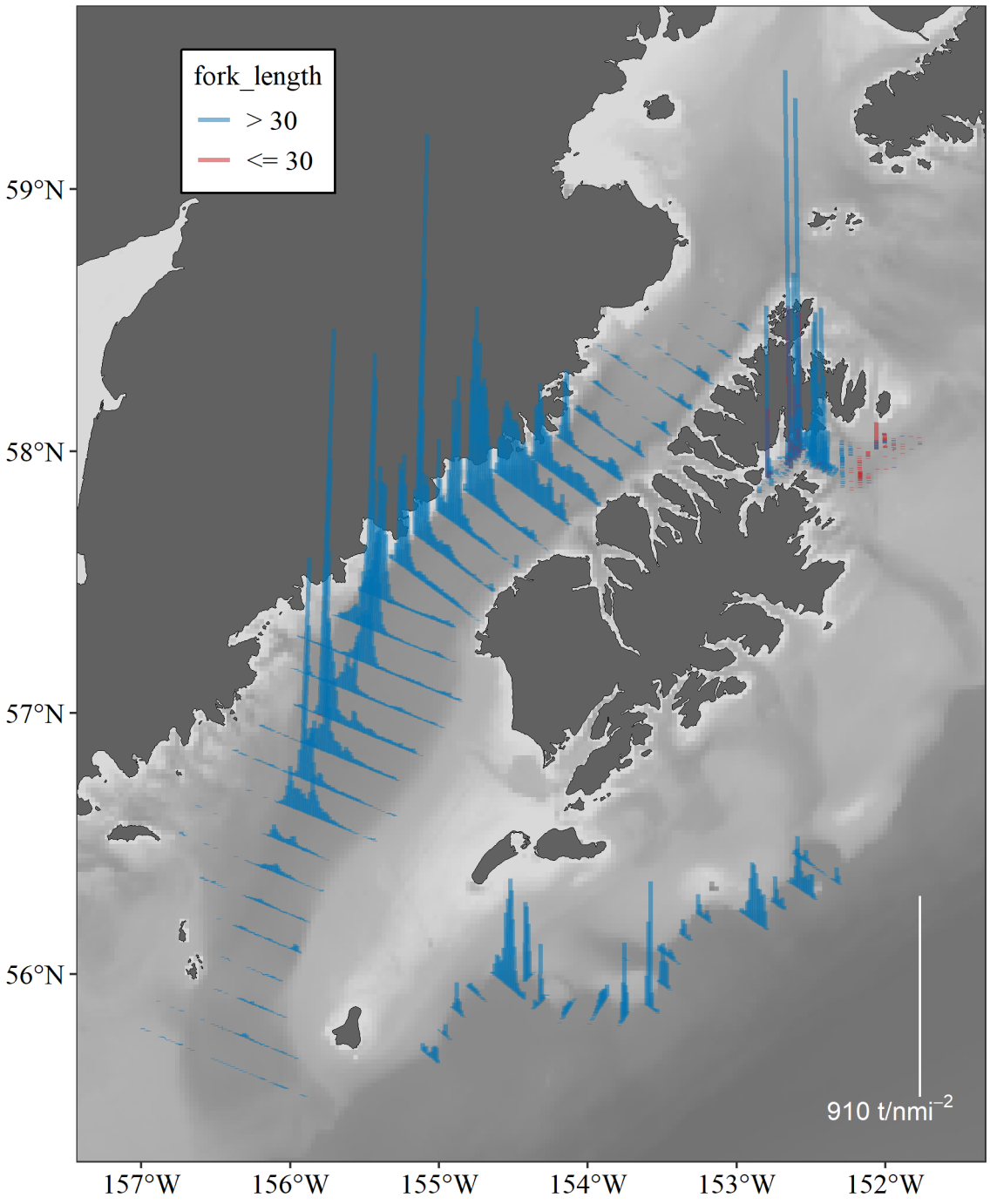

Figure 20. -- Biomass per unit area (tnmi^{-2}) attributed to pollock (vertical lines) along tracklines surveyed during the winter 2023 acoustic-trawl survey of Shelikof Strait, Chirikof shelfbreak, and Marmot Bay. Biomass densities are categorized based on haul catches of mostly large (> 30 cm FL, blue) or small (≤ 30 cm FL, red) pollock.

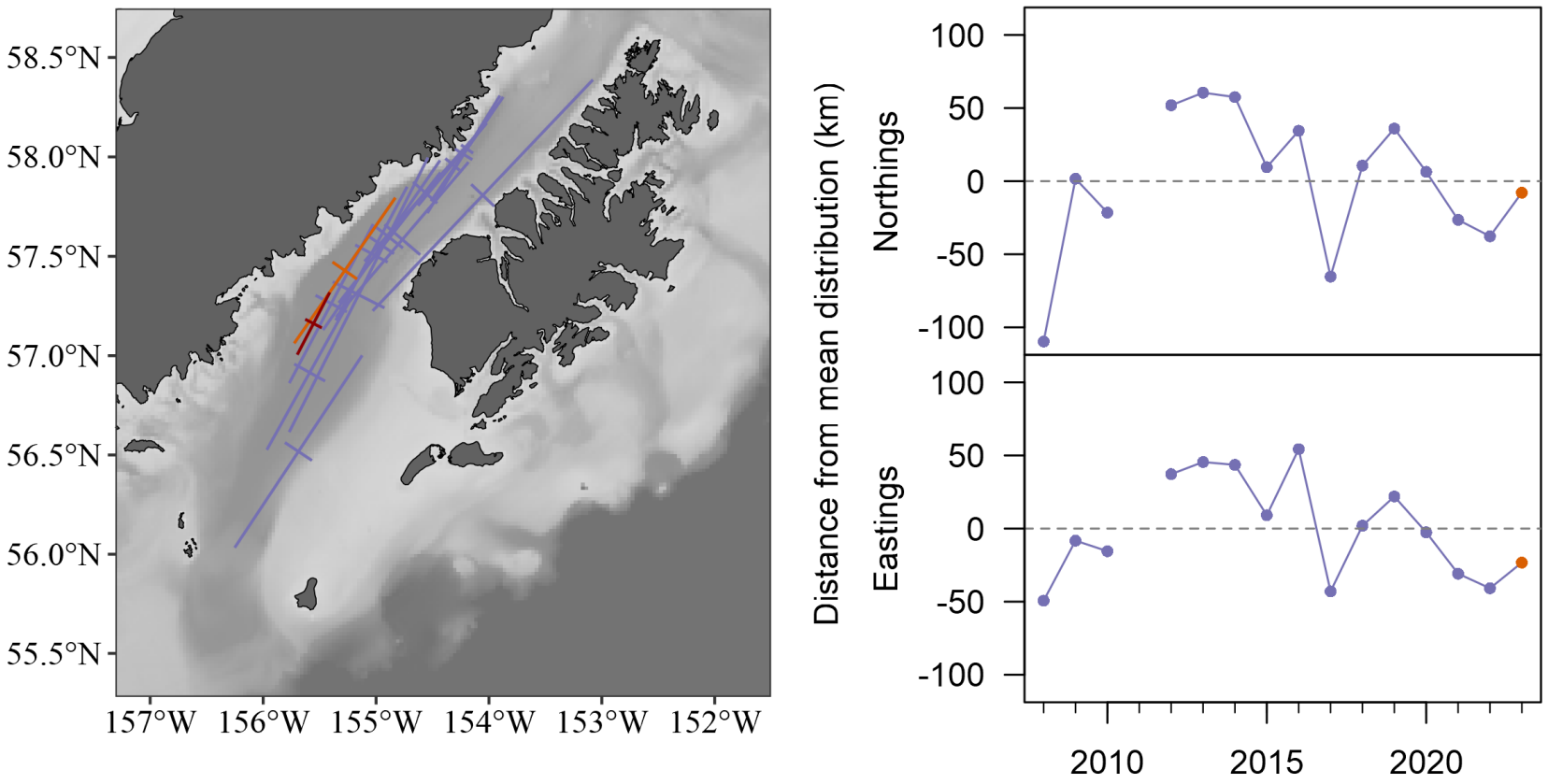

Figure 21. -- Geostatistical characterizations of pollock biomass distributions from 2008 to 2023. Center of gravity (COG, line intersection) and inertia (line length) estimates (left map) indicate the mean location and dispersion of the distribution around its COG during the 2023 survey (orange), the 2022 survey (red), and each of the other survey years (purple). Time series of COG estimates (right plots) centered by the 15-year mean are shown along latitudinal ('Northings') and longitudinal ('Eastings') axes.

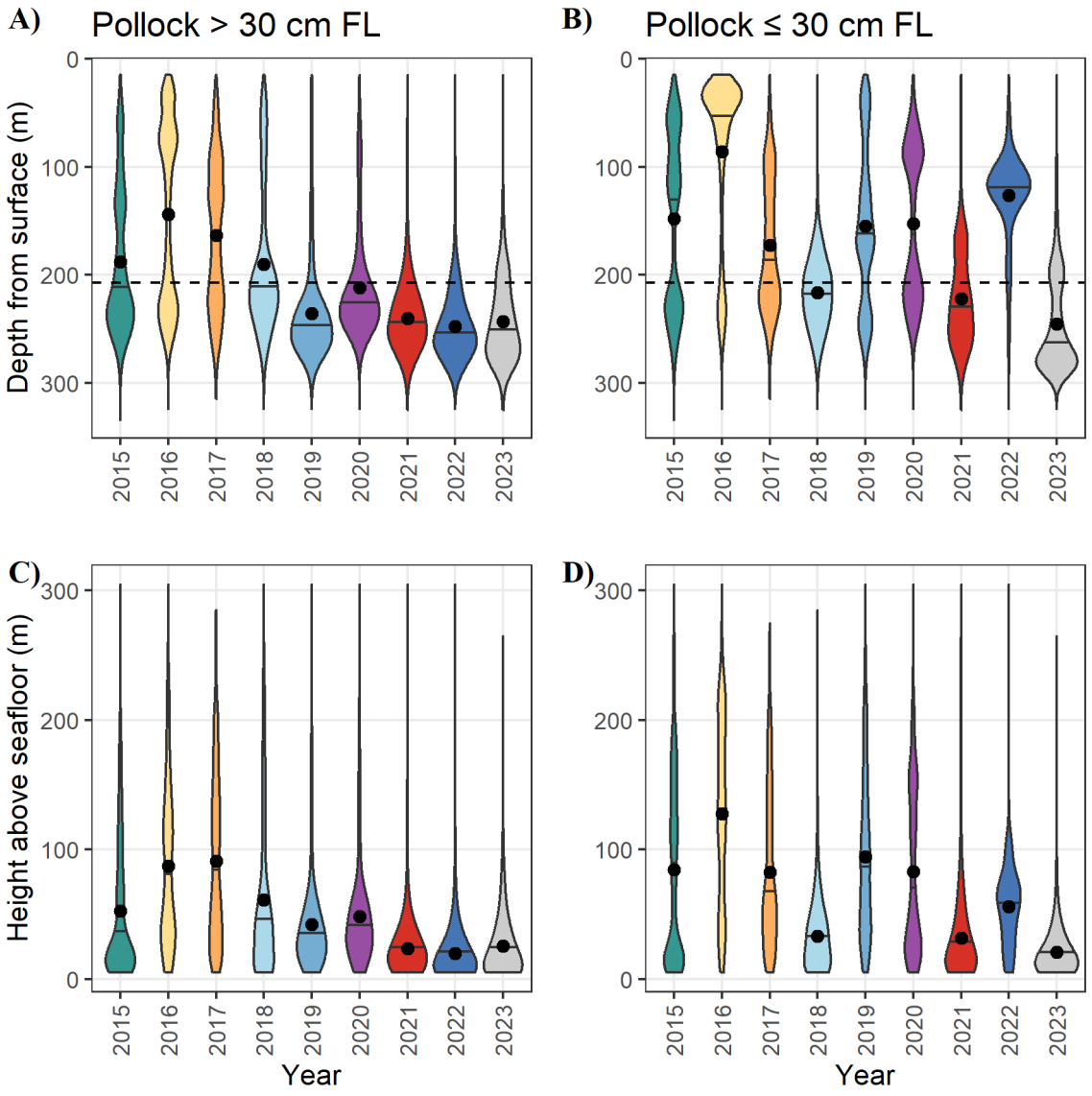

Figure 22. -- Estimated biomass distributions of larger pollock (> 30 cm FL) by depth (A) and height above the seafloor (C), and smaller pollock (≤ 30 cm FL) by depth (B) and height above the seafloor (D) in the in the Shelikof Strait 2023 acoustic-trawl survey. Results for the winter 2015-2022 acoustic-trawl surveys are included for comparison. Depth is referenced to the surface and height is referenced to the bottom. Data were averaged in 10 m depth bins. Mean bottom depth for 2023 is shown in panels A) and B) (dashed line). Plots show the probability density of pollock distribution, with median pollock depth noted by black horizontal lines, and the mean weighted pollock depth indicated by black points.

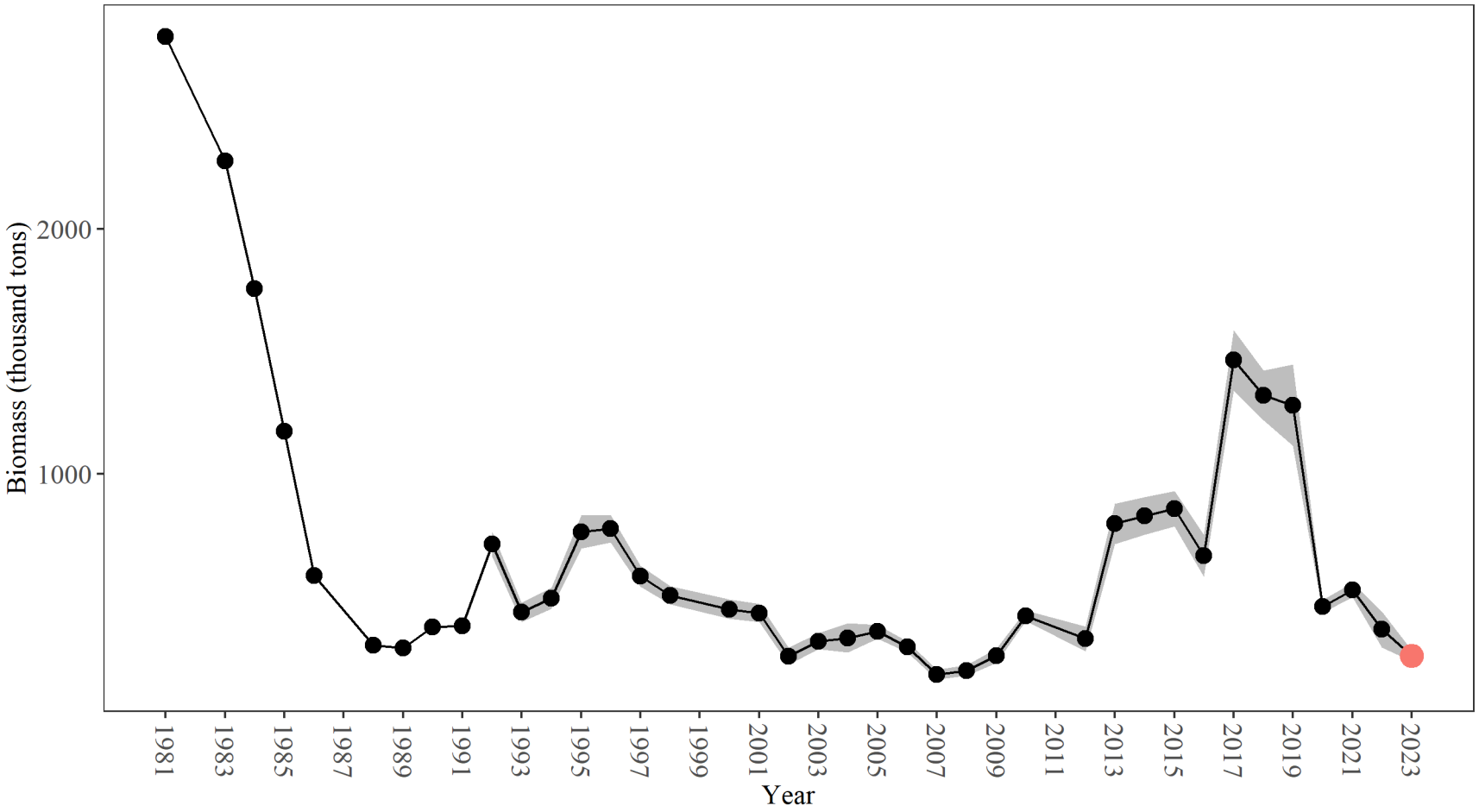

Figure 23. -- Summary of age-1+ pollock biomass estimates (thousands of metric tons) for Shelikof Strait based on acoustic-trawl surveys from 1981-2023 (except 1982, 1987, 1999, and 2011). Estimates for 2008-2023 include selectivity corrections for small fish escapement (see text for explanation). Current survey estimate in red, and shaded area indicates 1-D geostatistical 95% confidence intervals for 1992-2023.

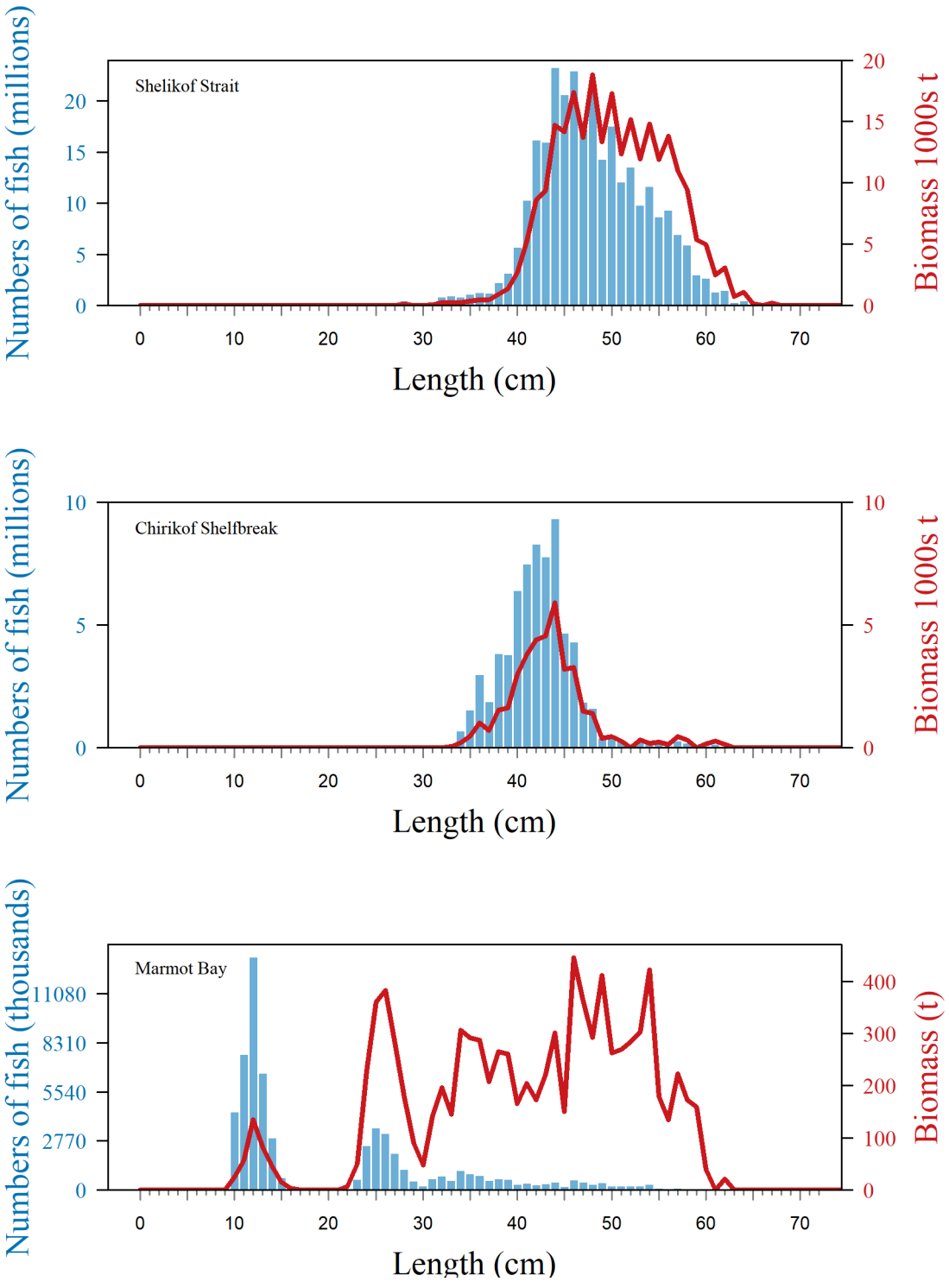

Figure 24. -- Numbers- (blue bars) and biomass- (red line) at-length estimates of pollock for the 2023 acoustic-trawl survey of Shelikof Strait, Chirikof shelfbreak, and Marmot Bay.

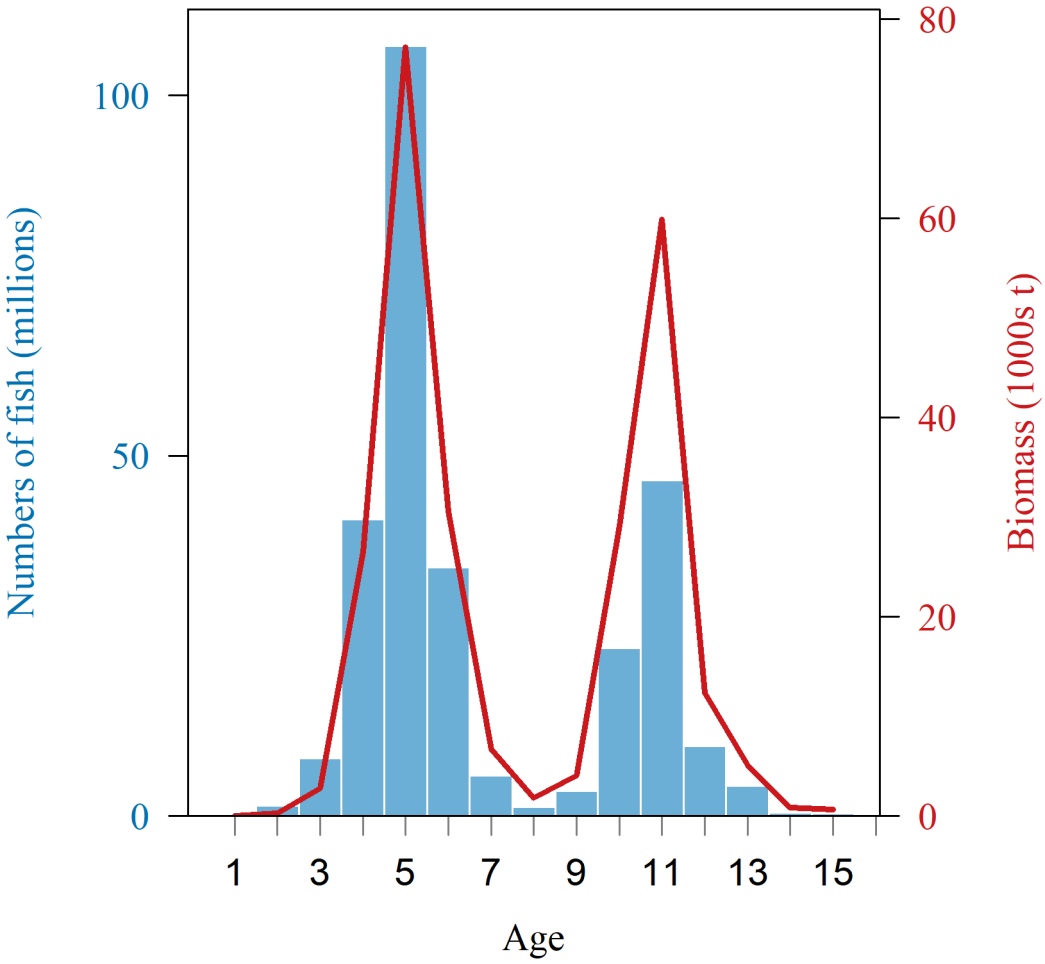

Figure 25. -- Numbers- (millions of fish, blue bars) and biomass- (1,000s t, red line) at-age estimates of pollock for the 2023 acoustic-trawl survey of Shelikof Strait.

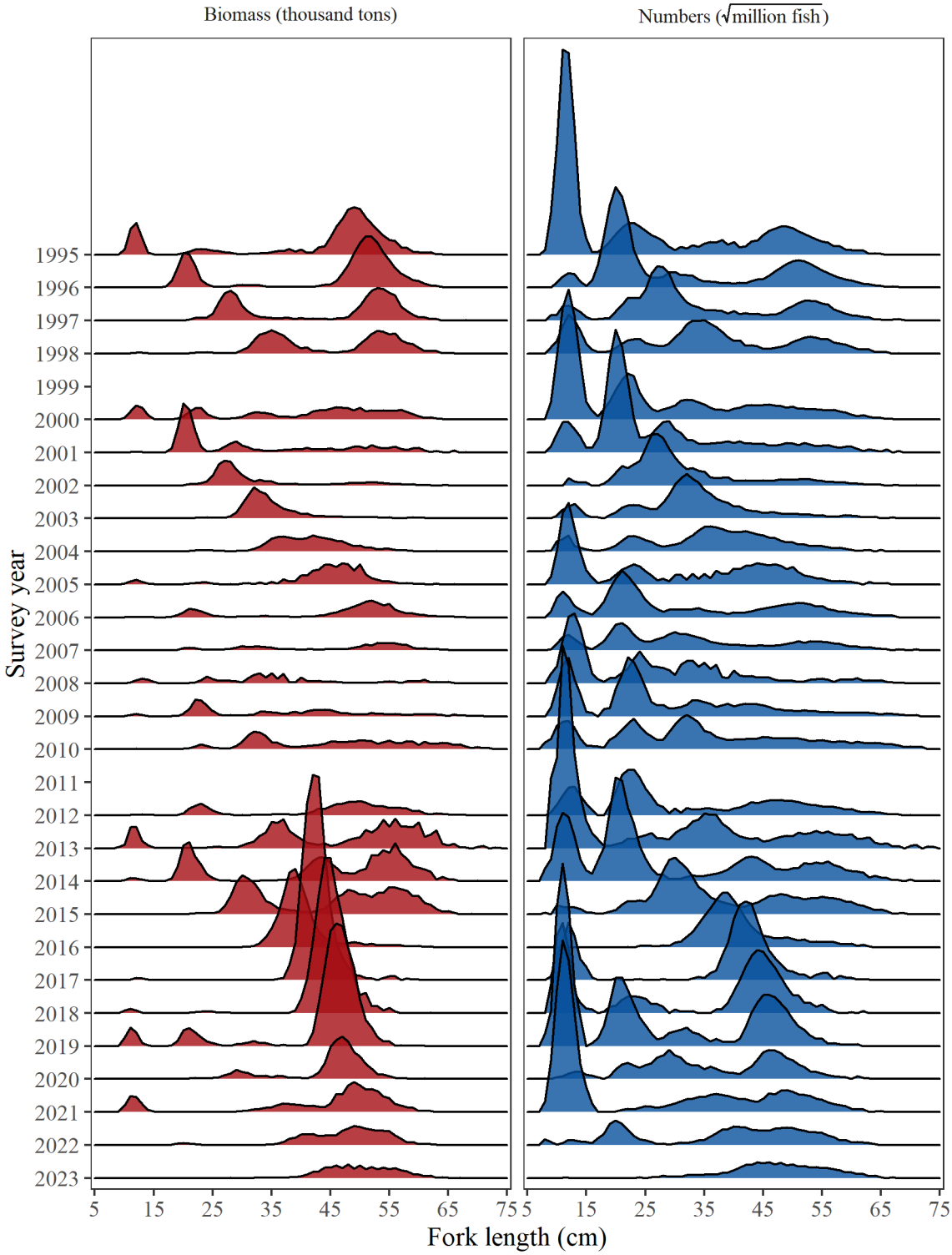

Figure 26. -- Time series of pollock population length composition by weight (left panel, thousand t) and numbers (right panel, million fish) from acoustic-trawl surveys of the Shelikof Strait for 1995-2023. Estimates for 2008-2023 include selectivity corrections for small fish escapement (see text for explanation).

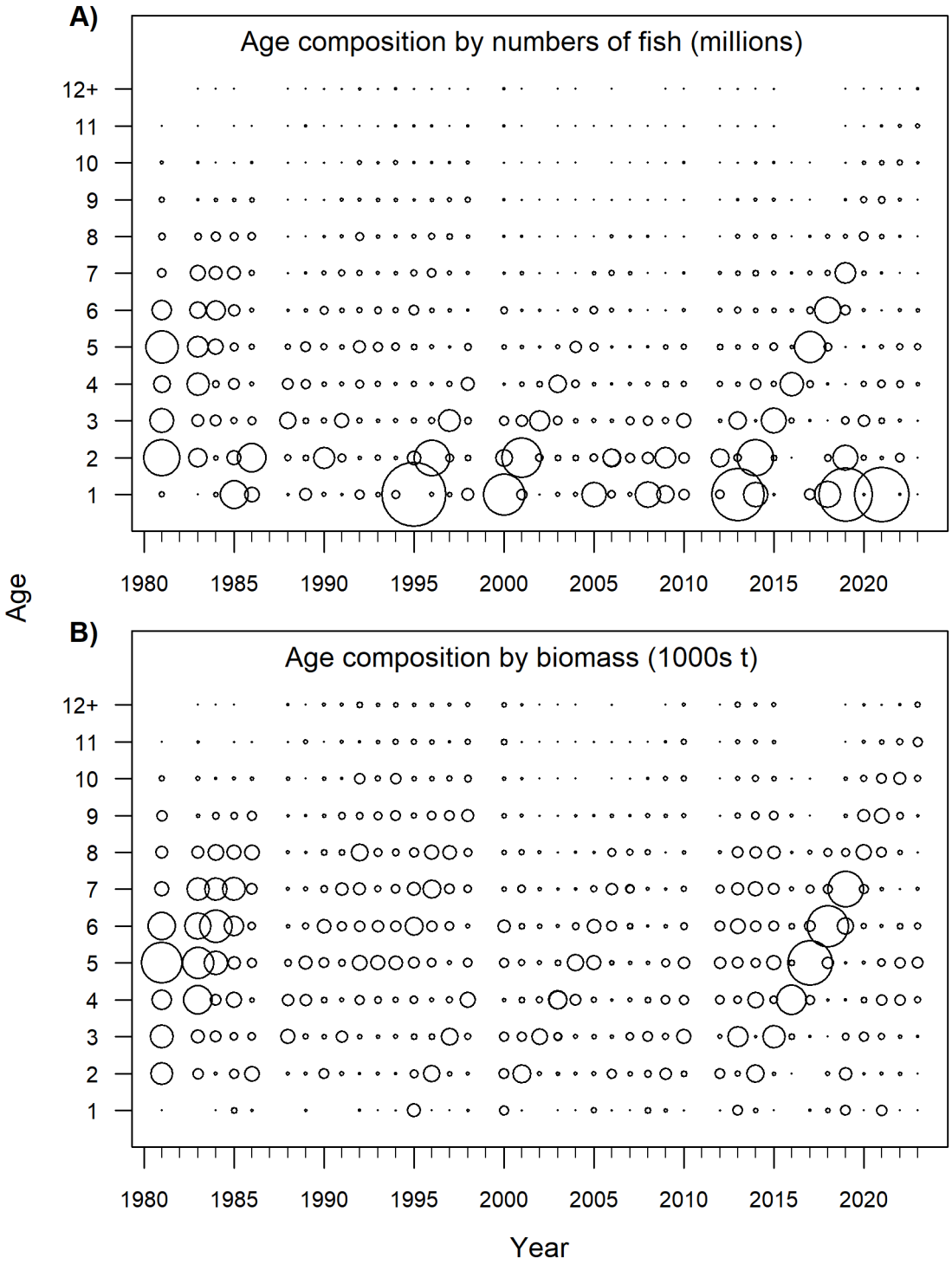

Figure 27. -- Time series of pollock population age composition by A) numbers (millions of fish) and B) biomass (1000s t) from acoustic-trawl surveys of Shelikof Strait area for 1981-2023. Estimates for 2008-2023 include selectivity corrections for small fish escapement (see text for explanation). Bubble size is scaled based on square root transform of numbers/biomass estimate by age.

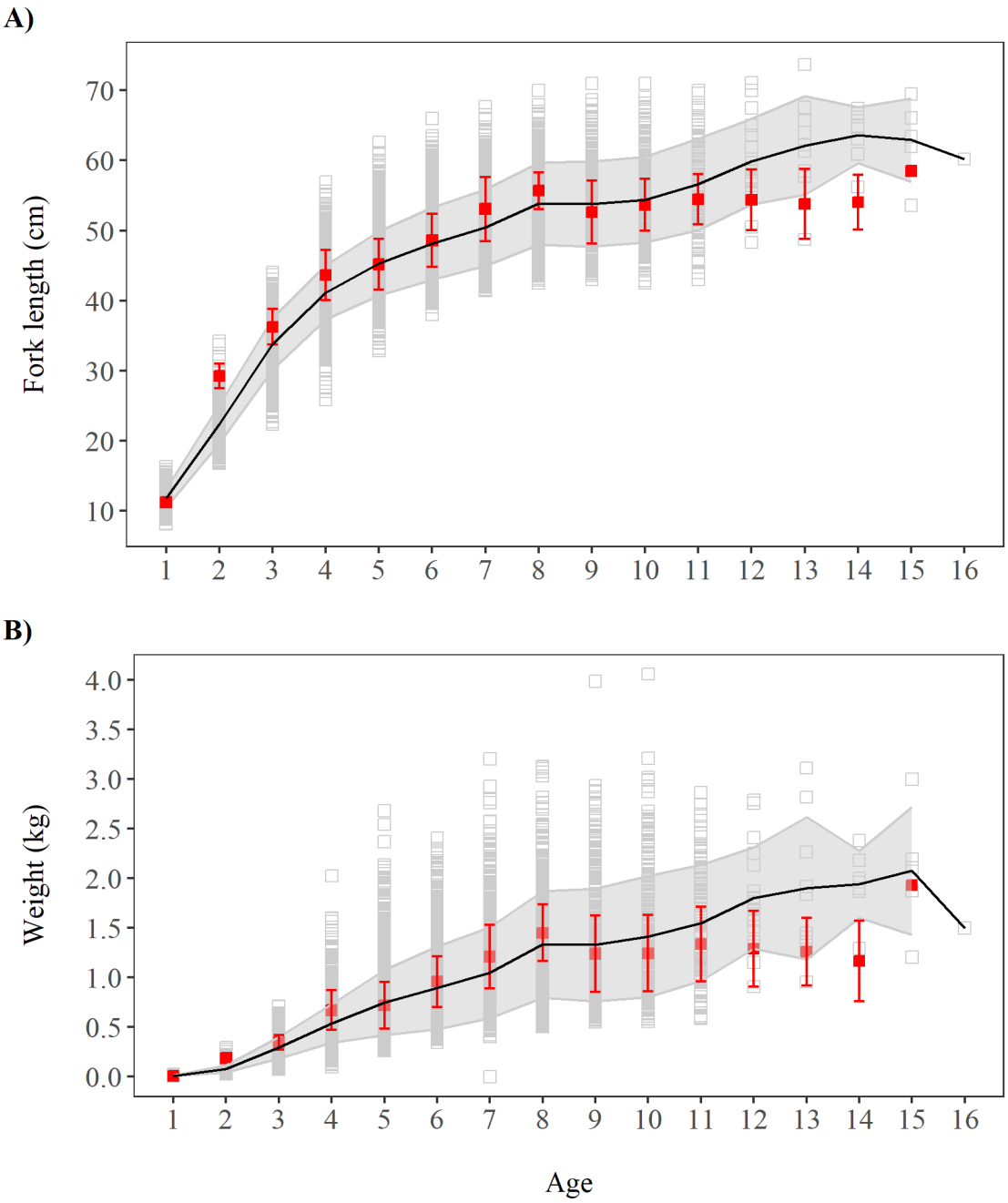

Figure 28. -- Pollock A) length- and B) weight-at-age for Shelikof Strait. The 2023 survey is highlighted in red (mean +/- 1 standard deviation). Gray squares indicate the range of observations in previous surveys (2008-2022), and the black line and gray ribbon indicate mean length- or weight-at-age in previous surveys +/- 1 standard deviation.

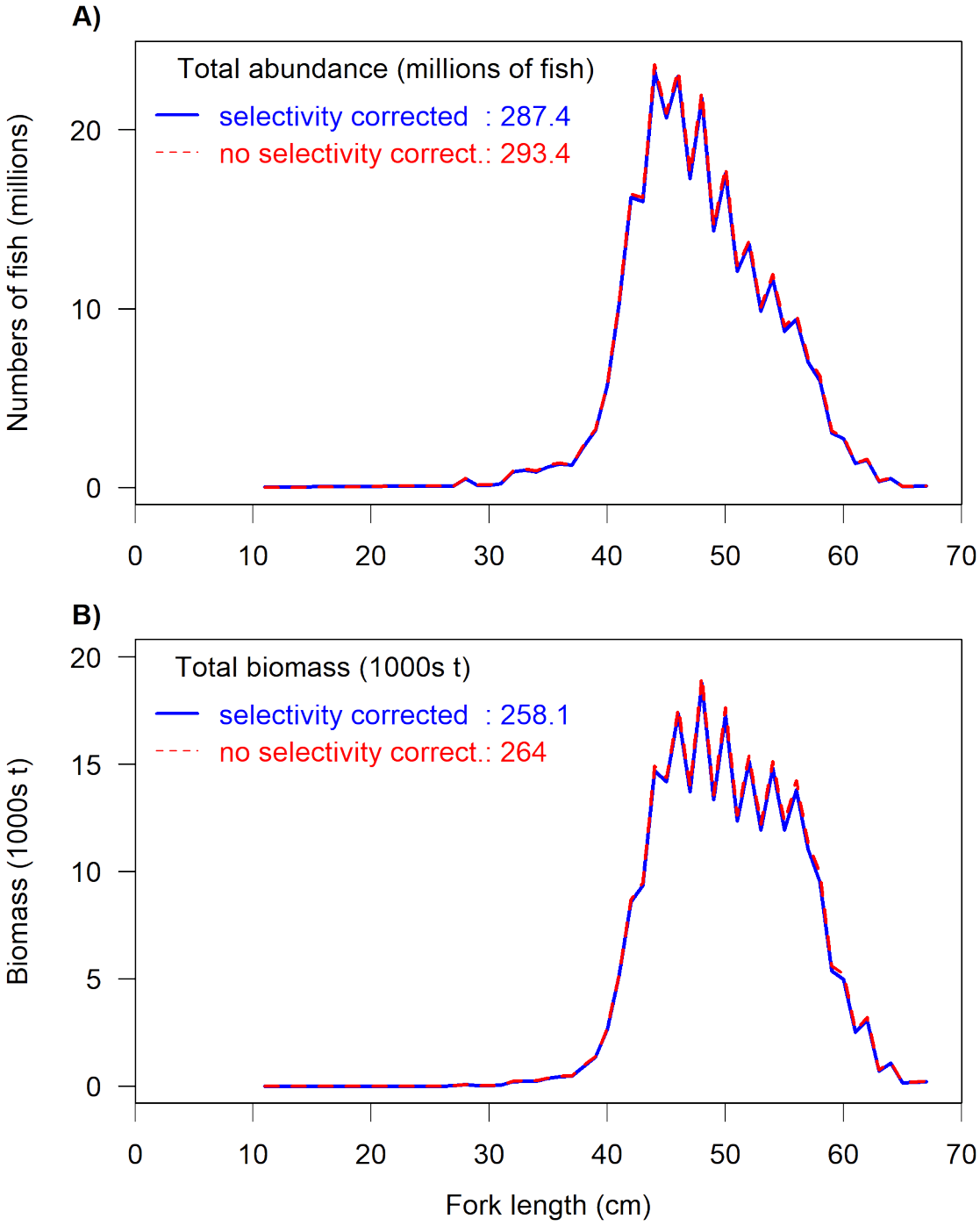

Figure 29. -- A) Numbers- and B) biomass-at-length estimates for the Shelikof Strait primary analysis corrected for net selectivity ('selectivity corrected') compared with estimates for the 'no-selectivity' analysis that do not include the effect of net selectivity ('no selectivity correct.'). The total numbers of fish (millions) and biomass (1,000s t) are also presented for each analysis.

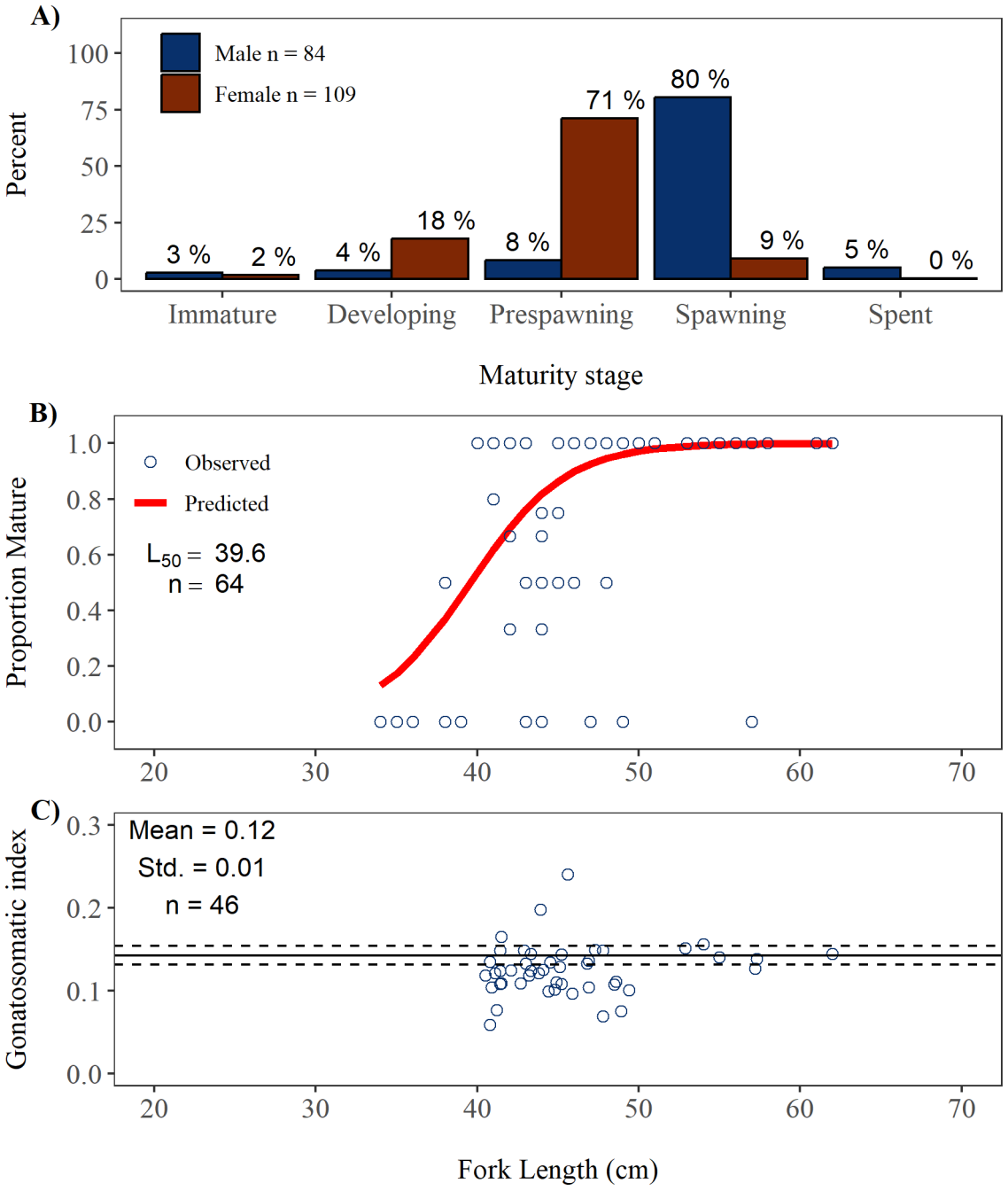

Figure 30. -- Pollock maturity in Chirikof shelfbreak. A) Maturity composition for male and female pollock > 40 cm fork length (FL) within each stage; B) proportion mature (i.e., pre-spawning, spawning, or spent) by 1-cm size group for female pollock; C) gonadosomatic index for females > 40 cm FL (with historic survey mean ± 1 standard deviation (Std.)). All maturity quantities are weighted by local pollock abundance.

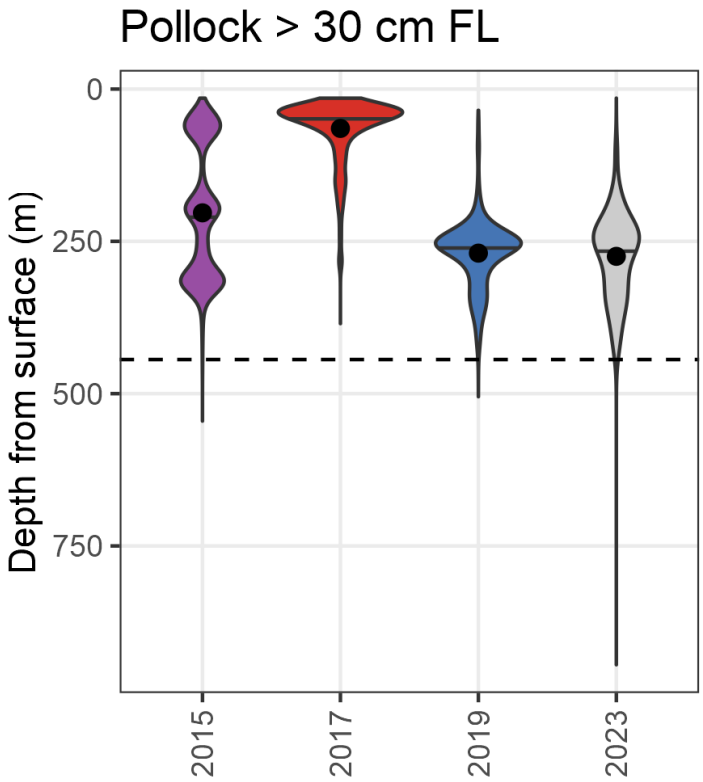

Figure 31. -- Estimated biomass distributions of pollock (> 30 cm FL) depth in the Chirikof shelfbreak 2023 acoustic-trawl survey. Results for the winter 2015-2019 acoustic-trawl surveys are included for comparison. Depth is referenced to the surface. Data were averaged in 10 m depth bins. Mean bottom depth for 2023 is shown (dashed line). Plots show the probability density of pollock distribution, with median pollock depth noted by black horizontal lines, and the mean weighted pollock depth indicated by black points.

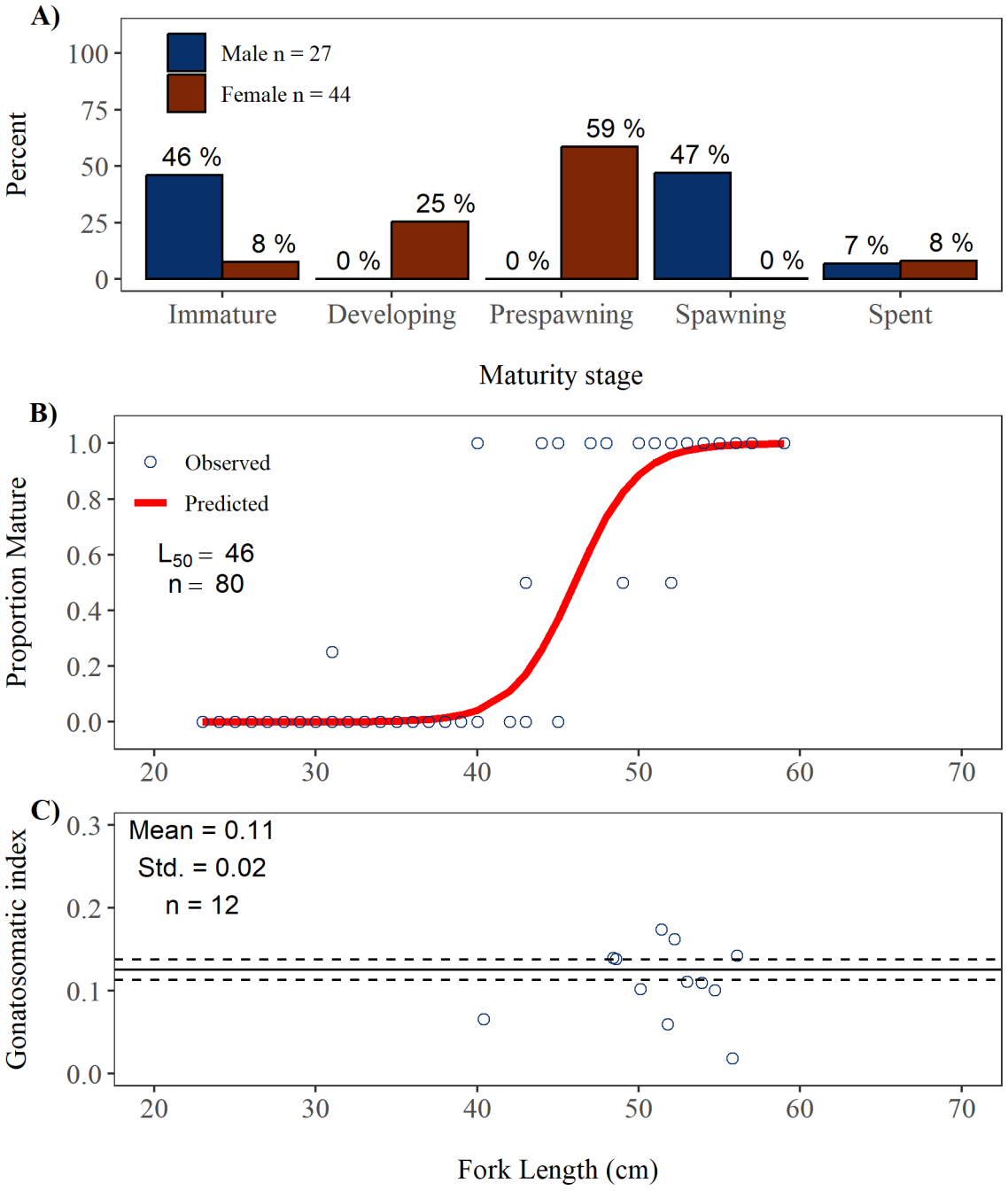

Figure 32. -- Pollock maturity in Marmot Bay. A) Maturity composition for male and female pollock > 40 cm fork length (FL) within each stage; B) proportion mature (i.e., pre-spawning, spawning, or spent) by 1-cm size group for female pollock; C) gonadosomatic index for females > 40 cm FL (with historic survey mean ± 1 standard deviation (Std.)). All maturity quantities are weighted by local pollock abundance.

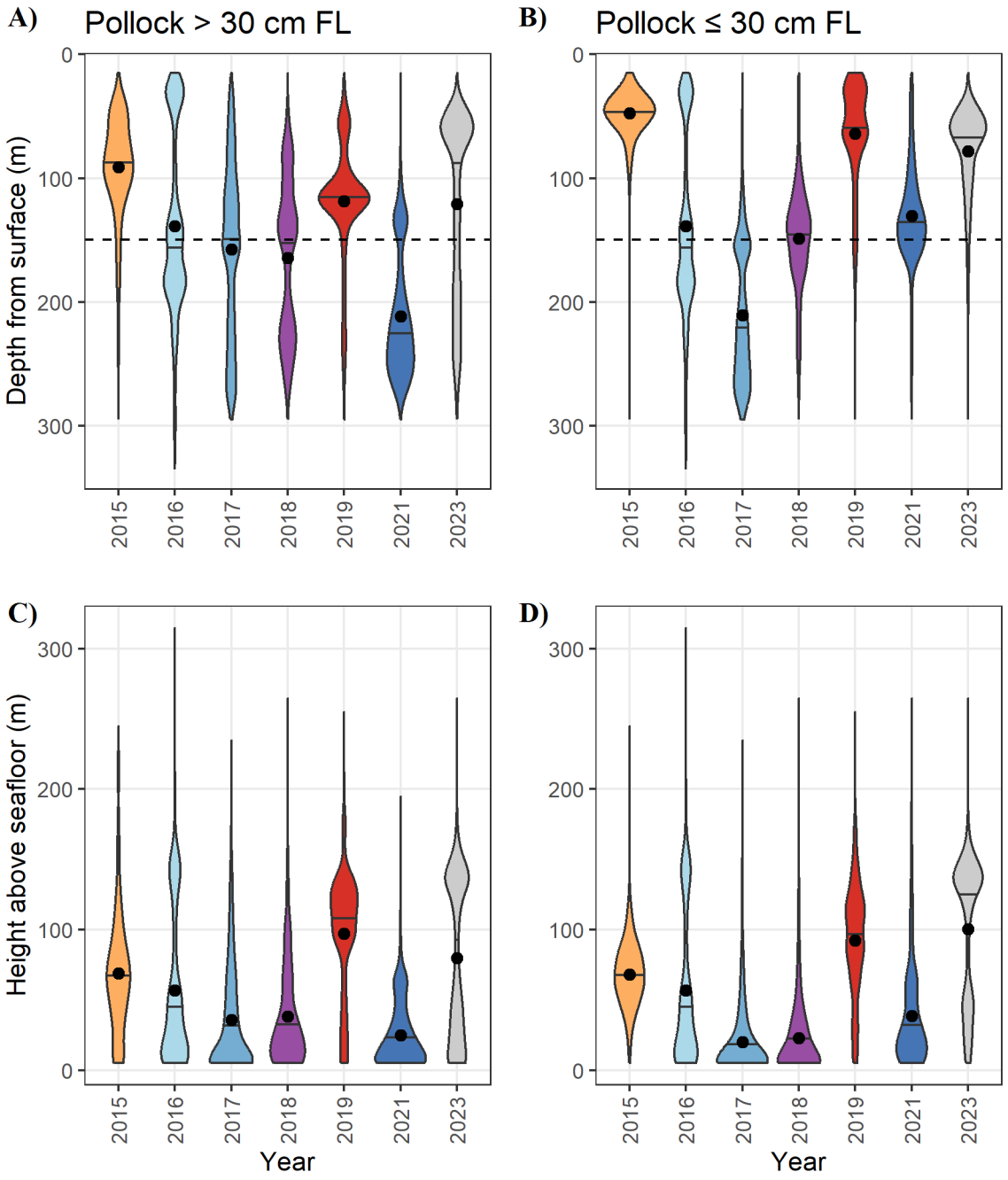

Figure 33. -- Estimated biomass distributions of larger pollock (> 30 cm FL) by depth (A) and height above the seafloor (C), and smaller pollock (≤ 30 cm FL) by depth (B) and height above the seafloor (D) in the Marmot Bay 2023 acoustic-trawl survey. Results for the winter 2015-2022 acoustic-trawl surveys are included for comparison. Depth is referenced to the surface and height is referenced to the bottom. Data were averaged in 10 m depth bins. Mean bottom depth for 2023 is shown in panels A) and B) (dashed line). Plots show the probability density of pollock distribution, with median pollock depth noted by black horizontal lines, and the mean weighted pollock depth indicated by black points.

APPENDIX I. ITINERARY

Shumagin Islands

10 February	Depart Kodiak, AK
10 February	Return to Kodiak (medical emergency)
11 February	Depart Kodiak
12 February	Arrive Uyak Bay, Kodiak Island (weather delay)
12 February-13 February	Acoustic sphere calibration in Uyak Bay
14 February	Arrive Castle Bay (medical emergency)
15 February-17 February	Acoustic-trawl survey of the Shumagin Islands
17 February-18 February	Acoustic-trawl survey of Pavlof Bay
18 February-19 February	Acoustic-trawl survey of Morzhovoi Bay
19 February-21 February	Acoustic-trawl survey of the Shumagin Islands (continued)
21 February	Transit to Kodiak
22 February	In port Kodiak

Shelikof Strait

4 March	Depart Kodiak, AK
4 March-5 March	Transit to survey start area
5 March-11 March	Acoustic-trawl survey of the Shelikof Strait
12 March-15 March	Acoustic-trawl survey of the Chirikof shelfbreak
13 March-14 March	Acoustic sphere calibration in Kaiugnak Bay
15 March-17 March	Acoustic-trawl survey of Marmot Bay
17 March	Transit to Kodiak
17 March	In port Kodiak

APPENDIX II. SCIENTIFIC PERSONNEL

Shumagin Islands

Name	Position	Organization
Denise McKelvey	Chief Scientist	AFSC
David Bryan	Fishery Biologist	AFSC
Alex De Robertis	Fishery Biologist	AFSC
Scott Furnish	Computer Spec.	AFSC
James Gossom	Fishery Biologist	AIS, Inc.
Dave McGowan	Fishery Biologist	AFSC
Matthew Phillips	Fishery Biologist	AFSC

[1]AFSC = Alaska Fisheries Science Center, National Marine Fisheries Service, Seattle, WA; AIS, Inc. Scientific and Environmental Services, Inc.

Shelikof Strait

Name	Position	Organization
Taina Honkalehto	Chief Scientist	AFSC
Scott Furnish	Computer Spec.	AFSC
James Gossom	Fishery Biologist	AIS, Inc.
Darin Jones	Fishery Biologist	AFSC
Mike Levine	Fishery Biologist	AFSC
Sandi Neidetcher	Fishery Biologist	AFSC
Matthew Phillips	Fishery Biologist	AFSC
Sam Urmy	Fishery Biologist	AFSC

[1]AFSC = Alaska Fisheries Science Center, National Marine Fisheries Service, Seattle, WA; AIS, Inc. Scientific and Environmental Services, Inc.

APPENDIX III. ABUNDANCE CALCULATIONS

The abundance of target species was calculated by combining the echosounder measurements with size and species distributions from trawl catches and target strength (TS) to length relationships from the literature (see De Robertis et al. 2017b for details). The echosounder measures volume backscattering strength, which is integrated vertically to produce the nautical area scattering coefficient, s_A (units of m^2 nmi^{-2}; MacLennan et al. 2002). The backscatter from an individual fish of species s at length l is referred to as its backscattering cross-section, $\sigma_{bs_{s,l}}$ (m^2), or in logarithmic terms as its target strength, $TS_{s,l}$ (dB re 1 m^2):

$$TS_{s,l} = 10\log_{10}\left(\sigma_{bs_{s,l}}\right) \quad . \qquad \text{Eqn.}i$$

The numbers of individuals of species s in length class l ($N_{s,l}$) captured in the nearest haul h were used to compute the proportion of acoustic backscatter associated with each species and length. First, the number of individuals in the catch were converted to a proportion ($P_{s.l,h}$):

$$P_{s,l,h} = \frac{N_{s,l,h}}{\sum_{s,l} N_{s,l,h}} \ , \quad \text{where} \sum_{s,l} P_{s,l,h} = 1 \quad . \qquad \text{Eqn.}ii$$

In analyses where trawl selectivity was considered, the selectivity-corrected numbers $N_{s_{corr},l,h}$ were used in place of $N_{s,l,h}$ in Eq. ii. This correction corrects the catch for trawl escapement. The corrected catch is that expected for an unselective sampling device. Refer to the main text for a description of the selectivity corrections applied.

The mean backscattering cross-section (an areal measure of acoustic scattering in m^2; MacLennan et al. 2002) of species s of length class l is:

$$\sigma_{bs_{s,l}} = 10^{\left(0.1 \cdot TS_{s,l}\right)} \ , \qquad \text{Eqn.}iii$$

where TS is the target strength (dB re 1 m^2) of species *s* at size *l* (Table 1).

The proportion of backscatter from species s of length class l in haul h ($PB_{s,l,h}$) is computed from the proportion of individuals of species s and length class l estimated from haul h ($P_{s,l,h}$) and their backscattering cross-section:

$$PB_{s,l,h} = \frac{P_{s,l,h} \cdot \sigma_{bs_{s,l}}}{\sum_{s,l}\left(P_{s,l,h} \cdot \sigma_{bs_{s,l}}\right)} \quad . \qquad \text{Eqn.}iv$$

The measured nautical area backscattering coefficient (s_A) at interval i was allocated to species s and length l as follows:

$$s_{A_{s,l,i}} = s_{A_i} \cdot PB_{s,l,h} \quad , \qquad \text{Eqn.}v$$

where haul h is the nearest haul within a stratum assigned to represent the species composition in a given 0.5 nmi along-track interval i. The nearest geographic haul was determined by using the great-circle distance to find the nearest trawl location (defined as the location where the net is at depth and begins to catch fish) out of the pool of hauls assigned to the same stratum (see above for details) closest to the start of interval i.

The abundance of species of length l in an area encompassing a series of transect intervals i was estimated from the area represented by that interval (A_i, nmi^2), the mean areal backscatter attributed to species s in given length/size class l ($s_{A_{s,l,i}}$, m^2 nmi^{-2}), and mean backscattering cross-section of species s at that size ($\sigma_{bs_{s,l}}$ m^2) as follows:

$$\text{Numbers at length } l\text{: } N_{s,l} = \sum_i \left(\frac{s_{A_{s,l,i}}}{4\pi\sigma_{bs_{s,l,i}}} \times A_i \right) \qquad \text{Eqn. } vi$$

$$\text{Biomass at length } l\text{: } B_{s,l} = \sum_i \left(W_{s,l} \times N_{s,l,i} \right) \quad , \qquad \text{Eqn. } vii$$

where $W_{s,l}$ is the mean weight-at-length for species s in each 1-cm length l derived from length-weight regressions. In the case of pollock, when five or more individuals were measured within a length interval, the mean weight at length was used. Otherwise (i.e., for length classes of pollock with < 5 weight measurements, or other species), weight-at-length was estimated using a linear regression of the natural log-transformed length-weight data (De Robertis and Williams 2008).

The abundance at age was computed from $Q_{s,l,j}$, the proportion of j-aged individuals of species s in length class l, and the abundance of that species and age class in each surveyed interval follows:

$$\text{Numbers at age } j\text{: } N_{s,j} = \sum_{i} \left(Q_{s,l,j} \times N_{s,l}\right) \qquad \text{Eqn. } viii$$

$$\text{Biomass at age } j\text{: } B_{s,j} = \sum_{i} \left(Q_{s,l,j} \times B_{s,l}\right) \quad . \qquad \text{Eqn. } ix$$

Appendix Table 1. -- Target strength (TS) to size relationships from the literature used to allocate 38 kHz acoustic backscatter to most species in this report. The symbols in the equations are as follows: r is the bell radius in cm and L is length in cm for all groups except pelagic crustaceans, in which case L is in m.

Group	TS (dB re 1 m^2)	Length type	TS derived for which species	Reference
walleye pollock	$TS = 20 \log_{10} L - 66$	L = fork length	*Gadus chalcogrammus*	Foote and Traynor (1988), Traynor (1996)
Pacific capelin	$TS = 20 \log_{10} L - 70.3$	L = total length	*Mallotus catervarius*	Guttormsen and Wilson (2009)
Pacific herring[1]	$TS = 20 \log_{10} L\text{-}2.3 \log_{10}(1 + depth/10) - 65.4$	L = fork length	*Clupea harengus*	Ona (2003)
eulachon	$TS = 20 \log_{10} L - 84.5$	L = total length	*Thaleichthys pacificus*	Gauthier and Horne (2004)
fish with swim bladders	$TS = 20 \log_{10} L - 67.4$	L = total length	Physoclist fishes	Foote (1987)
fish without swim bladders	$TS = 20 \log_{10} L - 83.2$	L = total length	*Pleurogrammus monopterygius*	Gauthier and Horne (2004)
jellyfish	$TS = 10 \log_{10}(\pi r^2) - 86.8$	r = bell radius	*Chrysaora melanaster*	De Robertis and Taylor (2014)
squid	$TS = 20 \log_{10} L - 75.4$	L = mantle length	*Todarodes pacificus*	Kang et al. (2005)
Pelagic crustaceans[2]	$TS = A * (\log_{10}(BkL)/(BkL))^c + D((kL)^6) + E((kL)^5) + F((kL)^4) + G((kL)^3) + H((kL)^2) + I(kL) + J + 20 \log_{10}(L/L_0)$	L = total length	*Euphausia superba*	Demer and Conti (2005)

[1] *depth* (m) is fixed at 75 m

[2] A = -930.429983; B = 3.21027896; C = 1.74003785; D = 1.36133896 x 10^{-8}; E = -2.26958555 x 10^{-6}
F= 1.50291244 x 10^{-4}; G = -4.86306872 x 10^{-3}; H = 0.0738748423; I = -0.408004891; J = -73.9078690; and L_0 = 0.03835
If L < 0.015 m, TS = -105 dB; and if L > 0.065 m, TS = -73 dB.
k = 2πfc, where f = 38,000 (frequency in Hz) and c = 1470 (sound speed in ms^{-1})

U.S. Secretary of Commerce
Howard Lutnick

Acting Under Secretary of Commerce
for Oceans and Atmosphere
Laura Grimm

Acting Assistant Administrator,
National Marine Fisheries Service
Emily Menashes

April 2025

www.fisheries.noaa.gov

OFFICIAL BUSINESS

National Marine
Fisheries Service
Alaska Fisheries Science Center
7600 Sand Point Way N.E.
Seattle, WA 98115-6349